8-2014

Fourth Moment Approximation of Instrinsic Mode Lifetimes in Solids

Yang Gao
Clemson University

Fourth Moment Approximation of Intrinsic Mode Lifetimes in Solids

---

A Dissertation
Presented to
the Graduate School of
Clemson University

In Partial Fulfillment
of the Requirements for the Degree
Doctor of Philosophy
Physics

---

by
Yang Gao
August 2014

Accepted by:
Dr. Murray S. Daw, Committee Chair
Dr. Bradley Meyer
Dr. Catalina Marinescu
Dr. Sumanta Tewari

Abstract

A new method (second moment approximation method) of calculating mode lifetimes of materials has been proposed by Dickel and Daw [14, 15]. The method was tested on an anharmonic lattice model, and it shows consistency with results from using traditional method (molecular dynamics with Green-Kubo [2]) at high temperatures, but deviates at low temperatures. Based on this method, we developed the fourth moment approximation method, and tested it on various models from 1D anharmonic chain to the FCC cube with Lennard-Jones potential. Calculations showed that the fourth moment approximation method provides a fast and reliable scheme to calculate mode lifetimes at wide range of temperatures, and this scheme can be used on many different materials.

Acknowledgments

I would like to thank my advisor, Dr. Murray S. Daw, for all the knowledge and skills I have been given, the great patience he showed me and all the interesting conversations we had. It is my honor and great fortune to be a student of his.

I want to thank my committee members: Dr. Bradley Meyer, Dr. Catalina Marinescu and Dr. Sumanta Tewari, for all the valuable suggestions on my research. I thank Dr. Bradley Meyer for the great E&M course. I thank Dr. Catalina Marinescu and Dr. Sumanta Tewari for the everything I have learned in quantum physics.

I thank Mr. Hengjia Wang and Mr. Andrew Garmon for joining Dr. Daw to continue our project.

Research supported by the U. S. Department of Energy, Office of Basic Energy Science, Division of Materials Sciences and Engineering under Award ER 46871.

Table of Contents

List of Tables

List of Figures

Chapter 1

Introduction

1.1 Background

In this dissertation, we investigate and develop a new method of calculating the mode lifetimes in insulating solids, where lattice vibrations dominate the thermal behavior.

Any lattice motion can be considered as a superposition of normal modes with their own frequency. These vibrations are normal modes (or phonons in quantum mechanics). The lifetime of one normal mode measures the time duration for this mode to diminish. If the system only has a harmonic interatomic potential, there is no interaction among normal modes and each normal mode vibrates forever once it starts, thus the mode lifetime is infinite. Systems with anharmonic interatomic potentials on the other hand involve interactions among normal modes, so energy and motion of one vibrating normal mode dissipates and transfers to other modes and the mode lifetime in this case is finite. In general, longer mode lifetimes represent normal modes having less interactions with other normal modes than ones with shorter mode lifetimes. Mode lifetimes microscopically describe vibrational behavior of systems and thus energy equilibration and they are very important property to investigate thermal and transport properties of materials, such as the thermal conductivity.

The calculation of mode lifetimes must include two steps: Step 1 is to obtain forces, and it can be done using first-principles method [1] or empirical potentials. Step 2 is to extract mode lifetimes using forces that have been calculated in step 1.

[1] Here we use "first-principles method" as a common terms relating to a method of solving for the electronic-structure.

Theoretically, any combination of a method from step 1 (obtaining forces) and from step 2 (extracting mode lifetimes) would be able to serve as a means to calculate the mode lifetimes (Figure: 1.1). Many examples in the mode lifetime calculations can be found in the literature. In the following few paragraphs, we will look back very briefly on these methods.

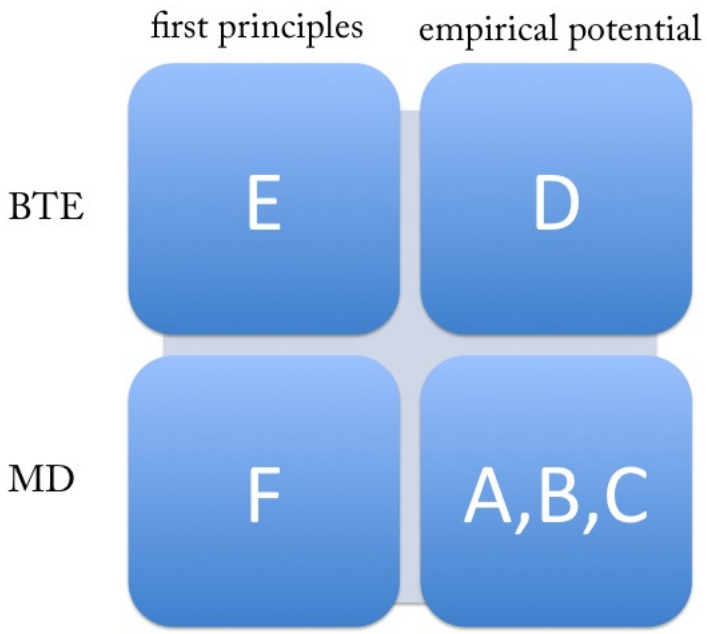

Figure 1.1: Classic methods of calculations of mode lifetimes: letters refer to examples discussed in text

1.2 Review of literature

1.2.1 Molecular dynamics and Green-Kubo (MD-GK): Examples A-C

Example A: Ladd *et al.* [1] calculated mode lifetimes (Eq:1.1, in which n represents phonon occurpation number, and δn is the fluctuation of n from its equilibrium value) of a monatomic fcc lattice at low temperatures using both MD-GK (equilibrium molecular dynamics with Green-Kubo) and anharmonic perturbation theory.

$$\tau = \frac{\int_0^\infty \langle \delta n(t) \delta n(0) \rangle dt}{\langle (\delta n(0))^2 \rangle} \tag{1.1}$$

Averages such as $\langle \delta n(0) \delta n(t) \rangle$, which depend on both time and ensemble properties (such as T) are obtained typically as in [1]. Ensemble Molecular Dynamics (EMD) is a numerical technique in which many different initial conditions have been drawn from some ensemble (such as NPT or NVT), and from each initial condition the dynamics of the system follows Newton's law. The Green-Kubo relation (GK) [2] is a formally exact expression of transport coefficients in terms of correlation functions which describes the decay of fluctuations in microscopic fluxes. Molecular Dynamics method simulates particles interactions with forces derived from potentials and thus calculates correlation functions. The correlation functions are therefore functions of the time and the ensemble variables (e.g., NVT). In this paper, the interatomic potential is "soft-sphere" potential (Eq:1.2). Calculations showed the agreement between MD-GK calculation and anharmonic perturbation theory at low temperatures. Calculations also showed the great complexity of phonon lifetimes. For example the dependence of the magnitude and direction of wave vector $\vec{k}$ shows no generality, and the temperature dependence of the mode lifetimes is as expected from the perturbation theory: $\tau \propto T^{-1}$

$$\phi_{\vec{r}} = \epsilon(\sigma/|\vec{r}|)^{12} \tag{1.2}$$

Transport and thermal-dynamic properties of materials can be extracted from the normal mode lifetimes. Ladd *et al.* also calculated the lattice thermal conductivity of the system using MD-GK directly with the dynamic variable heat current q (it can be represented by volume V, velocity $\vec{v}$, relative coordinate $\vec{r}_{mn}$ and force $\vec{F}_{mn}$) (Eq:1.3) to compare with the results extracted from the mode lifetimes.

$$\vec{q} = \frac{1}{2V} \sum_m m v_m^2 \vec{v}_m + \frac{1}{2V} \sum_{m>n} [\phi_{mn}(\vec{v}_m + \vec{v}_n) + \vec{F}_{mn} \cdot (\vec{v}_m + \vec{v}_n) r_{mn}] \tag{1.3}$$

Example B: By applying the same technique, Dong *et al.* [3] investigated LTC of Germanium Clathrates. The time dependent autocorrelation function is evaluated using MD and the forces is obtained from the Tersoff potential. Both crystals with and without guest atoms in their fullerane cages are studied at room temperature, and their work shows consistent results with experiments.

Example C: Schelling *et al.* [4] conducted the thermal conductivity calculation using both equilibrium and non-equilibrium MD on Sillinger-Weber silicon. The main purpose of this article is to represent both methods as established means for calculating the thermal conductivity, and resolve some of the main methodological issues. The first issue is the finite-size effect, and it has

been demonstrated in the article how to calculate the reliable results using non-equilibrium MD and extrapolation to the infinite size systems. The second issue is the choice of definition of local energy, and calculations showed that the thermal conductivity is relatively insensitive to the choices. At the end, the article showed the consistency between the two methods and with experiments.

1.2.2 Boltzmann Transport Equation with the Empirical Potential: Example D

Example D: Broido *et al.* [5] investigated lattice thermal conductivity (LTC) of silicon using BTE with empirical potentials.

Without any approximation to BTE (such as elastic continuum approximation and relaxation time approximation), calculations are done using a full inelastic phonon Boltzmann equation approach with empirical potentials (specifically the Stillinger-Weber(SW) potential, the Tersoff potential and the environment-dependent (ED) interatomic potential) providing second and third order force constants (Eq:1.4, 1.5).

$$K^{\alpha_1,\alpha_2}_{n_1 i_1, n_2 i_2} = \left.\frac{\partial^2 V}{\partial u^{\alpha_1}_{n_1 i_1} \partial u^{\alpha_2}_{n_2 i_2}}\right|_0 \tag{1.4}$$

$$K^{\alpha_1,\alpha_2,\alpha_3}_{n_1 i_1, n_2 i_2, n_3 i_3} = \left.\frac{\partial^3 V}{\partial u^{\alpha_1}_{n_1 i_1} \partial u^{\alpha_2}_{n_2 i_2} \partial u^{\alpha_3}_{n_3 i_3}}\right|_0 \tag{1.5}$$

where K is Nth order force constant, α specifies Cartesian component, n represents the unit cell and i is the index of atoms, V is an interatomic potential in general, and thus this formula applies to empirical potentials as well. The force constants are used as input to the inelastic phonon BTE in which three-phonon scattering processes, isotopic defect and boundary scattering are incorporated.

Their calculation results show agreement with experimentally measured LTC in the low temperatures, while at higher temperatures, all 3 empirical potentials give thermal conductivities that are larger than the measured ones.

1.2.3 Boltzmann Transport Equation (BTE) with First Principles: Example E

Example E: Broido *et al.* [6] combine First Principles method and Boltzmann transport equation (BTE). The article presents calculated LTC of both Silicon and Germanium using their

proposed method which agrees with experimentally measured LTC from 100K to 300K. Although the calculation is done to determine LTC and mode lifetimes were not directly computed, they could have been done by the same technique with some additional expense.

The Boltzmann transport equation (BTE) [7], is a semi-classical description of dynamic systems:

$$\frac{\partial f}{\partial t} + \vec{v} \cdot \bigtriangledown_{\vec{r}} f + \vec{F} \cdot \bigtriangledown_{\vec{p}} f = \frac{\partial f}{\partial t}|_{coll} \tag{1.6}$$

where f is the probability distribution function of any dynamic systems in phase, and $\frac{\partial f}{\partial t}|_{coll}$ describes the event "collision" which is composed of in-scattering and out-scattering process.

While it could simplify calculations tremendously using relaxation time approximation with BTE, the assumptions behind the approximation don't truly describe the behavior of most materials (for example, one assumption is elastic scattering, while anharmonic phonon-phonon scattering is inelastic). Instead, there are no adjustable parameters invoked in their proposed method. The calculation is done by solving BTE explicitly including phonon-phonon scattering process, and the only input is interatomic force constants using density functional perturbation theory (DFPT).

1.2.4 Molecular Dynamics with the First Principles: Example F

Example F: Stackhouse *et al.* [8] used non-equilibrium MD in combination with first-principles to determine the LTC of periclase (MgO, the main constituent of the Earth's deep mantle). The purpose of this work to estimate the LTC of periclase at extreme pressure-temperature conditions (conditions similar to Earth's core) where no experiments have been done and numerical methods using potentials tend not to work (empirical potentials won't give accurate descriptions of the system in such conditions). Computations have been done using density functional code VASP [9]. The code has been modified so that it can perform non-equilibrium MD by including the algorithm for kinetic energy exchange. Approximations have been made in this article to simplify the calculations in any possible way: 1. Only linear temperature gradient is considered in the calculation of the conductivity. 2. The contributions of defects, grain boundaries have been ignored. 3. This First Principles calculation uses Local Density Approximation(LDA) [10].

1.2.5 Discussion

The mode lifetime can be calculated using the schemes that have been discussed before, but each method has its strength & weakness.

The method of MD-GK in combination with interatomic potentials shows the possibility to calculate with reasonable efficiency mode lifetimes on different materials, the only downside is that potentials are limited to materials that have already been well studied. Thus it is hard to apply this method to new materials and materials with no empirical potentials to describe.

The method of BTE with first-principles is encouraging, and lots of work has been done using this technique [11, 12, 13] (such as calculation of thermal conductivities of different materials: diamond nanowires, GaN and boron arsenide). However the calculation is very demanding and expensive to generalize, and the challenge of calculation increases significantly with both size and complexity of cells.

The method of BTE with empirical potentials shows two drawbacks: 1. Solving BTE directly usually involves approximations. In this article the calculation only involves the second and third order force constants (Eq: 1.4), and higher order anharmonicity is ignored. 2. Usage of empirical potentials brings error to calculations which is very hard to correct. As is pointed out in the article [5]: at low temperatures, all 3 models can well describe the LTC, however at higher temperatures where phonon-phonon scattering dominates the behavior of the systems, none of the model gives the correct result. What is even worse is that the calculated LTC from each model doesn't agree with results from others which can be explained by the fact that none of these empirical potentials captures the accurate anharmonicity and phonon dispersions and each model might give a good description of the anharmonicity and be inaccurate about the rest.

The wide application of the method of MD with first principles is formidable especially for large complex systems because of its computational cost.

Overall it is safe to say that so far there is no clear way of conducting mode lifetimes calculations on wide variety of materials.

1.3 Present work

In this dissertation, we develop a computational technique of calculating mode lifetimes which is based on moments approximations which involves the Monte Carlo method (MC) only,

and deploy this method on various models. This method was originally proposed by Dickel and Daw (D&D) [14, 15], and the details of this proposed method will be discussed in Chapter 2. As a comparison, the method of MD has also been implemented on the same models, and our conclusions are the following:

- The results for mode lifetimes from the moments approximation method is consistent with that from the method of MD.
- The method of moments approximation is significantly faster than the method of MD and Green-Kubo.
- The method of moments approximation provides a very general paradigm to calculate mode lifetimes of a wide variety of materials.

In short, our work[2] provides a general and practical approach to calculate the intrinsic mode lifetimes of solids within relative short computational times and explore the physical properties of wide range of materials from the perspective of mode lifetimes. Thus it is beneficial to consider our proposed method as a new means of calculation of mode lifetimes Fig:(1.2)

[2]The method is inspired by a sequence of work from Haydock *et al.* [16, 17, 18] which provide a possible alternative to calculate mode lifetimes and thermal conductivities by using Liouville operator and recursion method.

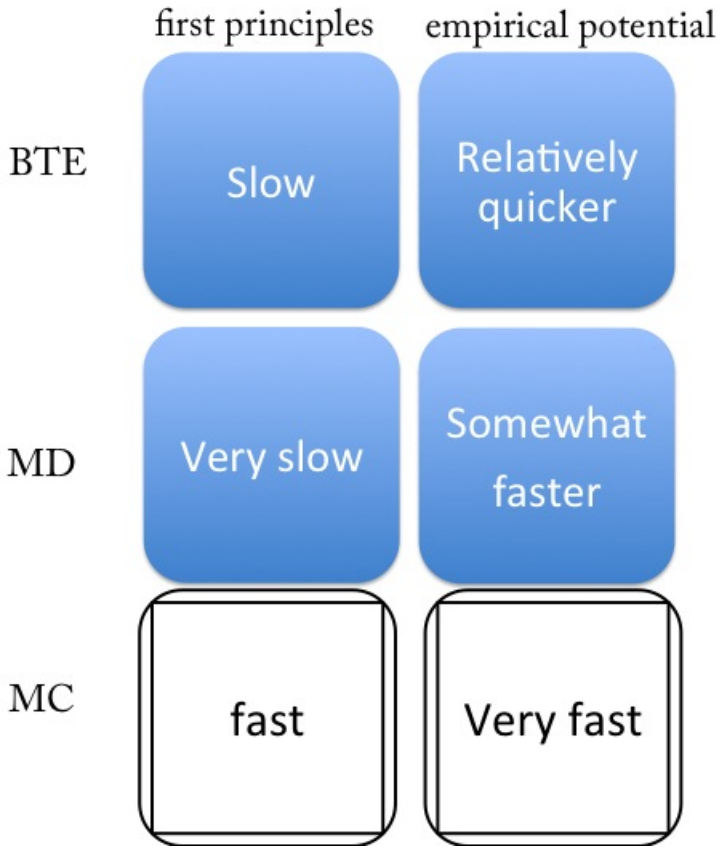

Figure 1.2: The relationship of new methods of calculations of mode lifetimes to previous methods

The remainder of this dissertation is organized as follows:

- Chapter 2: Review the work of DD who developed the second moment approximation method.
- Chapter 3: Build upon the work of DD by developing the fourth moment approximation method and implementing it on low dimension models.
- Chapter 4: Implement the fourth moment approximation method on 1D anharmonic chain and 3D lattice models.
- Chapter 5: Using the fourth moment approximation method on face cubic models with Lennard-Jones(LJ) potential.
- Chapter 6: Summary and future work.

Chapter 2

Second Moment Approximation (from Dickel & Daw)

2.1 Introduction

In this chapter, we review[1] the work from Ted Dickel and Murray Daw [14, 15]. They proposed a formal and practical scheme of calculations of mode lifetimes in solids, which is based on the Liouville operator and the recursion method. Instead of calculating mode lifetimes directly, they formalize the lifetimes in terms of moments of the power spectrum of the Liouvillian as projected onto the relevant subspace of phase space. Mathematically speaking, the moments are calculated as ensemble averages of dynamical quantities, and numerically the calculation is done with Monte Carlo (MC) only. The proposed method not only provides another way of analyzing mode lifetimes, also leads to a significantly faster calculations compared to the current methods.

The analysis of vibrational mode lifetimes was encompassed as part of the general theory of energy dissipation in dynamical systems begun in the seminal work of Van Hove [19, 20], and further developed by Prigogine and co-workers [21, 22, 23, 24, 25, 26, 27], and along similar lines by Zwanzig [28, 29, 30] and Mori [31]. The basic formalism considered the evolution of classical dynamical systems using the Liouvillian [32, 33]. Zwanzig and Moris projector operator approach was applied by Wilson and Kim specifically to the problem of mode lifetimes and lattice thermal

[1] Much of the text and most figures in this chapter are from [14, 15]

conductivity [34]. While the formalism provided insights into the mechanism of equilibration of energy, there have been no quantitative predictions of mode lifetimes using this formalism.

A recent breakthrough has been made in extracting the long-term dynamics within the Liouvillian formalism by applying the recursion method [16, 17, 18]. Haydock *et al.* [17] have recently proposed a practical scheme for calculating macroscopic rates from the resolvent of the Liouvillian. In this view, dissipation results from the flow of energy from large to small scale structures in phase space. By using the recursion method, along with careful considerations of the required analytical properties of the resolvent, Haydock and company investigated a way of extracting the long-time behavior from a finite amount of information about the resolvent. This new insight forms the inspiration and basis of the current work.

This chapter is organized as the follows: First, we recap the approximation proposed by Dickel & Daw (DD), which includes Green-Kubo formula, canonical transformation and the Liouville operator. Secondly, we look into the numerical work, where DD investigated the dependence of mode lifetimes on cell size and temperatures also they compared their method with other popular methods. At last, we draw conclusions.

2.2 Theory

2.2.1 Mode Lifetimes and the Green-Kubo Formula

In DD's work, they chose the fluctuation of the occupancy factor to describe the system's behavior and to calculate mode lifetime:

$$\delta n_k = n_k - \langle n_k \rangle$$

According to the Green-Kubo(GK) approach, the mode lifetime is defined as:

$$\tau_k = \int_{-\infty}^{+\infty} dt \ \chi_k(t) \tag{2.1}$$

where $\chi_k(t)$ represents the autocorrelation function:

$$\chi_k(t) = \frac{\langle \delta n_k(0) \ \delta n_k(t) \rangle}{\langle \delta n_k(0)^2 \rangle} \tag{2.2}$$

In the equation above, k is the mode index, angular brackets indicate ensemble average over the equilibrium distribution in phase-space:

$$\langle A \rangle = Z^{-1} \int d\Gamma e^{-\beta H(\{p_i\},\{q_i\})} A(\{p_i\},\{q_i\}) \tag{2.3}$$

$$Z = \int d\Gamma e^{-\beta H(\{p_i\},\{q_i\})} d\Gamma \equiv \prod_i dp_i dq_i \tag{2.4}$$

The autocorrelation function is a function of time and ensemble conditions. The system starts from an initial state drown from the ensemble, then giving one trajectory advances forward in time (using MD) for a period of time t. The autocorrelation is the ensemble average of the product of one dynamic variable at later time t and itself at time 0. If the interaction in the system is simply harmonic, the auto-correlation won't go to 0 and stay at 0. However, if the interactions involves anharmonicities, the autocorrelation will decay to 0. The mode lifetime defined by GK approach is the integral of the autocorrelation function, so it captures the "decaying" aspect of the dynamic of the system.

One general property of the autocorrelation function is the following:

$$\dot{\chi}(0) = 0 \tag{2.5}$$

2.2.2 Canonical Transformation

To have an expression of the occupancy factor n_k, two transformations have been implemented:

- Normal mode transformation: coordinates (p_i, q_i) to normal modes
- Hamilton-Jacobi transformation: normal modes to action-angle variables

The Hamilton-Jacobi theory originally was developed to study the perturbations of planetary orbits by other planets. Some planets still behave within nearly periodic orbits, while altering the action and relative phases of the other orbits. This coupled periodic orbital motion is clearly quite similar to the case of coupled anharmonic vibrations, where the underlying periodic motion of the normal modes is influenced by possibly strong coupling to other normal modes. So even in the presence of strong coupling, the action-angle transformation can be very helpful.

The simple SHO Hamiltonian involving coordinate and momentum variables (q,p)

$$H(q,p) = \frac{p^2}{2m} + \frac{kq^2}{2}$$

can be transformed to action-angle variables(S,α) by a transformation with an arbitrary frequency ω^X

$$q = \sqrt{\frac{2S}{m\omega^X}}\sin\alpha \tag{2.6}$$

$$p = \sqrt{2Sm\omega^X}\cos\alpha \tag{2.7}$$

to

$$K(S,\alpha) = S(\omega^X\cos^2\alpha + \frac{k}{m\omega^X}\sin^2\alpha)$$

so that the equations of motions are:

$$\dot{\alpha} = \omega^X\cos^2\alpha + \frac{k}{m\omega^X}\sin^2\alpha \dot{S} = -2S(-\omega^X + \frac{k}{m\omega^X})\sin\alpha\cos\alpha \tag{2.8}$$

If ω^X is chosen to match the harmonic frequency:$\omega^X = \omega^H = \sqrt{\frac{k}{m}}$, the equations of motion will be simplified so that S is a constant and $\alpha = \omega^H t$. Then $K = \omega S$ (we can find the connection with quantum mechanics here).

With any value of ω^X, the transformation is always canonical, and when ω^X is not the same as the harmonic frequency, the dynamical variables are still periodic. It is worth noticing that their averages over a period of the motions are $\bar{S} = 0$ and $\bar{\dot{\alpha}} \approx \omega^H$ if ω^X is close the the value of ω^H.

The action angle transformation is canonical regardless of what hamiltonian it applies to. If the transformation applies to the following hamiltonian:

$$H(q,p) = \frac{p^2}{2m} + \frac{kq^2}{2} + \lambda q^4$$

The motion of this anharmonic system is still periodic, so that the angle α will have an overall linear behavior in time with a periodic oscillation superimposed. With a chosen anharmonic

frequency trying to simplify the equations, α is no longer linear in time, but the slope of α has the mean value of a quasi-harmonic frequency ($\bar{\dot{\alpha}} \equiv \omega^Q$). This quasi-harmonic frequency is useful in the later numerical work.

Here is the two consecutive transformations applied to a 1D anharmonic chain in DD's scheme:

The system with the hamiltonian:

$$H = \frac{1}{2}\sum_n p_n^2 + \sum_n V(u_{n,n+1})$$

where

$$V(d) = \frac{d^2}{2} + \frac{d^4}{24}$$

Normal-mode transformation are:

$$q_k = \frac{1}{N}\sum_n u_n e^{-ikn} \pi_k = \frac{1}{N}\sum_n p_n e^{-ikn} \tag{2.9}$$

which are widely used for harmonic approximation method, and in the harmonic case, all modes will decouple.

Next, action-angle transformation is applied:

$$S_k = \frac{N}{2\omega_k^X}|\pi_k + i\omega_k^X q_k|^2 = \hbar n_k \alpha_k = arg(\pi_k + i\omega_k^X q_k) \tag{2.10}$$

To minimize the fluctuation caused by anharmonicity, it is beneficial to use the following equation to define the quasi-harmonic oscillation:

$$\langle \dot{\alpha}_k \rangle = \omega_k^Q(\beta) \tag{2.11}$$

It is expected that at low temperatures, where harmonic potential dominates the system behavior, the quasi-harmonic frequency will converge to the harmonic frequency.

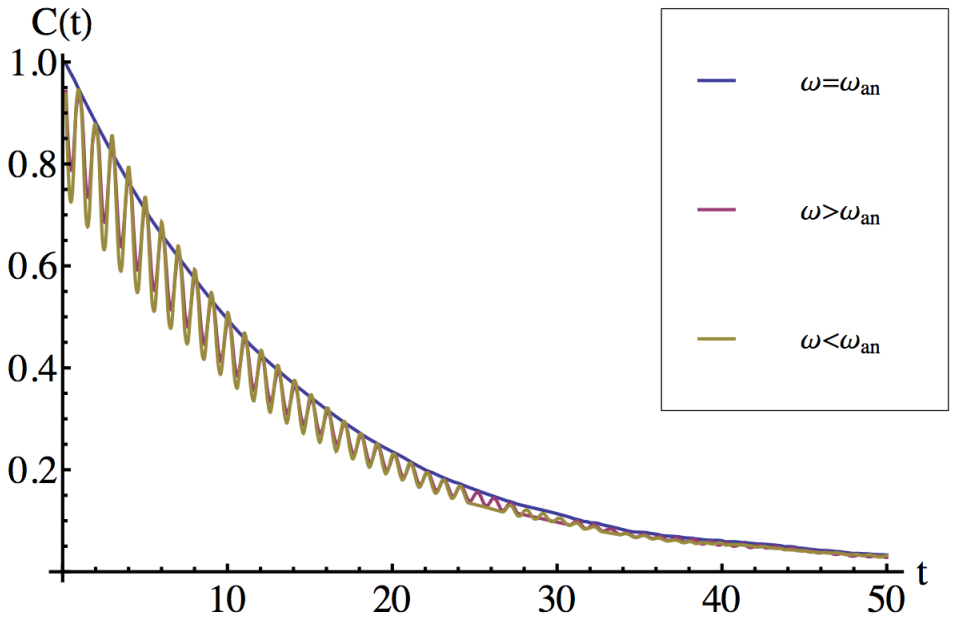

Figure 2.1: The autocorrelation function χ with different ω vs time at a certain temperature from article [14]

2.2.3 Liouville operator and moments

Here is the elaboration of this method. DD are interested in the autocorrelation function(ACF) of δn_k. To get the time evolution of ACF or any quantity $f(p, q, 0)$, Liouville operator [21, 32, 33] is introduced:

$$\hat{L} = i\{H, \} = i \sum_l (\frac{\partial H}{\partial q_l} \frac{\partial}{\partial p_l} - \frac{\partial H}{\partial p_l} \frac{\partial}{\partial q_l}) \tag{2.12}$$

so that:

$$f(p, q, t) = e^{-it\hat{L}} f(p, q, 0) \tag{2.13}$$

The Liouville operator has many general properties that are helpful when it comes to actual calculation (Fig: 2.2):

	Liouville Equation	Schrodinger Equation
Operator	$\hat{L} = \sum_i [-i(\frac{\partial H}{\partial p_i})(\frac{\partial}{\partial q_i}) + i(\frac{\partial H}{\partial q_i})(\frac{\partial}{\partial p_i})]$	$\hat{H} = \frac{p^2}{2m} + V(r)$
Time Evolution Equation	$i(\frac{\partial \rho}{\partial t}) = \hat{L}\rho$	$i\hbar(\frac{\partial \phi}{\partial t}) = \hat{H}\phi$
Hermitian	$\hat{L} = \hat{L}^\dagger$	$\hat{H} = \hat{H}^\dagger$
Formal Solution	$\rho(p_i, q_i, t) = e^{-i\hat{L}t}\rho_0(p_i, q_i)$	$\phi(t) = e^{-i\frac{\hat{H}t}{\hbar}}\phi_0$
Linearity	$\hat{L}(f+g) = \hat{L}f + \hat{L}g$	$\hat{H}(\phi_1 + \phi_2) = \hat{H}\phi_1 + \hat{H}\phi_2$
Specialty	L is a linear operator even if the Hamiltonian is not.	

Figure 2.2: Property of Liouville operator

In terms of τ, the autocorrelation of velocity has the form:

$$\chi(t) = \frac{\langle v(0)\ v(t)\rangle}{\langle v(0)^2\rangle} = \frac{\langle v(0)\ e^{-it\hat{L}}v(0)\rangle}{\langle v(0)^2\rangle} \tag{2.14}$$

$\chi(t)$ can be written as a Taylor Series:

$$\chi(t) = 1 - \mu_2\frac{t^2}{2!} + \mu_4\frac{t^4}{4!} - \mu_6\frac{t^6}{6!} + ... \tag{2.15}$$

where μ_s are called moments:

$$\mu_m = \frac{\langle \delta n(0)\ (-iL)^m \delta n(0)\rangle}{\langle \delta n(0)^2\rangle} \tag{2.16}$$

and first few low-order moments are not difficult to calculate analytically, which ideally could give

insight to the system. In principle, knowledge of all the moments μ_s could specify the lifetime:

$$\tau = F(\mu_2, \mu_4, \mu_6, \ldots)$$

which can be re-expressed (using dimensional analysis) as

$$\tau/\tau_2 = G(\gamma_4, \gamma_6, \ldots)$$

where $\tau_2 = \mu_2^{-1/2}$, G is a generally unknown function, and the γ's are dimensionless parameters

$$\gamma_n = \frac{\mu_n}{(\mu_2)^{n/2}}$$

that characterize the shape of the DOS. (Note that $\gamma_n \geq 1$.) The moments of the Liouvillian are also the moments of the density of states (DOS) derived from $\chi(t)$. That is, taking the Fourier transform of $\chi(t)$ to get $n(\omega)$, the moments are also

$$\mu_m = \int_{-\infty}^{+\infty} d\omega \; \omega^m \; n(\omega)$$

While it is not generally possible to know all of the moments, DD proposed that in certain circumstances the lifetime might be practically approximated from a knowledge of only the lowest moments. This suggests a series of approximations, starting with only the second moment

$$\tau = c\tau_2 \tag{2.17}$$

and including successively higher moments. The fourth moment approximation would then be

$$\tau = \tau_2 K(\gamma_4) \tag{2.18}$$

where K is some function yet to be determined. The higher moments correspond to ensemble averages of higher powers of the Liouvillian, and so each higher moment involves higher time derivatives of the dynamical variables.

2.3 Numerical Work

2.3.1 Model

The model DD used to demonstrate the methods is a three-dimensional lattice. The basic structure is $(8 \times 8 \times 8)$ simple cubic (SC) with periodic boundary condition. The Hamiltonian of the model is given by the following equation such that only the nearest neighbor lattice sites are connected by anharmonic potentials:

$$H = \sum_i \frac{1}{2} |\vec{p}_i|^2 + \sum_{<i,j>} V(\vec{d}_i - \vec{d}_j) \tag{2.19}$$

where $\vec{p}_i$ is the momentum of the particle at i^{th} lattice site and $V(\vec{d})$ is given by:

$$V(\vec{d}) = \frac{1}{2}|\vec{d}|^2 + \frac{1}{24}|\vec{d}|^4 \tag{2.20}$$

Following are the advantages and characters of the chosen model

- It is a simple model with enough complex nonlinear dynamic behavior.
- The lattice is fixed, and there is no mass flow. the only motions are vibrations about equilibrium states.
- There is no melting point or any other phase transition critical temperature, so that DD can examine the proposed scheme over a wide range of temperature.
- The Hamiltonian of the system does not have particle flow, so DD can study the vibrations of the anharmonic lattice exclusively.
- The system behaves differently in two temperature regimes: At low temperatures, simple harmonic potential dominates the behavior, which is characterized by harmonic heat capacity and long mode lifetimes. At high temperatures, the system behavior is dominated by the anharmonic potential (the quartic part of the potential), which is characterized by shorter mode lifetimes.

2.3.2 Calculations

To calculate auto-correlation function $\chi_k(t)$,the numerical calculations can be described as follows:

- By using Monte Carlo (MC) sampling at a fixed temperature, an initial position in phase space (a state of the system) is chosen.
- This initial state of the state starts evolving in time by carrying out Molecular Dynamics(MD) (specifically, DD used velocity Verlet algorithm [54]).
- Calculate occupation number (the dynamics DD chose to calculate the mode lifetimes) by applying canonical transformation.
- Auto-correlation function $\chi_k(t)$ is calculated with the states of each time step in MD and initial states.
- Fluctuation of the auto-correlation function $\chi_k(t)$ is minimized by choosing anharmonic frequency ω_a as the transformation frequency wisely(such as choosing ω_a which maximize lifetimes τ_k)
- Repeat the above steps many times(until the results converges) with different initial states chosen by MC method, and calculate the average.

In their numerical work. DD tested a simple moment approximation:

$$\begin{aligned} \tau &= C\tau_2 \\ \tau_2 &= 1/\sqrt{\mu_2} \end{aligned} \tag{2.21}$$

2.3.3 Results

The following is a typical auto-correlation of the chosen model, one thing that is worth noticing is $\chi_k(t)$ does not go to zero. One explanation is that as long as the system is finite, the ensemble will have some memory of its initial states at any later time (In other words, the states of the system at any time is more or less correlated with the initial states of the system.). DD chose to solve this numerical issue by truncating the autocorrelation once it dropped below 0.5% of its original value.

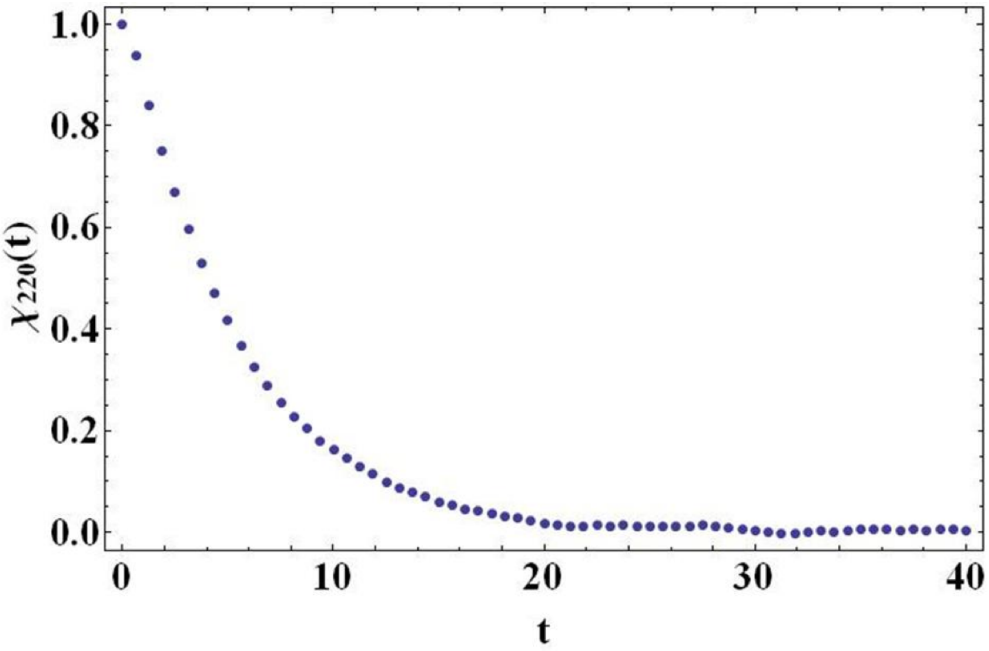

Figure 2.3: A typical autocorrelation of the 3D lattice model from article [15]

The behavior of the mode lifetimes change over temperatures (Fig:2.4). DD focused on the high temperatures, while low temperature calculation is limited by substantially increasing computing times. In the low-temperature regime, change of τ more sensitive to the change of temperatures than that in high temperatures, and in the high-temperature regime (above 10), mode lifetimes behave as:

$$\tau(T) \propto T^{-\frac{1}{3}} \tag{2.22}$$

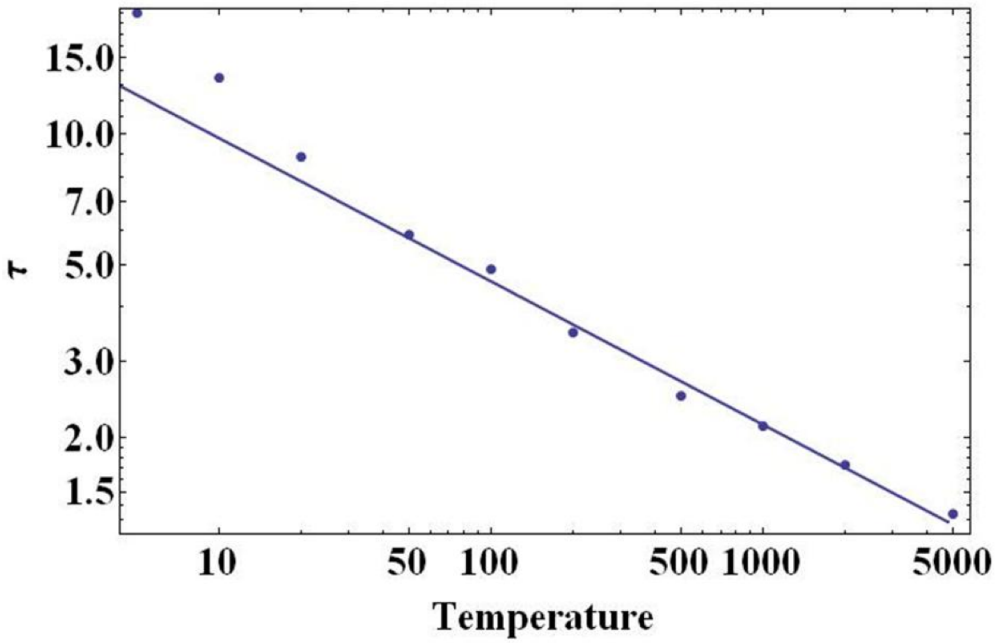

Figure 2.4: The mode lifetime τ as a function of the temperature in the direction of [220] from article [15]

Frequency of transformation is chosen to be the anharmonic mode frequency which depends on both temperature and wavevector, so to see how τ is related to temperature and wave vector, it is important to investigate the anharmonic frequency($\omega_a(k)$). The harmonic frequency is defined by:

$$\omega_0(\vec{k}) = \sqrt{6 - 2\cos\frac{2\pi k_x}{l_x} - 2\cos\frac{2\pi k_y}{l_y} - 2\cos\frac{2\pi k_z}{l_z}} \tag{2.23}$$

Calculations showed that the ratio between the frequency shift ($\delta\omega(\vec{k}) \equiv \omega_a(\vec{k}) - \omega_0(\vec{k})$) and $\omega_0(\vec{k})$ was independent of wave vector, but, it depended on temperature (Fig: 2.5) with the following relation:

$$\frac{\delta\omega(\vec{k})}{\omega_0(\vec{k})} = f(T) = (\frac{T}{T_0})^{\frac{1}{3}} \tag{2.24}$$

Because of the similarities between Eq. 2.24 and Eq. 2.22, DD continued examining the relation between τ and $\delta\omega$ at a fixed temperature (Fig/ 2.6).

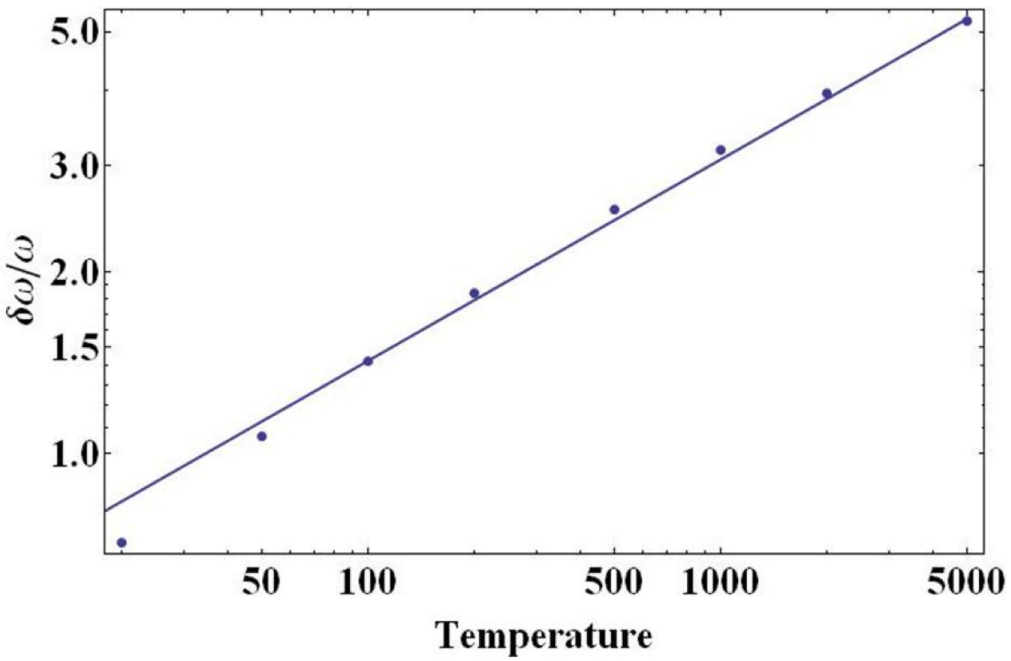

Figure 2.5: The fractional shift in frequency $\frac{\delta\omega}{\omega}$ vs the temperature, it is universal for all anharmonic frequencies with different wave vector from article [15]

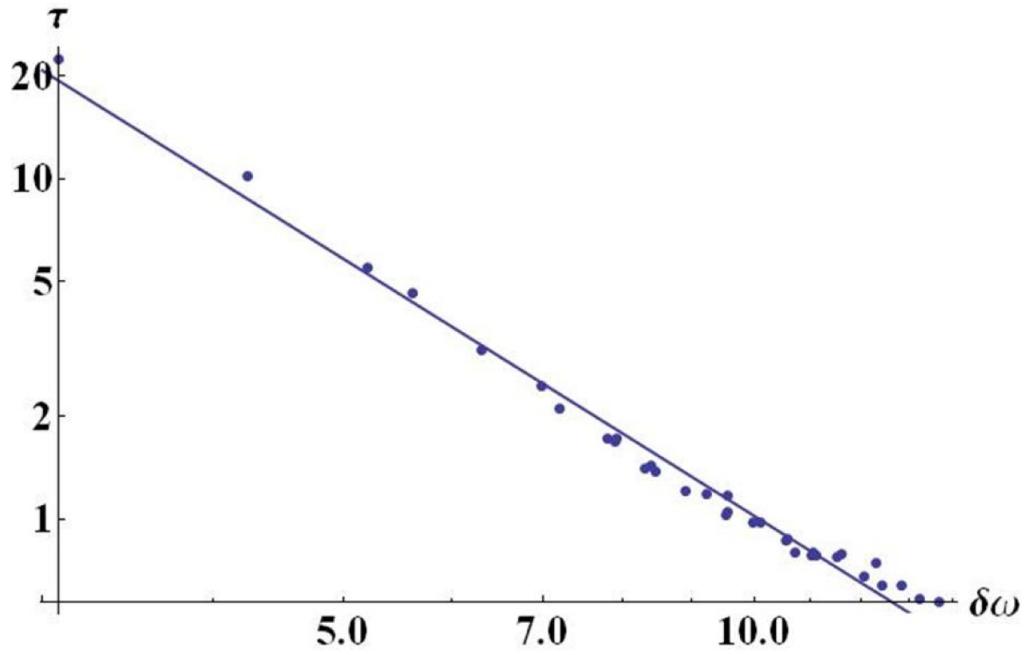

Figure 2.6: The mode lifetime τ vs frequency shift $\delta\omega$, at temperature of 2000 from article [15]

After investigating the characters of the behavior of the mode lifetime of the model with respect to temperature and wave-vector, DD did another set of numerical work to complete the approximation method.

This part of numerical work has the following features:

- It does not require any time evolution of the dynamics of the system
- MC is needed only which is significantly faster than the numerical method considered above.

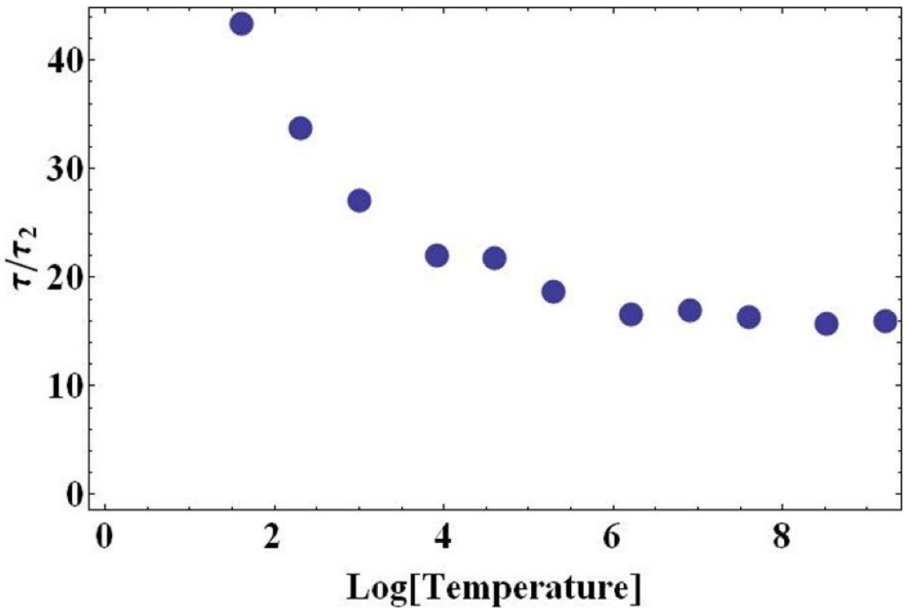

Figure 2.7: The ratio τ/τ_2 vs temperatures from article [15]

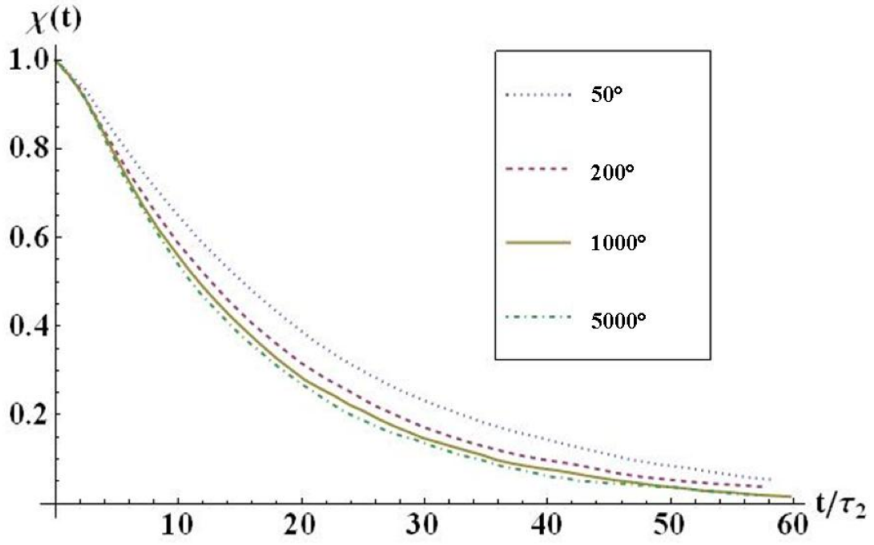

Figure 2.8: The data collapse of $\chi(t)$ for the [222] wave-vector at different temperatures from article [15]

2.3.4 Conclusion

By analyzing the mode lifetime in an 3D anharmonic lattice with quartic interaction between neighbors, DD drew some important conclusions. First, for this specific model, mode lifetimes τ have a very simple relation with anharmonic frequency, which depends separably on the harmonic frequency and the temperature. While these properties are certainly not universal, they certainly give some insight to the method. Second, this numerical work is the first attempt to use a much less computational expensive method than any available methods that we are aware of to calculate the mode lifetime and the thermal conductivity. While there are some deviations at low temperatures, it works quite well at high temperature region. Third, this method promises to be applicable to other more complex and realistic systems.

Chapter 3

Fourth Moment Approximation in Low-Dimensional Models[1] (original work)

3.1 Introduction

As we have discussed in the previous Chapter, Dickel & Daw [14, 15] proposed an approximation to lifetimes of vibrational modes in nonlinear solids which involves ensemble averages of appropriate functions in phase space that can be carried out by conventional Monte Carlo in combination with a means of calculating forces, such as interatomic potentials or first-principles electronic structure codes. The approach was illustrated on a lattice model of non-linear interactions, where the dependence of the mode lifetimes on cell size and temperature was investigated numerically. In particular, calculations based on averages of the second power of the Liouvillian (that is, so-called "second moment" approximation) accounted for the mode lifetimes very well at high temperatures but diverged at lower temperatures.

While the aim of the original work was to lay out the formalism and carry out first-level (that is, second moment) calculations, the purpose of the this chapter is to examine in more depth the approximations involved and to investigate the improvement gained by including the fourth

[1] Some of the text and figures have appeared in [35].

moment. To this end we take up the same idea as applied to very simple systems of just one or two degrees of freedom. In considering systems of such simplicity, we analyze some aspects of the problem analytically as well as numerically. These insights prove fruitful, especially by indicating how the next level of approximation (that is, "fourth moment") is able to account for vibrational mode lifetimes even at much lower temperatures.

$$\tau = \tau_2 K(\gamma_4) \tag{3.1}$$

where K is some function yet to be determined. The higher moments correspond to ensemble averages of higher powers of the Liouvillian, and so each higher moment involves higher time derivatives of the dynamical variables. We then return to the lattice model, and find that the fourth moment results are reliable to much lower temperatures than the second moment.

In this chapter, we use several simple dynamical models as the basis for testing the fourth moment approximation and also using the density of states to provide an analysis of why the approximation might work and when it would be expected to fail. Each model has been laid out as follows:

- Apply dimensional analysis (DA) to the model
- Calculate the specific heat of the system (analytical or numerical)
- Calculate the moments and mode lifetimes at all temperatures
- Analyze the approximation method from the perspective of Density of States (DOS)

3.2 Numerical calculation

For numerical calculation, three techniques are tried.

The first technique combines the Monte-Carlo method (MC) and the Molecular Dynamic (MD) method. Specifically, one can sample the phase space of the initial state of the system by MC with a sufficient number of samples. From each initial state, the system is run by MD for a relatively short time, and at the end the average of quantities that one is interested over samples (ensemble average) can be found. In the MD part, Velocity Verlet method is applied:

$$x(t+\delta t) = x(t) + v(t)\delta t + \frac{1}{2}a(t)^2\delta t^2$$

$$v(t+\delta t) = v(t) + \frac{a(t)+a(t+\delta t)}{2}\delta t$$

The second method is that one can run a system according to MD for a long time and apply Fast Fourier Transform (FFT) twice (forward and backward) to get the autocorrelation of a quantity. Here, Convolution in Fourier transform is used: Suppose $F(\omega)$ is the Fourier Transform of $f(t)$, according to Convolution Theorem, Inverse Fourier Transform of $|F(\omega)^2|$ is nothing but $\int_{-\infty}^{\infty} f(x)f(x+t)dx$ which is the autocorrelation of $f(t)$.

The last technique is simply a mixture of the first two by using a relatively smaller number of samples, and running longer MD for each sample.

Our calculations showed that the second numerical method is the least efficient one to implement on our models, especially at low temperatures.

3.3 Models Considered

We consider three simple model hamiltonians in one (x) and two (x and y) dimensions. These models are chosen because they are simple, non-linear, and the ensemble averages can be obtained analytically. The momentum conjugate to x is p; that to y is q.

x^4 model:

$$H(p,x) = p^2 + x^2 + x^4 \tag{3.2}$$

The auto-correlation in the x^4 model has been studied extensively before [37, 38]. In that work, an analytic approximation to $\chi(t)$ was obtained at low temperature:

$$\chi(t) = \frac{\cos(t) - 3Tt\sin(t)}{9T^2t^2 + 1} \tag{3.3}$$

showing an oscillatory behavior with an *algebraically* decaying envelope. Our numerical auto-correlation conforms well to this analytical form at low temperatures.

x^2y^2 model:

$$H(p,x,q,y) = p^2 + q^2/M + x^2 + y^2 + x^2y^2 \tag{3.4}$$

The x^2y^2 model is a simple extension to two modes coupled nonlinearly. In this model, we investigate various values of the ratio (M) of the masses between the two modes, which controls the degree of resonance.

"cubic" model:

$$H(p,x,q,y) = p^2 + q^2 + x^2 + y^2 + \frac{\lambda}{4}(x^2+y^2)^2 + \frac{1}{3}(x^3 - 3xy^2) \tag{3.5}$$

The "cubic" model for certain parameters has multiple minima in the $x-y$ plane and exhibits a "structural" transformation (from multiple attractors to a single attractor) with temperature, which makes it interesting to include in the present study. To explore the effects produced by this transition, we tried various values of the strength (λ) of the quartic term. For $\lambda < 1/9$, there are three off-center global minima with one local minimum on-center. For $1/9 < \lambda < 1/8$, there is one global minimum at the center and three off-center local minima. Finally, for $\lambda > 1/8$, there is only one global minimum at the center.

Some examples of a calculated ACF are shown in Figs. 3.1-3.2. For the x^4 model, the function exhibits a simple oscillation and decay. In the "cubic model", the function displays less regularity because of the less symmetrical potential.

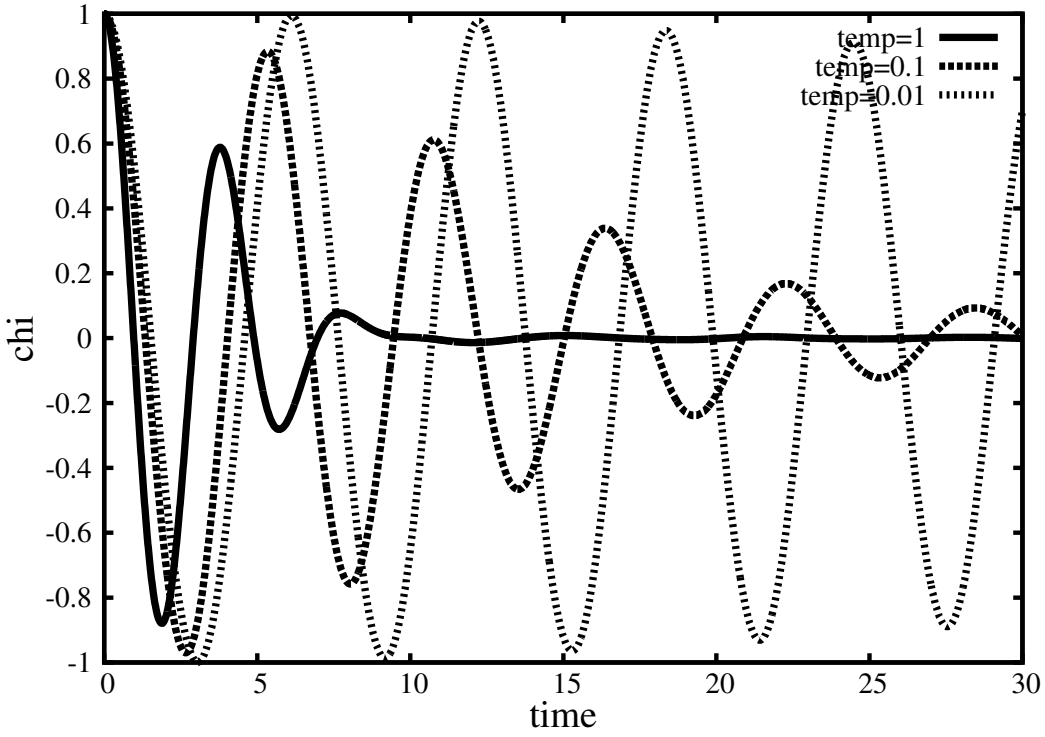

Figure 3.1: The ACF at three temperatures for the x^4 model.

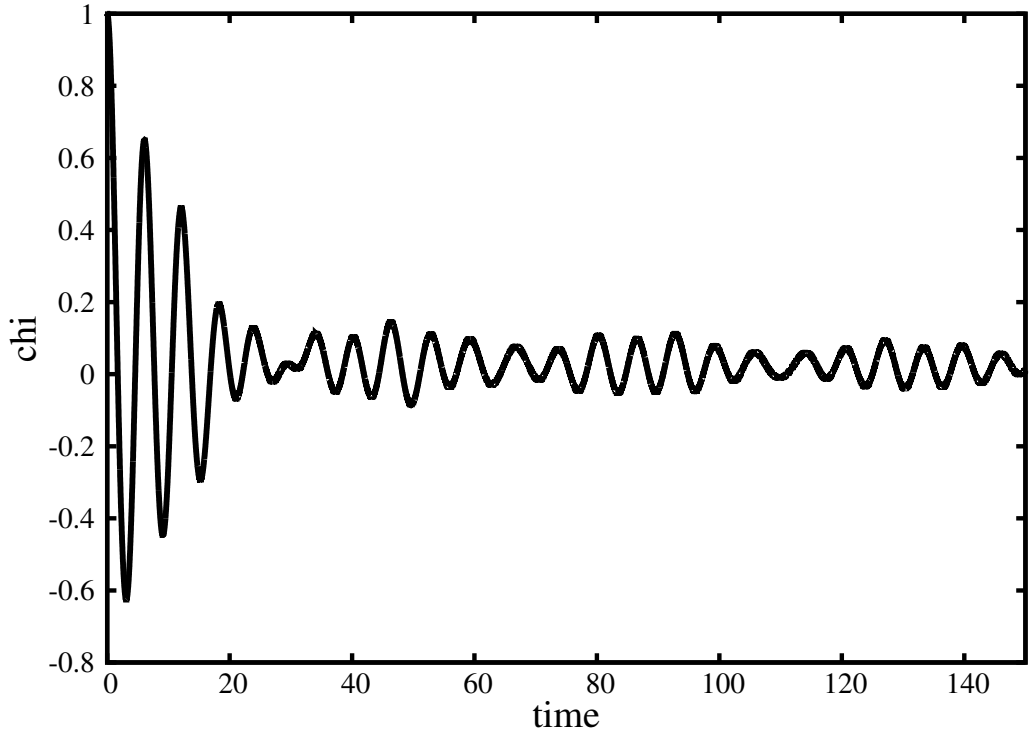

Figure 3.2: The ACF of the x-mode at $\lambda = 0.5$ and $T = 0.2$ for the "cubic" model.

These models are chosen because they are simple, non-linear, and the ensemble averages can be obtained analytically. The x^2y^2 model is a simple extension to two modes. In this model, we investigate various values of the ratio (M) of the masses between the two modes. The "cubic" model for certain parameters has multiple minima and exhibits a "structural" transformation (from multiple attractors minima to a single attractor) with temperature, which makes it interesting to include in the present study. To explore the effects produced by this transition, we tried various values of the strength (λ) of the cubic term.

3.4 "Clemson Time": an alternative definition of lifetime

From Figs(3.1, 3.2), it is clear to see that the integration of the ACF is not only very close to zero, but also it fails to encapsulate the information of the damping behavior of the system. Thus

we define lifetime as follows:

$$\tau = \int_0^\infty \chi(t)^2 dt \tag{3.6}$$

which doesn't have the problem of oscillation any more. For the rest of this article, the mode lifetimes (τ) is calculated by Eq. 3.6 unless otherwise noted. Also for everyone's convenience, it is defined as 'Clemson Time'.

3.5 Choice of dynamical variables

Ladd *et al.* [58] chose the occupation number autocorrelation function (OACF), which has an oscillation and decay in anharmonic systems. The problem with the OACF is that in finite systems, the OACF does not decay to zero as time increases. Instead, it has a residue, even though the residual decreases as the size of the system increases.

On the other hand, the velocity autocorrelation function (VACF) was used by Sen [37] to study the behavior of systems. The advantage of VACF is that it doesn't have residuals.

In the x^4 model, the OACF (and ACF of its derivative), VACF and XACF have been studied, while in the x^2y^2 and the cubic model, study is concentrated on the VACF and XACF. (The residuals of XACF is not zero in the cubic model due to the local and global minima of the potential.)

Following are the layout of results from each dynamic model.

3.6 The x^4 model

In this section, calculations are conducted in the x^4 model and they are organized as follows:

- Dimensional analysis(DA) of the x^4 model
- Calculation of heat capacity
- Calculation of moments and mode lifetimes of the chosen dynamic variables: the fluctuation of occupation number δJ and its derivative
- Calculation of moments and mode lifetimes of the chosen dynamic variables: displacement and velocity

- Density of States

3.6.1 Dimensional analysis(DA)

The x^4 model has the following hamiltonian: $H = \frac{1}{2}(\frac{p^2}{m} + kx^2 + \lambda x^4)$ which can be written in the reduced-parameter form $H = \frac{1}{2}(p^2 + x^2 + x^4)$ by doing the following dimensional analysis [55].

M, K, λ are taken as basis out of all variables:M, K, β and λ Following is the DA:

$$\begin{aligned} [m] = M, [\lambda] = ML^{-2}T^{-2}, \\ [\beta] = T^2 m^{-1} L^{-2}, [k] = MT^{-2}, \\ [\mu_2] = [(u_0, L^2 u_0)] = T^{-2} \end{aligned} \tag{3.7}$$

According to DA, one can set the following equations:

$$\begin{aligned} [\mu_2] * [\lambda]^a * [m]^b * [k]^c = M^0 L^0 T^0, \\ [\beta] * [\lambda]^{a1} * [m]^{b1} * [k]^{c1} = M^0 L^0 T^0, \end{aligned} \tag{3.8}$$

so that $\frac{m\mu_2}{k}$ and $\frac{\lambda}{\beta k^2}$ are both dimensionless and by the Buckingham Pi Theorem:

$$\mu_2 = \frac{k}{m}\phi(\frac{\lambda}{\beta k^2}) \tag{3.9}$$

Similarily, since $[\tau] = T$, we have the following equation:

$$\tau = \sqrt{\frac{m}{k}}\psi(\frac{\lambda}{\beta k^2}) \tag{3.10}$$

3.6.2 Heat Capacity

The value of the heat capacity of the x^4 model can be calculated analytically, and it is between 3/4 at high temperature and 1 at low temperatures,

At low temperature: Harmonic part of the hamiltonian dominates the behavior of the system, then partition function can be given by

$$\int_{-\infty}^{\infty}\int_{-\infty}^{\infty} e^{-\frac{1}{2}\beta(p^2+q^2)} dpdq = \frac{2\pi}{\beta}$$

which gives the extreme value of heat capacity at low temperatures.

While at high temperatures: anharmonic part of the hamiltonian dominates the behavior, and the partition function is approximately given by

$$\int_{-\infty}^{\infty}\int_{-\infty}^{\infty} e^{-\frac{1}{2}\beta\left(p^2+q^4\right)}dpdq = \frac{\sqrt{\pi}\ \Gamma[\frac{1}{4}]}{2^{1/4}\beta^{3/4}}$$

which gives the extreme value of C at high temperatures.

Here is the behavior of heat capacity C of the x^4 model at low and high temperatures:

	low T	high T
C	$1-3T$	$0.75+0.0597486\ T^{-\frac{1}{2}}$

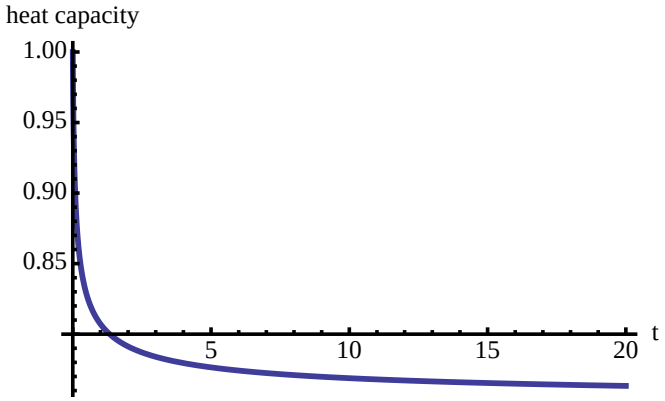

Figure 3.3: Heat capacity vs T

3.6.3 Lifetime of autocorrelation function of δJ and $\dot{J}$

In this part, the fluctuation of occupation number δJ and its derivative $\dot{J}$ are chosen as the dynamical variables we are interested in, and the corresponding autocorrelation function is called OACF and the autocorrelation function of $\dot{J}$:

$$\begin{aligned} J &= \frac{p^2+x^2}{2} \\ \delta J &= J - \langle J \rangle \\ \dot{J} &= \hat{L}J = -i2px^3 \end{aligned} \tag{3.11}$$

Next, the lifetimes of ACFs are extracted with a proper method. One popular way is based on the Green-Kubo Theorem, and mode lifetime can be defined as follows:

$$\begin{aligned} \tau &= \int_0^\infty \chi(t)dt \\ \chi(t) &= \frac{\langle \delta J(0)\delta J(t)\rangle}{\langle \delta J(0)^2\rangle} \end{aligned} \tag{3.12}$$

However, the application of the Green-Kubo Theorem on the x^4 model is problematic, which can be demonstrated by the following graph (Fig. 3.4): After elimination of the residual, the integration of $\chi(t)$ is almost zero, which fail to grasp the damping behavior of the system. Thus we use integration of $\chi(t)^2$ to calculate the mode lifetime Eq.(3.6).

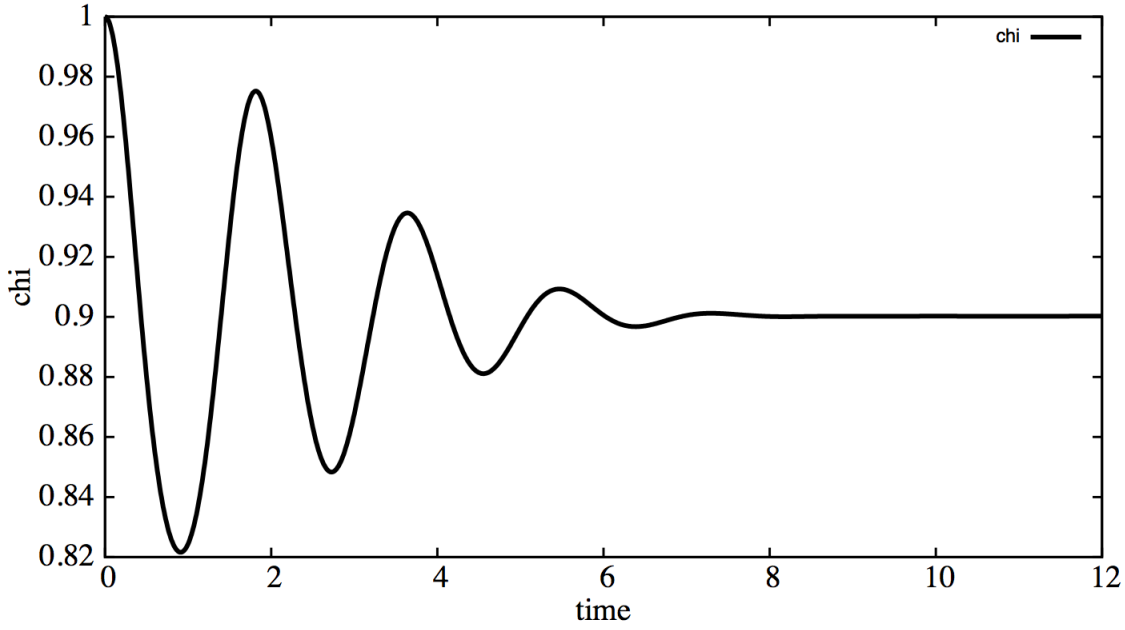

Figure 3.4: Autocorrelation function of δJ from the x^4 model at T=0.5

The numerical works have been done to calculate χ at different temperatures, and for each different temperature, according to the Eq.(3.6), there is a lifetime corresponding to the system.

3.6.4 Behavior of moments of OACF

To approximate the lifetime with moments, the low order moments and γ have been calculated at different temperatures and following are the behavior of the μ_s at extreme temperatures (T)

Table 3.1 shows the behavior of μ_s of δJ at low and high T

	low T	high T
μ_2	$60T^2 - 1260T^3$	$5.73587T^{\frac{1}{2}} - 3.62916$
μ_4	$384T^2 - 1008T^3$	$168T - 91.7738T^{\frac{1}{2}}$
μ_6	$3840T^2 + 60480T^3$	$8672.63T^{3/2} - 4287.29T$
μ_8	$52224T^2 + 1688832T^3$	$665280.T^2 - 313041.T^{3/2}$

Table 3.1: Asymptotic behavior of moments of δJ in the x^4 model at extreme temperatures

Table 3.2 shows the behavior of γ_s of δJ at both high and low T

	low T	high T
γ_4	$\frac{8}{75}T^{-2} + \frac{21}{5}T^{-1}$	$5.10636 + 3.67226\ T^{-\frac{1}{2}}$
γ_6	$\frac{4}{225}T^{-4} + \frac{7}{5}T^{-3}$	$45.9572 + 64.5145\ T^{-\frac{1}{2}}$
γ_8	$\frac{68}{16875}T^{-6} + \frac{293}{625}T^{-5}$	$614.623 + 1266.32\ T^{-\frac{1}{2}}$

Table 3.2: Asymptotic behavior of γ_s of δJ in the x^4 model at extreme temperatures

Table 3.3 shows the behavior of μ_s of $\dot{J}$ at low and high T

	low T	high T
μ_2	$\frac{32}{5} + \frac{588}{5}T$	$29.2894T^{\frac{1}{2}} + 2.5318$
μ_4	$64 + 2352\ T$	$1512T + 209.21T^{\frac{1}{2}}$
μ_6	$\frac{4352}{5} + \frac{232128}{5}T$	$115986T^{3/2} + 18809.9T$
μ_8	$13312 + 916224\ T + 16208640\ T^2$	$1.21081 \times 10^7\ T^2 + 1.85578 \times 10^6\ T^{3/2}$

Table 3.3: Asymptotic behavior of moments of $\dot{J}$ in the x^4 model at extreme temperatures

Table 3.4 shows the behavior of γ_s of $\dot{J}$ at low and high T

	low T	high T
γ_4	$\frac{25}{16} + \frac{140175}{1024}T^2$	$1.76251 - 0.0608331\ T^{-\frac{1}{2}}$
γ_6	$\frac{425}{128} - \frac{6075}{1024}T$	$4.61609 - 0.448445\ T^{-\frac{1}{2}}$
γ_8	$\frac{8125}{1024} - \frac{151875}{4096}T$	$16.4526 - 3.16705\ T^{-\frac{1}{2}}$

Table 3.4: Asymptotic behavior of γ_s of $\dot{J}$ in the x^4 model at extreme temperatures

Now both lifetimes and low order moments have been calculated at different temperatures (temperature: $T \in (0.001, 100)$), according to what have been found by DD [14, 15], behavior of the system over a wide range of temperatures might be described by the 2nd and 4th moments, to check the assumption, graphs have been made to analyze the relation between the lifetimes and the 2nd and 4th moments.

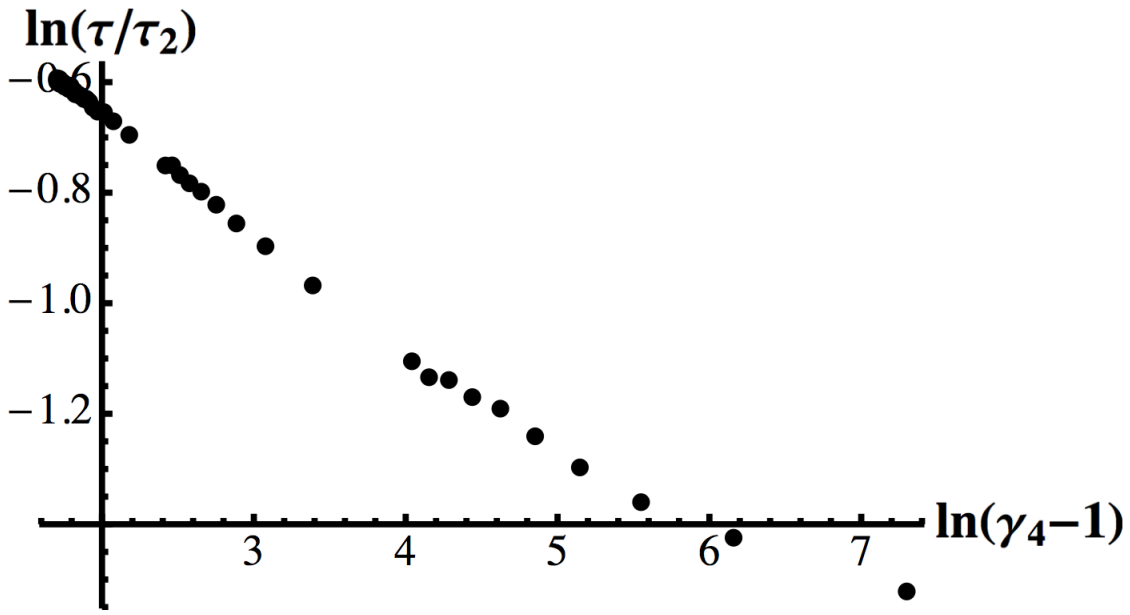

Figure 3.5: The ratio τ/τ_2 vs. γ_4 of autocorrelation function of δJ from the x^4 model

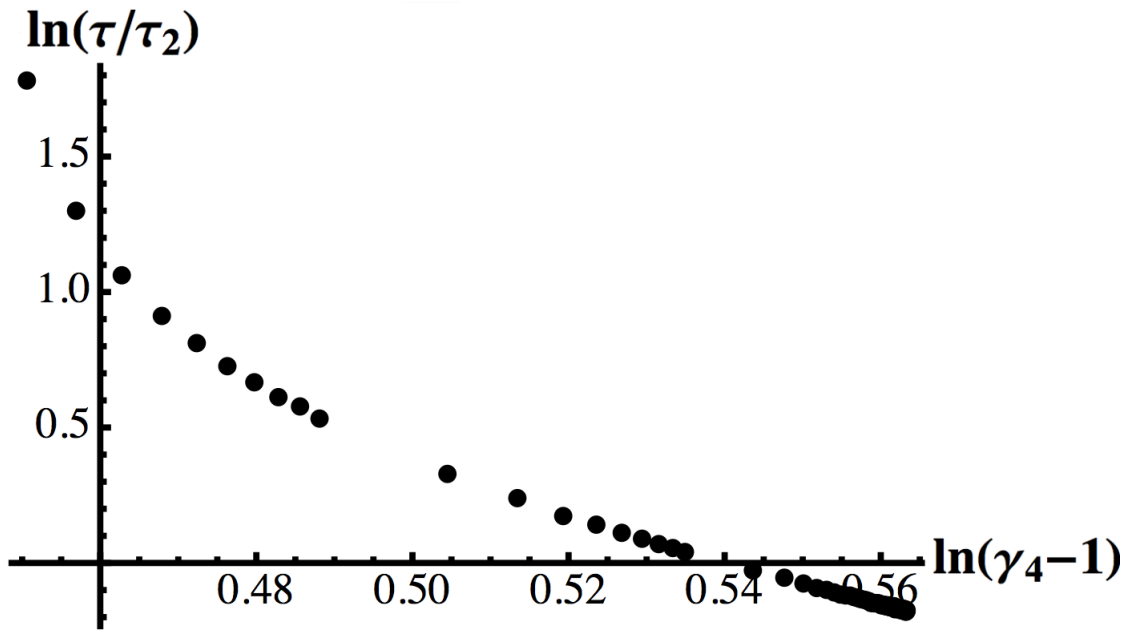

Figure 3.6: The ratio τ/τ_2 vs. γ_4 of autocorrelation function of $\dot{J}$ from the x^4 model

Clearly, Figs (3.5, 3.6) illustrate that there is a simple relation between the lifetimes τ and μ_2 γ_4 , which means, lifetime τ can be approximated by μ_2 and μ_4, and the assumptions made by

DD holds for the x^4 model.

3.6.5 lifetime of VACF and XACF

Similar calculations and procedures in the previous section have been applied to calculate the velocity autocorrelation function(VACF) and the displacement autocorrelation function(XACF). The advantage of the VACF and XACF is that both of them are simple quantities to calculate, and they have no residuals and yet they contain dynamical information of the system just like the OACF does.

Figures (3.7, 3.8) illustrate the VACF and XACF at both low and high temperatures. It is obvious that the higher the temperature the faster they decay to the equilibrium.

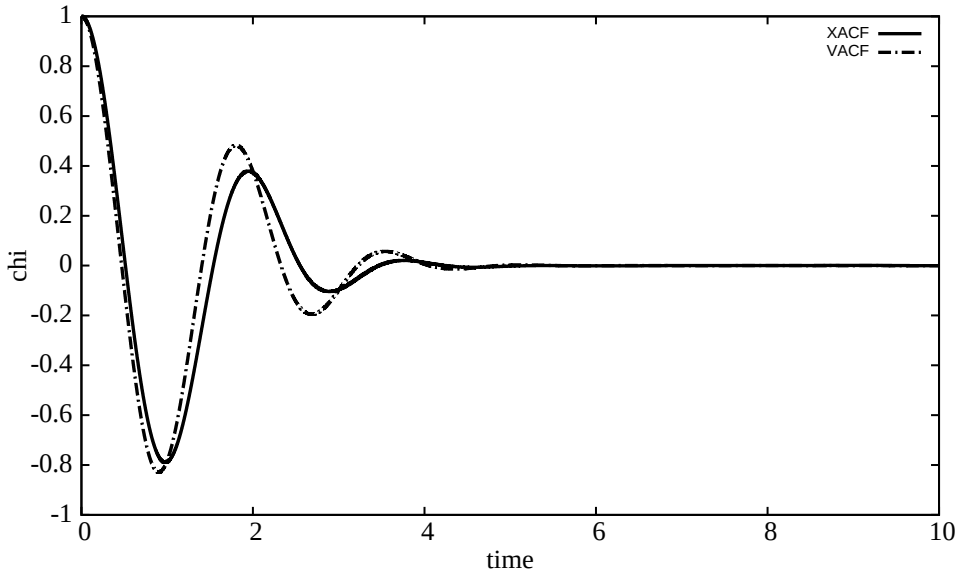

Figure 3.7: Autocorrelation functions at temperature=20 in the x^4 model

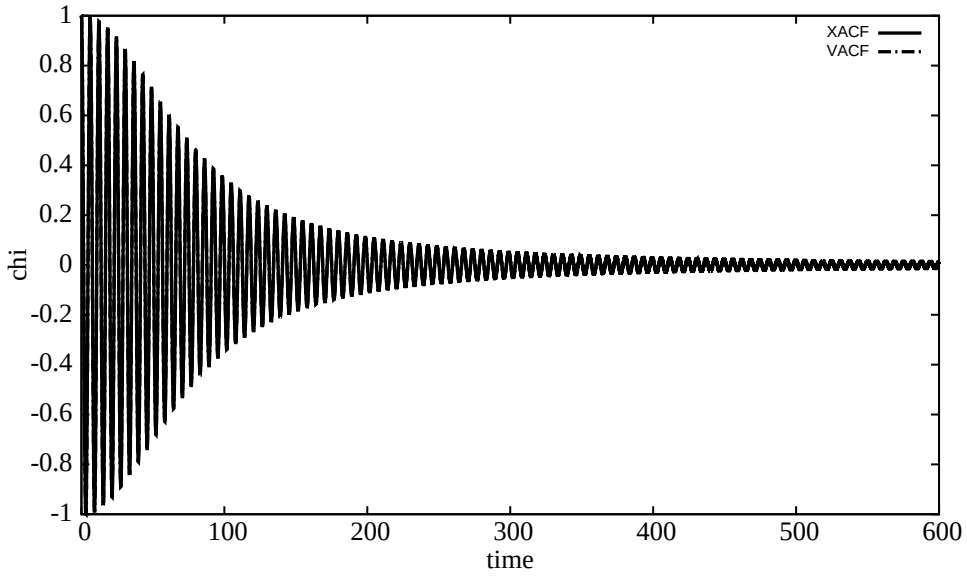

Figure 3.8: Autocorrelation functions at temperature=0.01 in the x^4 model

3.6.6 behavior of moments of VACF and XACF

The behavior of moments and γ_s of VACF and XACF have been illustrated in the following Tables (3.5, 3.6)

	low T	high T
μ_2	$1 + 6\ T$	$2.86793 T^{\frac{1}{2}} + 0.18542$
μ_4	$1 + 12\ T$	$18\ T - 2.86793 T^{\frac{1}{2}}$
μ_6	$1 + 18\ T$	$361.36\ T^{3/2} - 102.637\ T$
μ_8	$1 + 24\ T$	$12852\ T^2 - 3510.35\ T^{3/2}$

Table 3.5: Asymptotic behavior of moments of VACF in the x^4 model at extreme temperatures

	low T	high T
γ_4	$1 + 72\ T^2$	$2.18844 - 0.631661 T^{-\frac{1}{2}}$
γ_6	$1 + 648\ T^2$	$15.3191 - 7.32235 T^{-\frac{1}{2}}$
γ_8	$1 + 5616\ T^2$	$189.974 - 101.018 T^{-\frac{1}{2}}$

Table 3.6: Asymptotic behavior of γ_s of VACF in the x^4 model at extreme temperatures

Tables (3.7, 3.8) show the behavior of moments and γ_s of XACF

	low T	high T
μ_2	$1 + 6\ T$	$2.092099 T^{\frac{1}{2}} + 0.59422$
μ_4	$1 + 12\ T$	$6\ T - 2.092099 T^{\frac{1}{2}}$
μ_6	$1 + 18\ T$	$37.657786\ T^{3/2} - 4.695957\ T$
μ_8	$1 + 24\ T$	$756\ T^2$

Table 3.7: Asymptotic behavior of moments of XACF in the x^4 model at extreme temperatures

	low T	high T
γ_4	$1 + 24\ T^2$	$1.37084 - 0.300732 T^{-\frac{1}{2}}$
γ_6	$1 + 120\ T^2$	$4.11252 - 2.99141 T^{-\frac{1}{2}}$
γ_8	$1 + 720\ T^2$	$39.4632 - 44.835 T^{-\frac{1}{2}}$

Table 3.8: Asymptotic behavior of γ_s of XACF in the x^4 model at extreme temperatures

3.6.7 Fourth moment approximation

After lifetime (Eq:3.6) and low-order moments have been calculated at different temperatures, Figs 3.9 and 3.10 show the simple consistent relation between τ/τ_2 and γ_4 through the full range of temperatures.

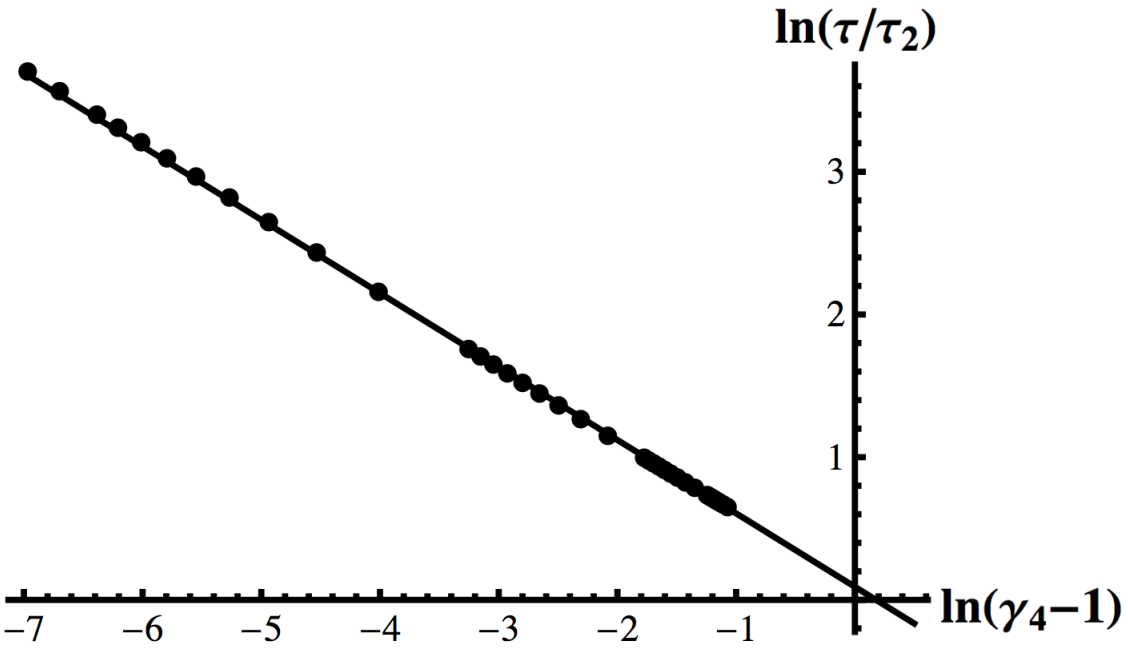

Figure 3.9: The ratio τ/τ_2 vs. γ_4 of XACF in the x^4 model

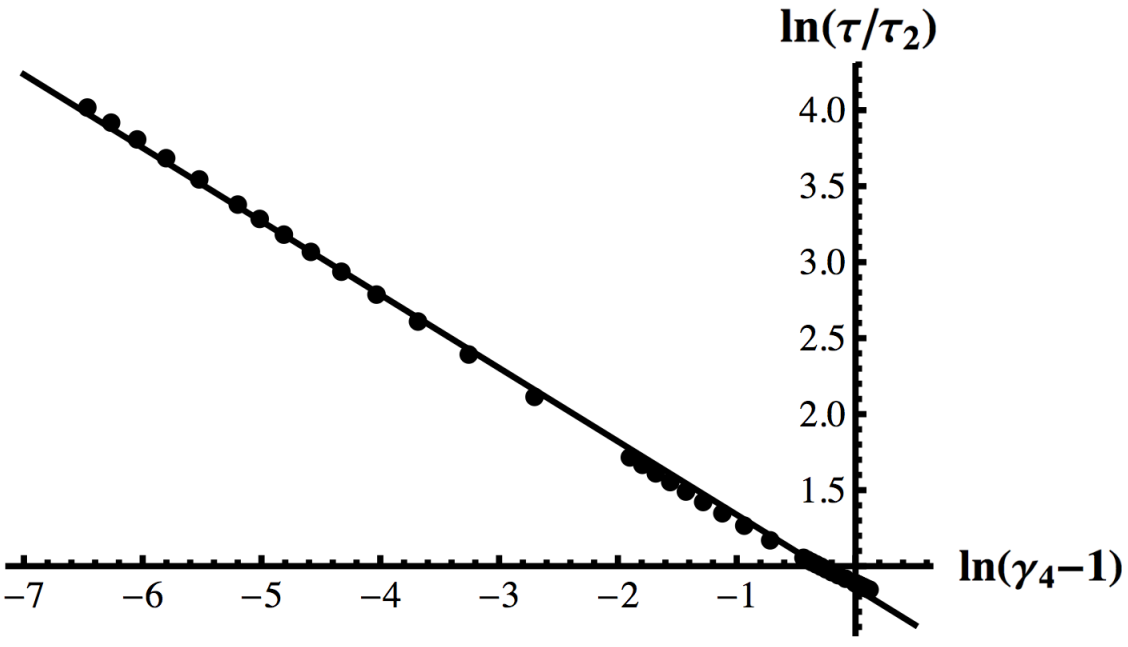

Figure 3.10: The ratio τ/τ_2 vs. γ_4 of VACF in the x^4 model

Both Figs 3.9 and 3.10 are captured well by:

$$\tau/\tau_2 = c/\sqrt{\gamma_4 - 1} \tag{3.13}$$

(c is a constant)

In Sen's paper [37], an analytic form was developed for the x^4 model at low temperature (high β):

$$\chi(t) = \frac{\beta^2 \cos(t) - \gamma\beta t \sin(t)}{\gamma^2 t^2 + \beta^2},\ \gamma = \frac{3}{4}\lambda \tag{3.14}$$

Our numerical work on x^4 model has been compared with this analytic result , which shows good consistency (Figure: 3.11).

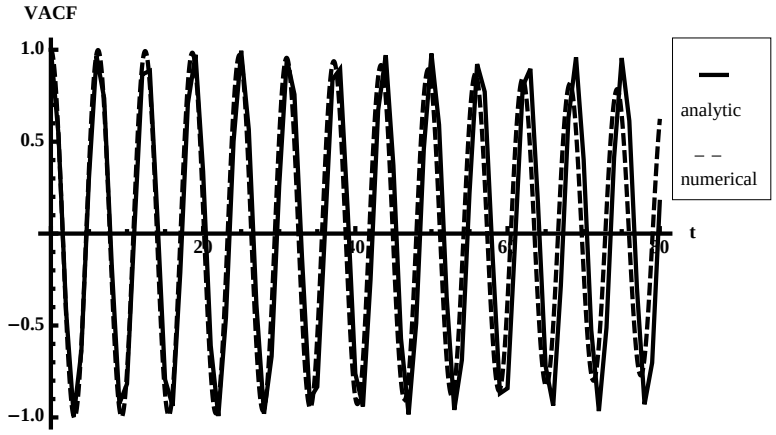

Figure 3.11: VACF at T=0.005 from analytical and numerical results

To verify the correctness of the lifetime, data collapse has been applied by plotting χ vs. t/τ in Figs (3.12, 3.13). Autocorrelation function at different temperatures are contained by the same envelope with different frequencies of oscillation.

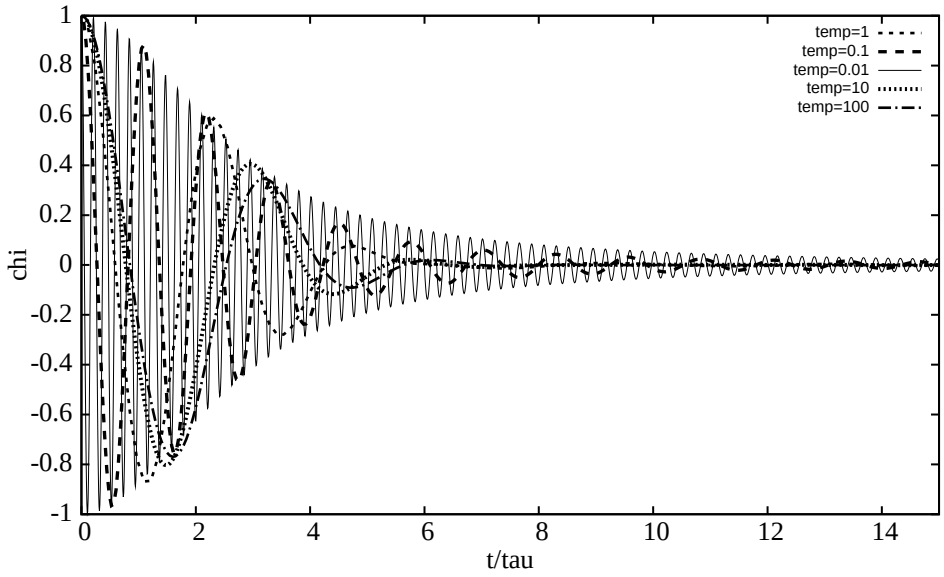

Figure 3.12: Data collapse of XACF in the x^4 model

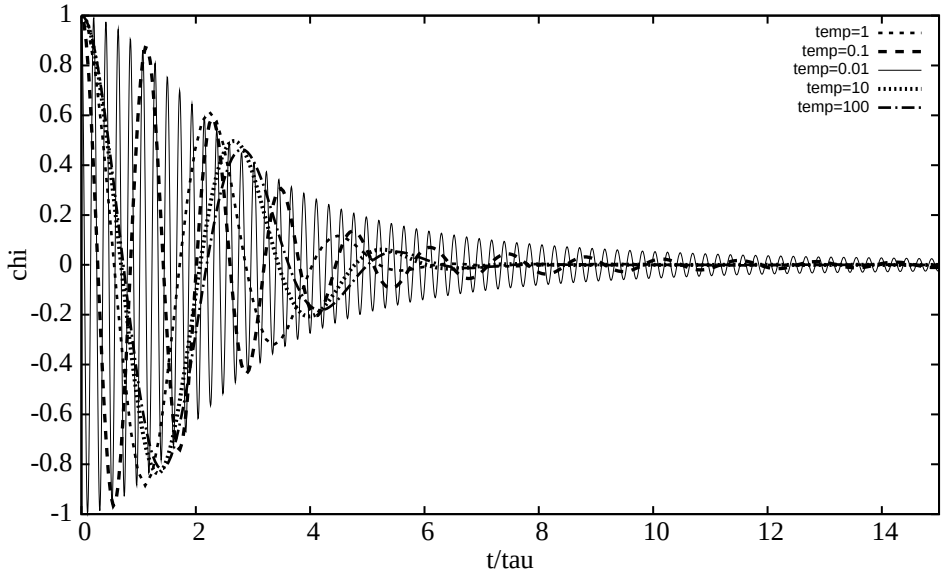

Figure 3.13: Data collapse of VACF in the x^4 model

Figures 3.9 and 3.10 show a simple relation between τ, τ_2 and γ_4. One explanation of that is from the perspective of density of states. Figures (3.14) shows that as temperature changes, the structure of the DOS changes, but it is always in a very simple form and can be well described by its width and the location of its peak. Thus the lifetime τ can be approximated by the first two

non-vanishing moments.

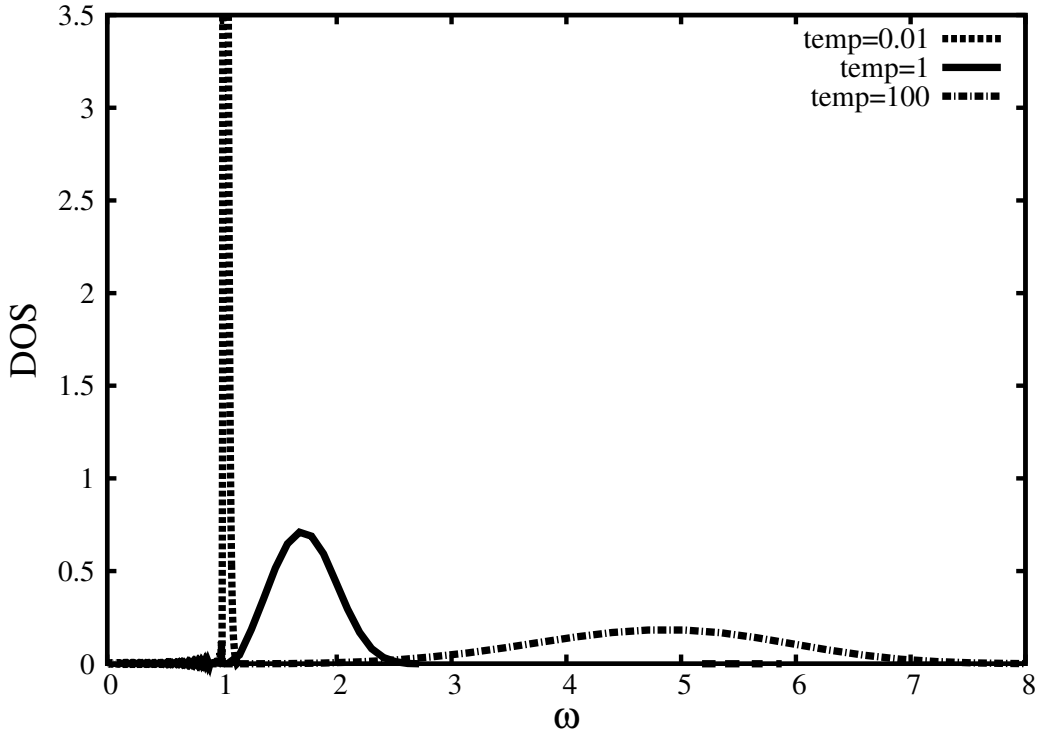

Figure 3.14: Density of states at various temperatures for the x^4 model.

3.7 The X^2Y^2 model

This section is organized as follows:

- Dimensional analysis(DA) of the x^2y^2 model
- Calculation of specific heat
- Calculation of moments and mode lifetimes of the chosen dynamic variables: displacement and velocity
- Density of States

3.7.1 Dimensional Analysis(DA)

The x^2y^2 model has the following hamiltonian :

$$H = \frac{1}{2}(\frac{p^2}{m_1} + \frac{q^2}{m_2} + k(x^2 + y^2) + \lambda x^2 y^2)$$

where M, K, λ are taken as basis out of all variables:M, K, β and λ Following is the DA:

$$\begin{aligned} [m_1] = M, [\lambda] = ML^{-2}T^{-2}, \\ [\beta] = T^2 m^{-1} L^{-2}, [k] = MT^{-2} \\ [\mu_2] = [(u_0, L^2 u_0)] = T^{-2} \end{aligned} \tag{3.15}$$

According to DA, one can set the following equations:

$$\begin{aligned} [\mu_2] * [\lambda]^a * [m_1]^b * [k]^c = M^0 L^0 T^0 \\ [\beta] * [\lambda]^{a1} * [m_1]^{b1} * [k]^{c1} = M^0 L^0 T^0 \\ [m_2] * [\lambda]^{a2} * [m_1]^{b2} * [k]^{c2} = M^0 L^0 T^0 \end{aligned} \tag{3.16}$$

so that $\frac{m\mu_2}{k}$, $\frac{\lambda}{\beta k^2}$ and $\frac{m_2}{m_1}$ are dimensionless, and by the Buckingham Pi Theorem:

$$\mu_2 = \frac{k}{m}\phi(\frac{\lambda}{\beta k^2}, \frac{m_2}{m_1}) \tag{3.17}$$

Similarily, since $[\tau] = T$, we have the following equation:

$$\tau = \sqrt{\frac{m}{k}}\psi(\frac{\lambda}{\beta k^2}, \frac{m_2}{m_1}) \tag{3.18}$$

Thus the model can be written in the reduced-parameter form to simplify calculations:

$$H = \frac{1}{2}(p^2 + \frac{q^2}{m} + x^2 + y^2 + \lambda x^2 y^2) \tag{3.19}$$

3.7.2 Heat Capacity

The value of the specific heat of the x^2y^2 model is between 2 and 1.5,

Here is the behavior of heat capacity C of the x^2y^2 model at low and high temperature T

	low T	high T
C	$2 - T + 6T^2 - 50T^3$	$1.5 + \frac{1}{\ln(T)}$

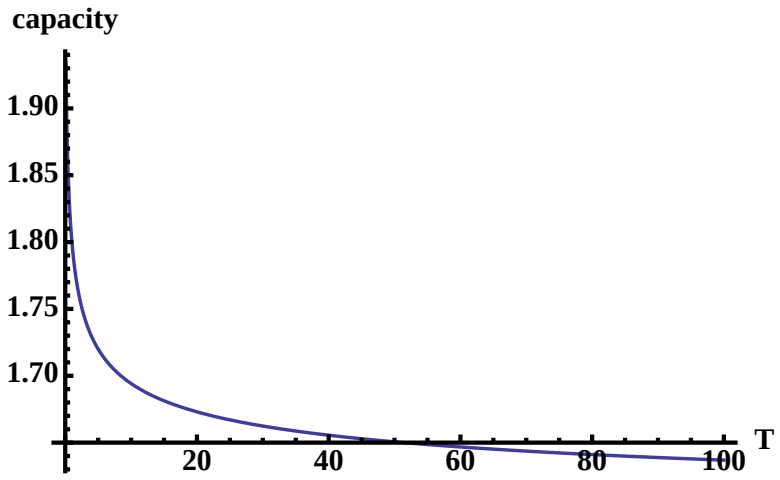

Figure 3.15: Heat capacity vs T

3.7.3 Low order moments of VACF

The moments of both the VACF and XACF have been calculated at all different temperatures, and following are the value of moments at extreme temperatures

Table 3.9 shows the behavior of μ_s of velocity at low and high temperatures

	low T	high T
μ_2	$1 + T - T^2 + 4T^3$	$0.5 + \frac{2.T}{\ln(T)}$
μ_4	$1 + 2T + \left(1 + \frac{4}{M}\right) T^2$	$\frac{4T^2}{\ln(T)} + \frac{4}{M} T$
μ_6	$1 + 3T + \frac{2\left(8+16M+3M^2\right)}{M^2} T^2$	$\frac{16\ T^3}{\ln(T)} + \frac{2\left(16.+32.M+3.M^2\right)T^2}{M^2 \ln(T)}$

Table 3.9: Asymptotic behavior of moments of vacf in the x^2y^2 model at extreme temperatures

Table 3.10 shows the behavior of γ_s of velocity at both high and low temperatures:

	low T	high T
γ_4	$1+\frac{2(2+M)T^2}{M}$	$\ln(T)+1.50223$
γ_6	$1+\frac{2\left(8+16M+3M^2\right)}{M^2}T^2$	$2\ln^2(T)+6.0089\ln(T)$

Table 3.10: Asymptotic behavior of γ_s of vacf in the x^2y^2 model at extreme temperatures

γ_4 of x mode	monotonically decreasing	monotonically increasing
$M=1$		$T>0$
$M=2$		$T>0$
$M=10$		$T>0$

Table 3.11: Relation of γ_6 to γ_4 of for y-component of VACF of x^2y^2 model

γ_4 of y mode	monotonically decreasing	monotonically increasing
$M=1$		$T>0$
$M=2$		$T>0$
$M=10$	$T>9.5$	$0<T<9.5$

Table 3.12: Relation of γ_6 to γ_4 of for y-component of VACF of x^2y^2 model

Figures (3.16, 3.17) here are parametric plot of γ_6 VS. γ_4

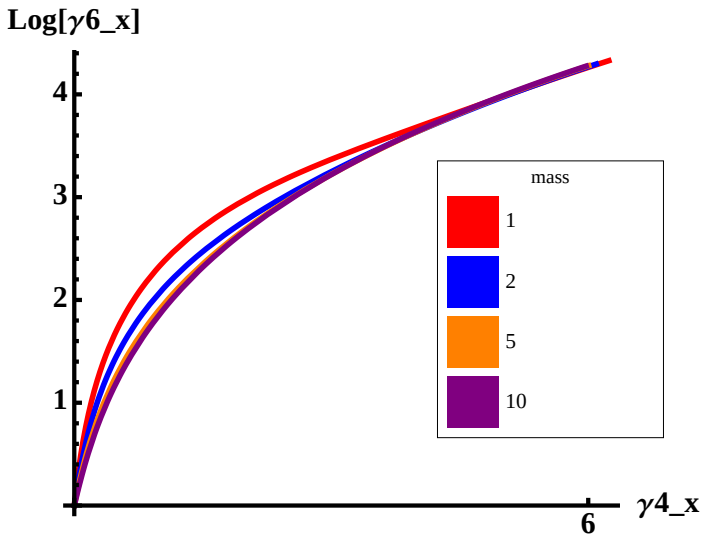

Figure 3.16: γ_6 vs γ_4 of x mode

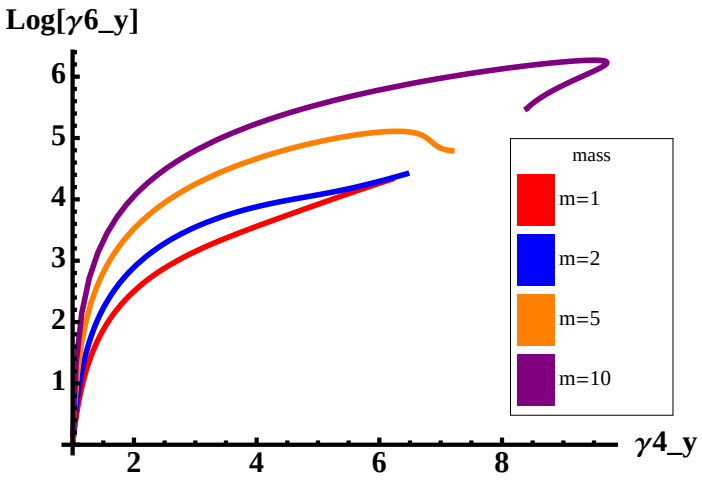

Figure 3.17: γ_6 vs γ_4 of y mode

3.7.4 lifetime of VACF and XACF

The numerical method mentioned in section 2, the VACF and XACF are shown in Figs (3.18, 3.19), and the lifetime is given by the equation (eq: 3.6).

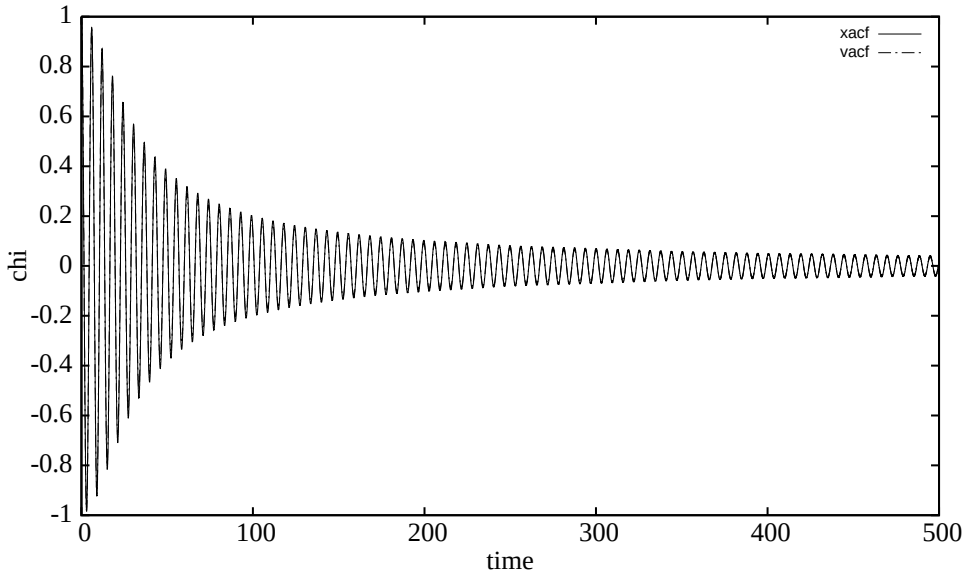

Figure 3.18: X mode autocorrelation functions at $m = 10$, temperature=2^{-3} in the x^2y^2 model

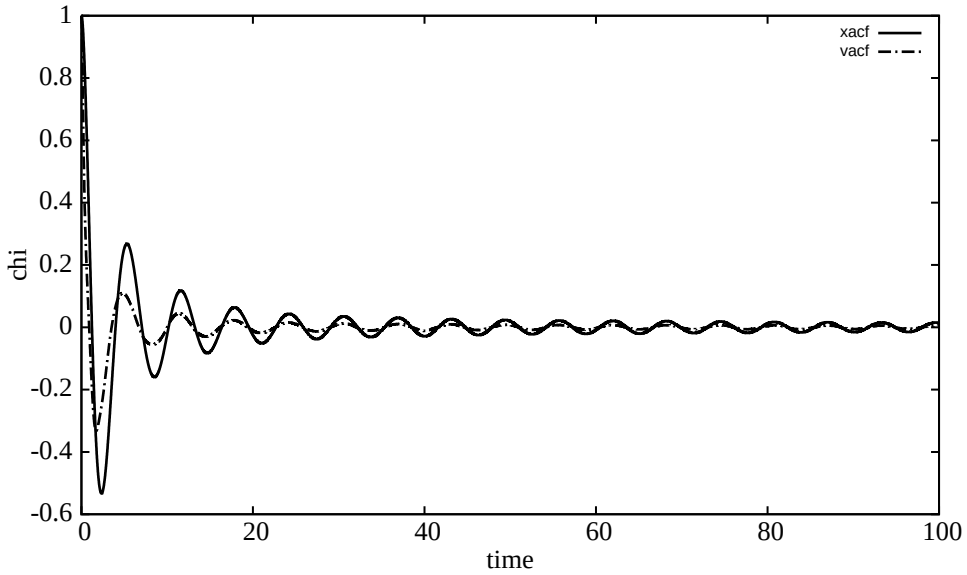

Figure 3.19: X mode autocorrelation functions at $m = 10$, temperature=2^6 in the x^2y^2 model

Again, after calculations at different temperatures have been done, Figures 3.20 and 3.20 show the consistent relation between τ/τ_2 and γ_4 at wide range of temperatures.

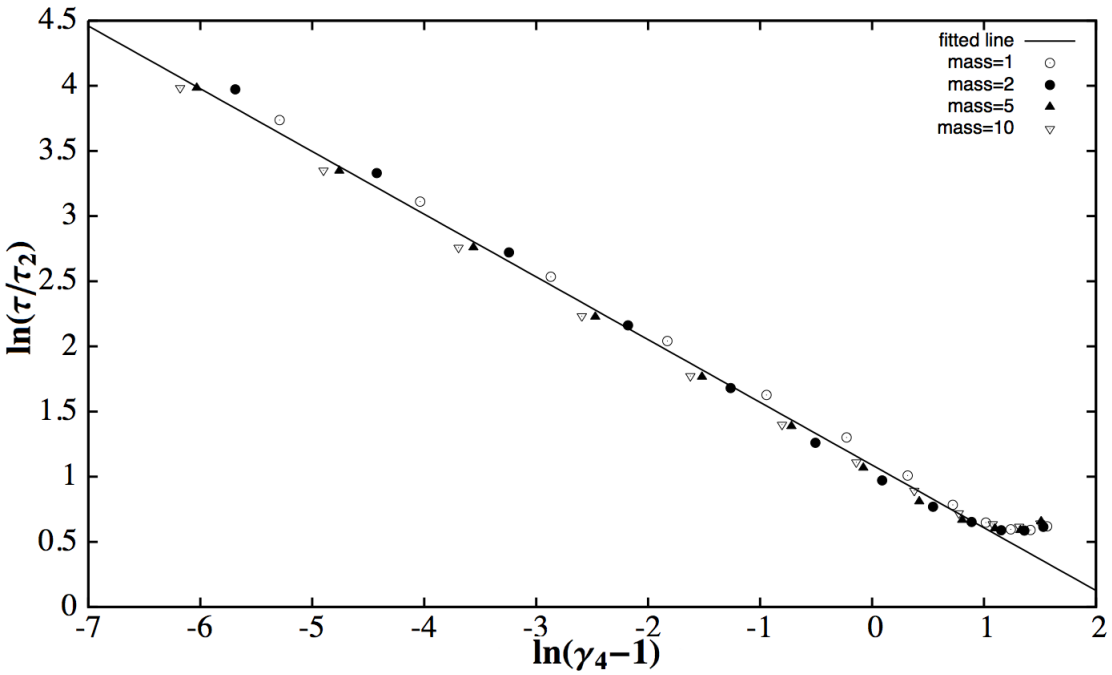

Figure 3.20: τ/τ_2 vs γ_4 of velocity of x mode in the x^2y^2 model

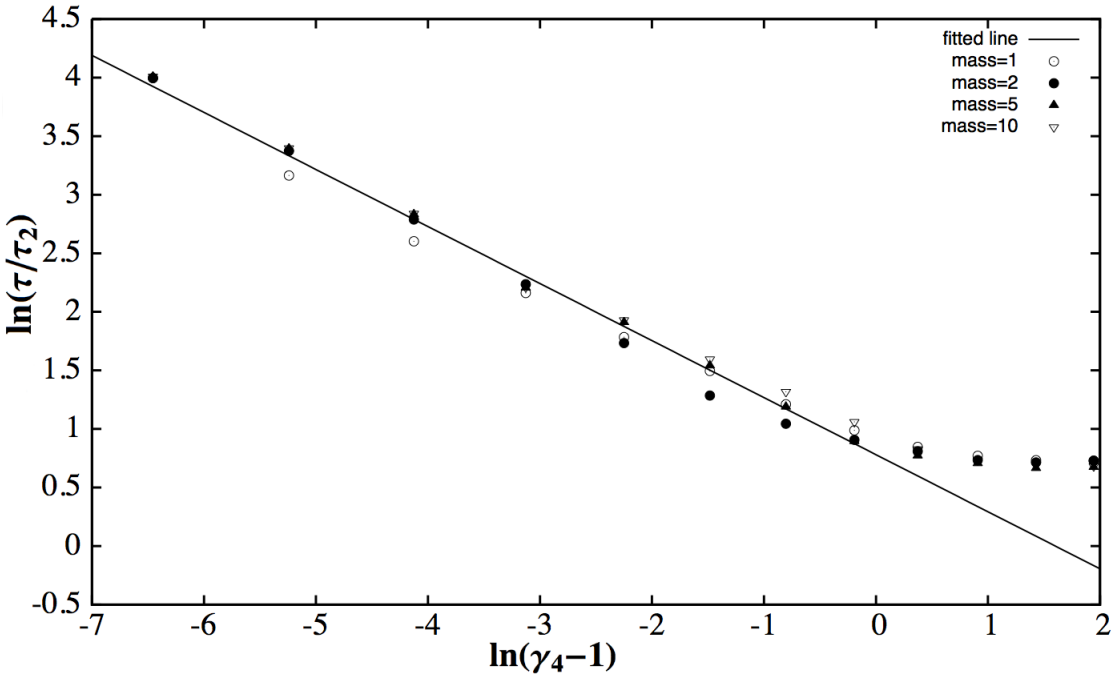

Figure 3.21: τ/τ_2 vs γ_4 of displacement of x mode in the x^2y^2 model

In Fig (3.22) the data collapse shows the university of the decay envelope.

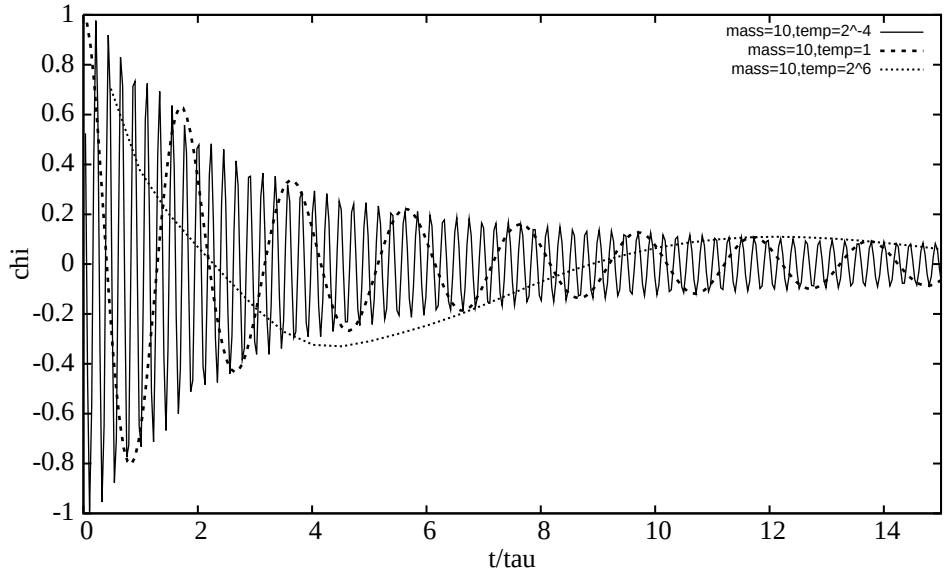

Figure 3.22: χ vs t/τ of VACF in x mode in the x^2y^2 model

In the x^2y^2 model, there is more than one parameters that mode lifetime depends on:

temperature and the mass ratio. Figure (3.23) shows the DOS in terms of temperature and mass ratio. It is shown that DOS in x^2y^2 is still can be described by two parameters: the height and width of the single peak.

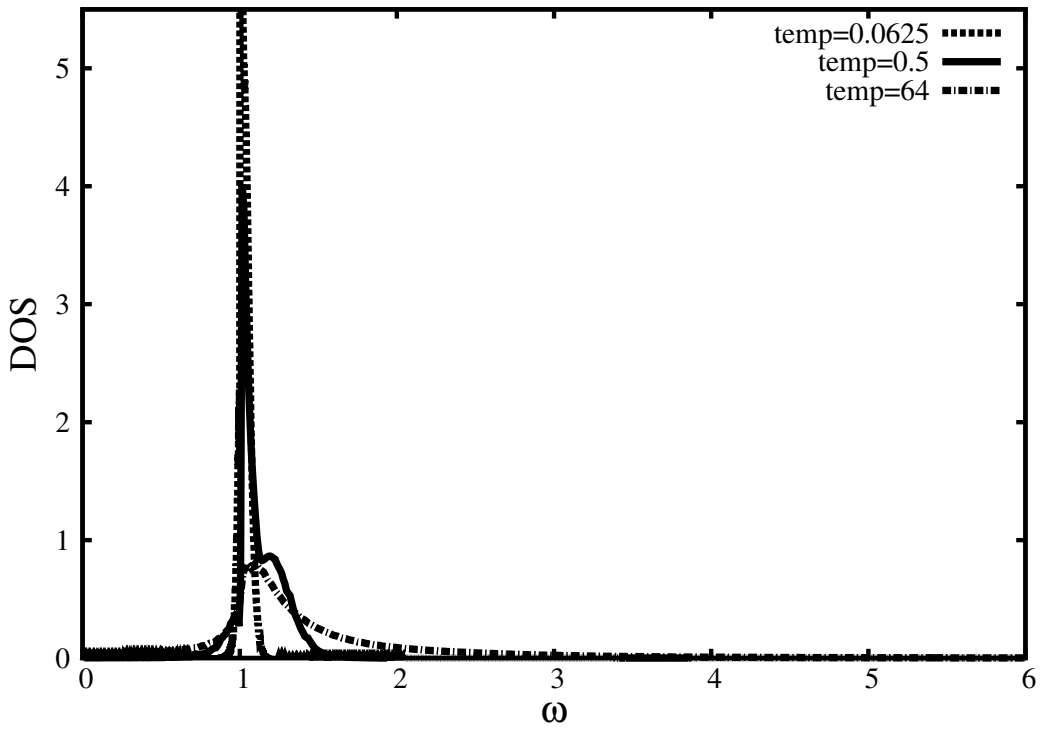

Figure 3.23: Density of states of the y-mode at $M = 1$ for the x^2y^2 model

Conclusion: At low T, the low moments for both x^4 and x^2y^2 models behave similarly, in that $\mu_2 \approx 1 + aT$ and $\mu_4 \approx 1 + 2aT$ so that γ_4 approaches 1 as T^2. Thus τ_2 is approaches a constant while $\gamma_4 - 1$ goes to zero, and the lifetime diverges like $\tau \approx T^{-1}$ at low temperature. The temperature dependence at low T is dominated by the approach of γ_4 to 1. At high temperature, the moments for the x^4 model go as $\mu_2 \approx aT^{1/2} + b$ and $\mu_4 \approx cT - dT^{1/2}$. So γ_4 saturates to a constant as $T^{-1/2}$, leaving only the variation in τ_2 to account for the change in lifetime. Thus the lifetime at high T, is governed by the behavior of τ_2 and $\tau \approx T^{-1/4}$. For the x^2y^2 model, by contrast, at high temperature, the moments go as $\mu_2 \approx 2T/\log T + 1/2$ and $\mu_4 \approx 4T^2/\log T + 4T/M$ which makes γ_4 go as $\log T$. This cancels a $\log T$ dependence in τ_2 leaving $\tau \approx T^{-1/2}$. Comparing with the result from the x^4 model, the relation between the lifetime τ, τ_2 and γ_4 is more complex in the x^2y^2 model (DOS from the x^2y^2 model shows more structure than that from the x^4 model), but overall both

models seem to be well-described by the simple combination of the first two moments.

3.8 Cubic model

This section is organized as follows:

- Dimensional analysis(DA) of the cubic model
- Anharmonic behavior of the cubic model
- Calculation of specific heat
- Calculation of moments and mode lifetimes of the chosen dynamic variables: displacement and velocity
- Density of States

3.8.1 Dimensional Analysis

This cubic model has the following hamiltonian :

$$H = \frac{1}{2}(\frac{p^2}{m} + \frac{q^2}{m} + k(x^2+y^2)) + \frac{\lambda}{4}(x^2+y^2)^2 + \frac{\lambda_1}{3}(x^3 - 3xy^2)$$

where m, k, λ_1 , are taken as basis out of all variables:m, k, β, λ and λ_1.

Following is the DA:

$$\begin{aligned} [m] = M, [\lambda] = ML^{-2}T^{-2} \\ [\beta] = T^2 m^{-1} L^{-2}, [k] = MT^{-2} \\ [\mu_2] = [(u_0, L^2 u_0)] = T^{-2} \\ [\lambda_1] = ML^{-1}T^{-2} \end{aligned} \tag{3.20}$$

using DA, one can set the following equations:

$$\begin{aligned} [\mu_2] * [\lambda_1]^a * [m]^b * [k]^c = M^0 L^0 T^0 \\ [\lambda] * [\lambda_1]^{a1} * [m]^{b1} * [k]^{c1} = M^0 L^0 T^0 \\ [\beta] * [\lambda_1]^{a2} * [m]^{b2} * [k]^{c2} = M^0 L^0 T^0 \end{aligned} \tag{3.21}$$

by Buckingham Pi Theorem:

$$\mu_2 = \frac{k}{m}\phi(\frac{\lambda k}{\lambda_1^2}, \frac{\beta k^3}{\lambda_1^2}) \tag{3.22}$$

Similarily, since $[\tau] = T$, we have the following equation:

$$\tau = \sqrt{\frac{m}{k}}\psi(\frac{\lambda k}{\lambda_1^2}, \frac{\beta k^3}{\lambda_1^2}) \tag{3.23}$$

Thus the Hamiltonian of the cubic model can be written in the reduced-parameter form:

$$H = \frac{1}{2}(p^2 + q^2 + k(x^2 + y^2)) + \frac{\lambda}{4}(x^2 + y^2)^2 + \frac{1}{3}(x^3 - 3xy^2) \tag{3.24}$$

3.8.2 Anharmonicity

Unlike the x^4 and x^2y^2 model, the value of the coefficient λ of the quartic term has the effect on the character of the anharmonic potential. Because of the complexity, this model is worth studying to test our method. The cubic model is studied at different values of λ such that one can describe all different anharmonic behavior of the system at potential with different character.

- $\lambda \in (0, \frac{2}{9})$ (Fig: 3.24): three equal off-center minima and one metastable minimum at center

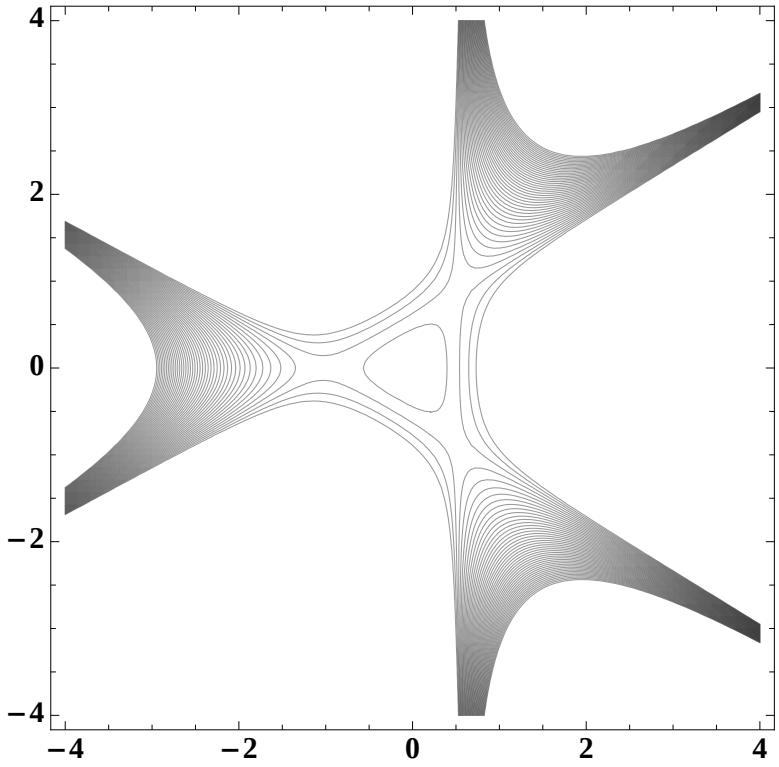

Figure 3.24: Cubic potential at $\lambda = 0.01$

- $\lambda = \frac{2}{9}$ (Fig: 3.25): four equal off-center minima at the center and corners of an equilateral triangle

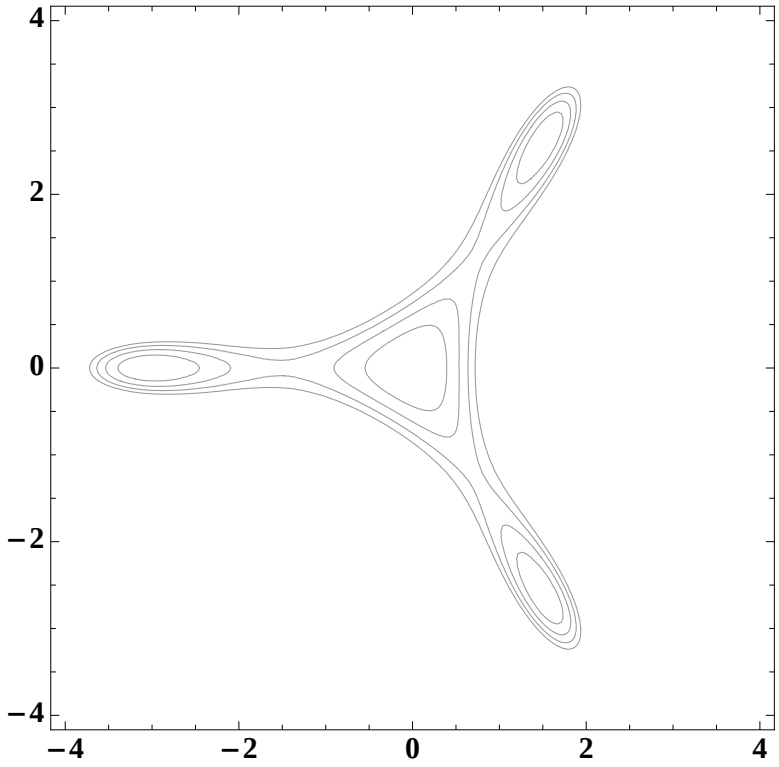

Figure 3.25: Cubic potential at $\lambda = 2/9$

- $\lambda \in (\frac{2}{9}, \frac{1}{4})$ (Fig: 3.26): one global minimum at the center and three metastable minima at corners of an equilateral triangle

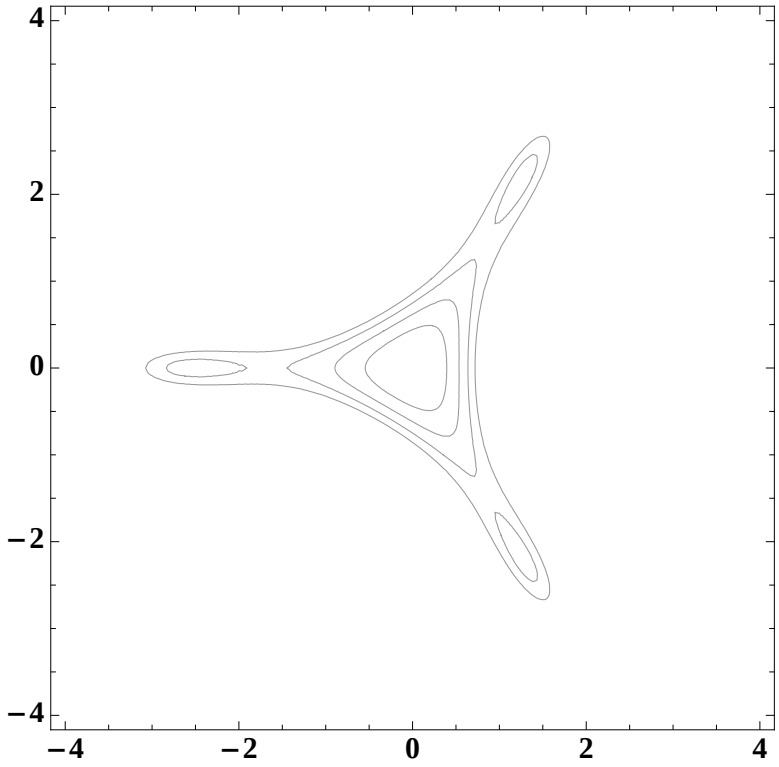

Figure 3.26: Cubic potential at $\lambda = 0.24$

- $\lambda \in (\frac{1}{4}, \infty)$ (Fig: 3.27): one global minimum at the center

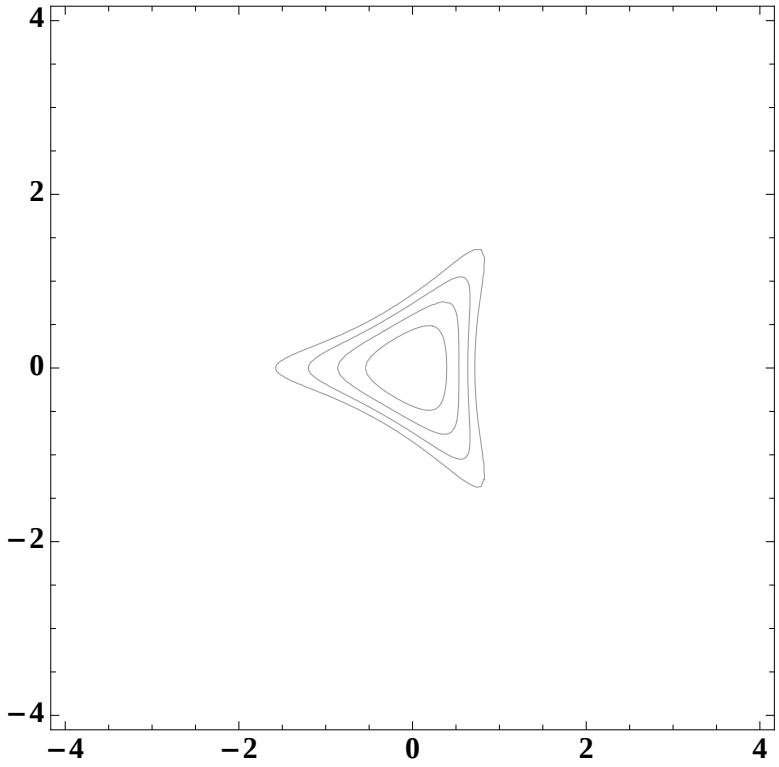

Figure 3.27: Cubic potential at $\lambda = 0.3$

3.8.3 Heat capacity

The anharmonic potential of the cubic model is composed by two parts: the quartic and the cubic part. Depends on the value of the λ, either part will dominate the nonlinear behavior of the system, for example: when λ is small ($\lambda < \frac{2}{9}$) the potential has three off-center minimum, and when $\lambda > \frac{1}{4}$, the potential has one minimum at center. Because of the complexity of the anharmonic potential, the heat capacity experiences a transition (Fig: 3.28) during the change of temperature (unlike the monotonic behavior of the heat capacity in the x^4 and x^2y^2 models), and the transition is defined where the thermal conductivity is at its maximum .

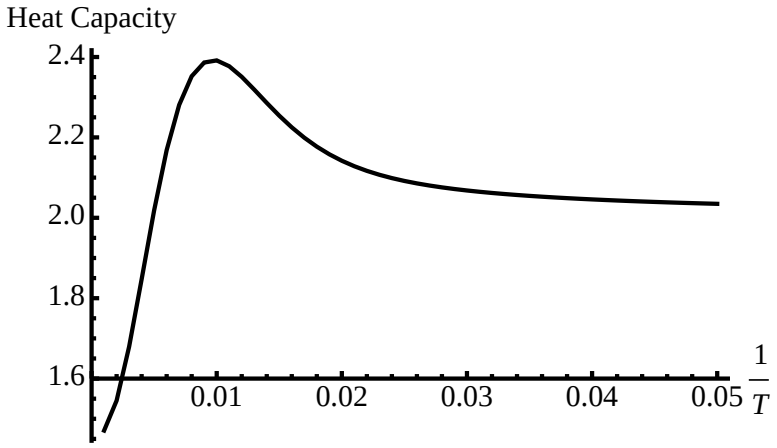

Figure 3.28: Heat capacity vs 1/T at $\lambda = 0.05$ in the cubic model

The behavior of the system on both sides of the transition point are significantly different, and the behavior of the system during the transition could be very complex. However it is possible that we can summarize the behavior of the system at two regions beyond the transition region. thus it is useful to list out the transition points (where heat capacity is maximum) at values of λ (Fig: 3.29).

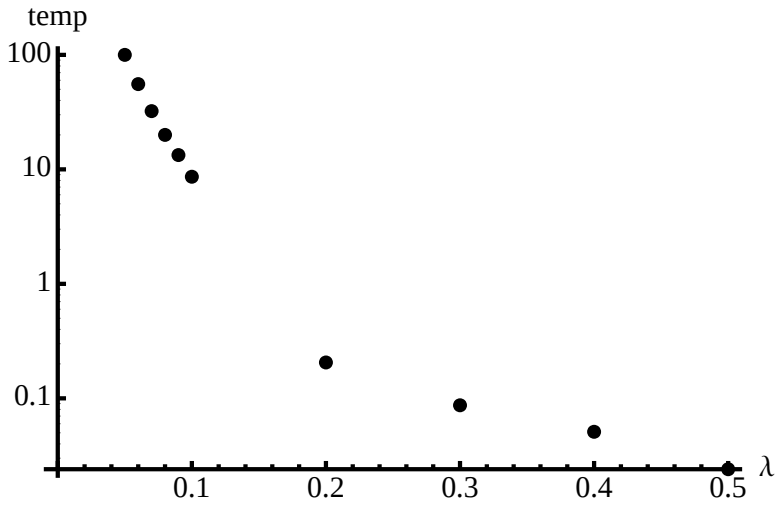

Figure 3.29: Transition points of the heat capacity in the cubic model

3.8.4 lifetime of VACF and XACF

The calculations and procedures that have been applied here are very similar to what has been done in the x^4 and x^2y^2 model:

- Step 1: Choose velocity v and displacement x as the dynamical variables to be investigated
- Step 2: Fix the value of $\lambda = 0.05$ (potential has 3 off-center global minima and one center local minimum), VACF and XACF have been calculated at different temperatures
- Step 3: Extract lifetime (Eq:3.6) from VACF and XACF, and calculate low order moments at corresponding temperature
- Step 4: Repeat Step 2 and 3 at value of $\lambda = 0.1$ (potential has 3 off-center global minima and 1 center local minimum)
- Step 5: Repeat Step 2 and 3 at value of $\lambda = 0.2$ (potential has 3 off-center global minima and 1 center local minimum)
- Step 6: Repeat Step 2 and 3 at value of $\lambda = 0.5$ (potential has 1 center global minimum)
- Step 7: Repeat Step 2 and 3 at value of $\lambda = 1.$ (potential has 1 center global minimum)
- step 8: Test the fourth moment approximation with plot τ/τ_2 vs γ_4
- analysis and reason from the perspective of DOS

Following are the examples of calculated autocorrelation functions Fig: 3.30 and 3.31

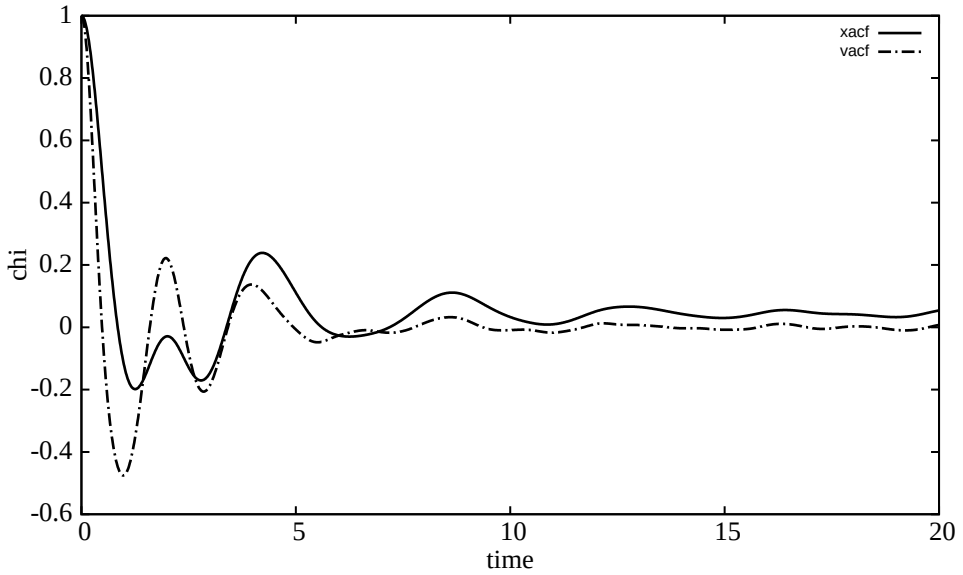

Figure 3.30: Autocorrelation functions of x mode at $\lambda = 0.1$ (potential with 3 global minima and one metastable minimum) and $T = 200$ in the cubic model

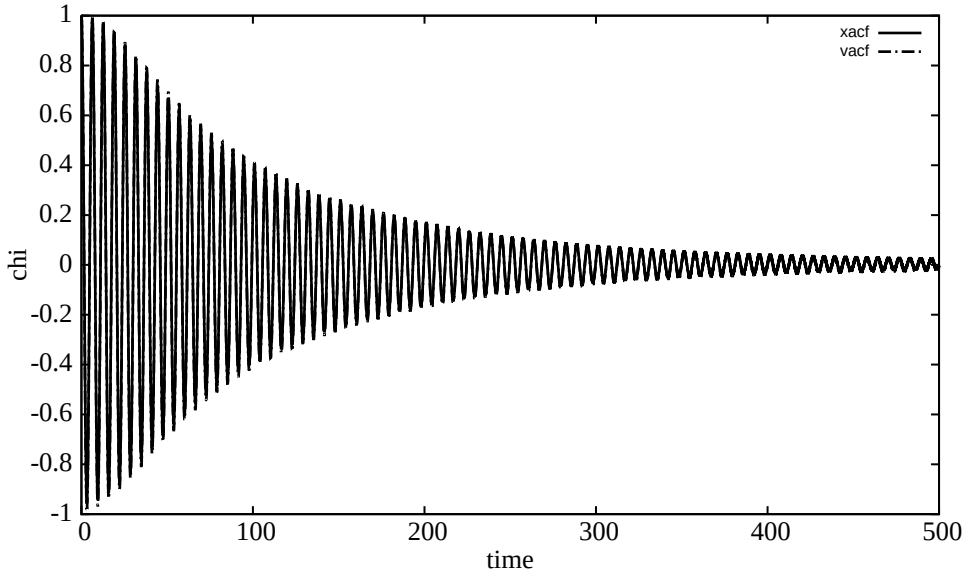

Figure 3.31: Autocorrelation functions of x mode at $\lambda = 0.1$ (potential with 3 global minima and one metastable minimum) and $T = 0.01$ in the cubic model

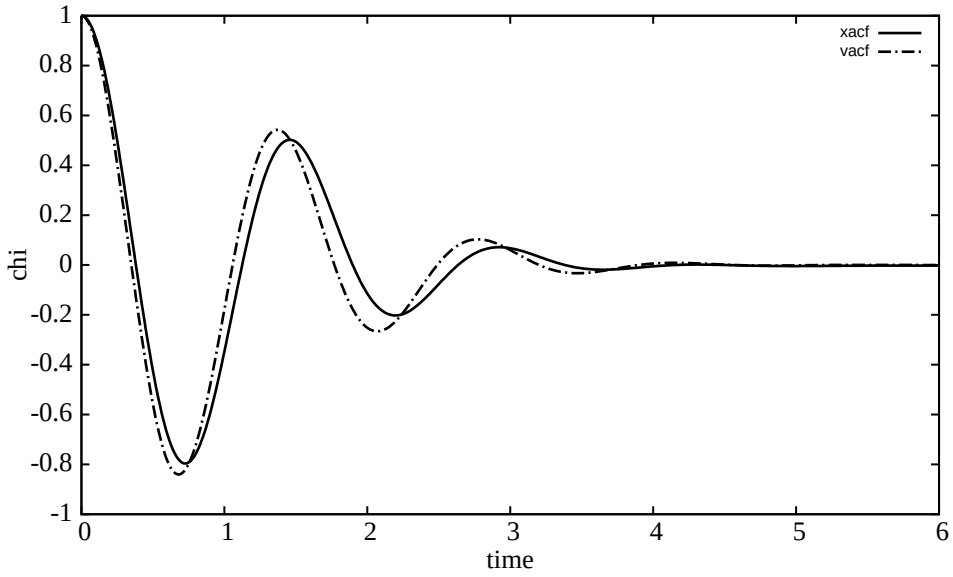

Figure 3.32: Autocorrelation functions of x mode at $\lambda = 1$ (potential with on minimum)and $T = 100$ in the cubic model

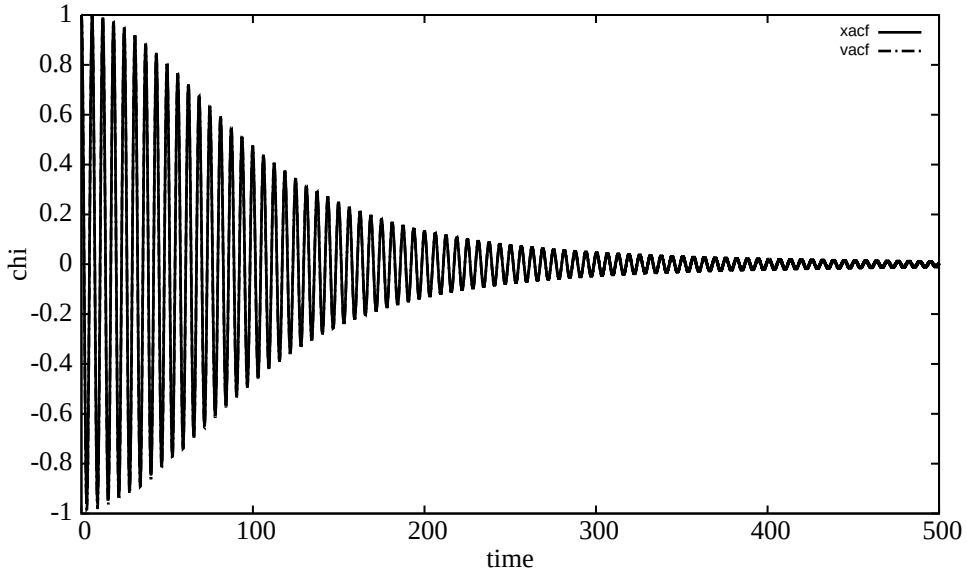

Figure 3.33: Autocorrelation functions of x mode at $\lambda = 1$ (potential with on minimum) and $T = 0.01$ in the cubic model

3.8.5 summary on plots on x mode of VACF

As what has been done in the x^4 and x^2y^2 model, lifetime and low order moments were calculated at different temperature, then plots of τ/τ_2 vs γ_4 at different values of λ were made (Fig: 3.34, 3.35, 3.36 and 3.37).

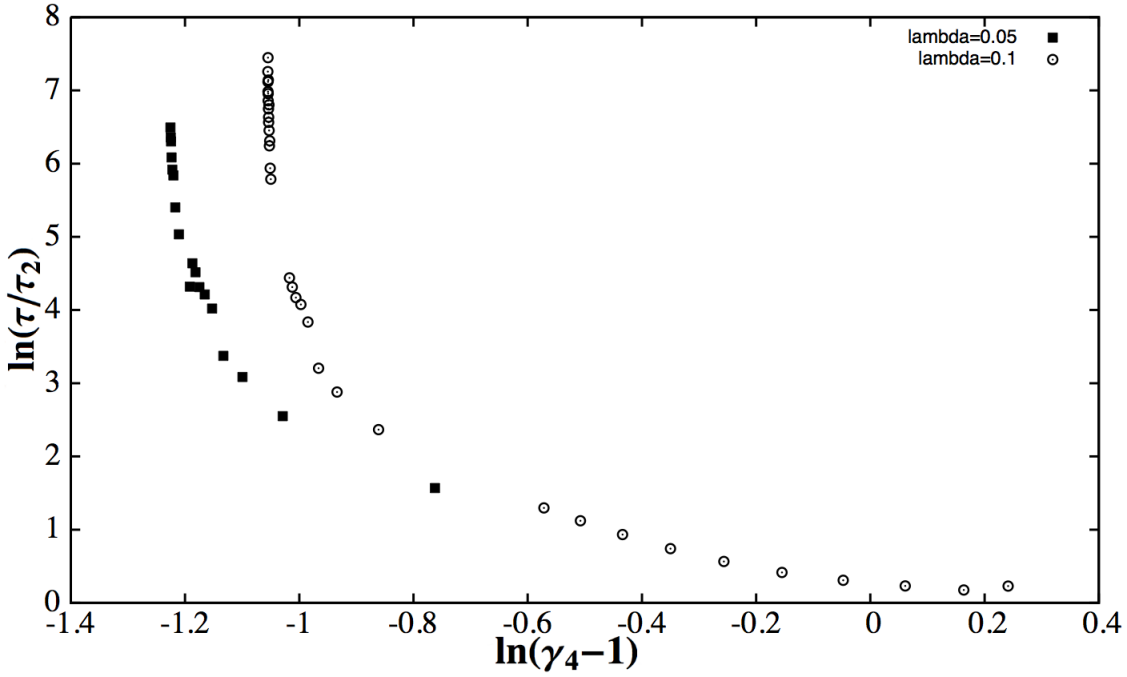

Figure 3.34: VACF of x mode at $\lambda = 0.1$ and $\lambda = 0.05$ in the cubic model

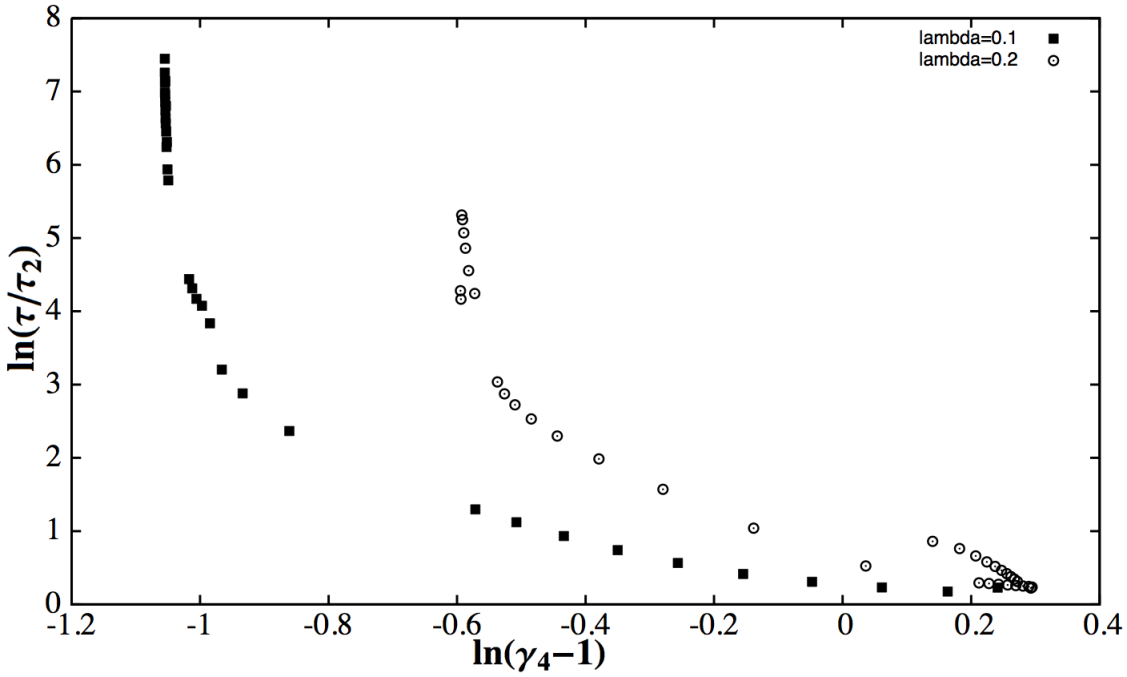

Figure 3.35: VACF of x mode at $\lambda = 0.1$ and $\lambda = 0.2$ in the cubic model

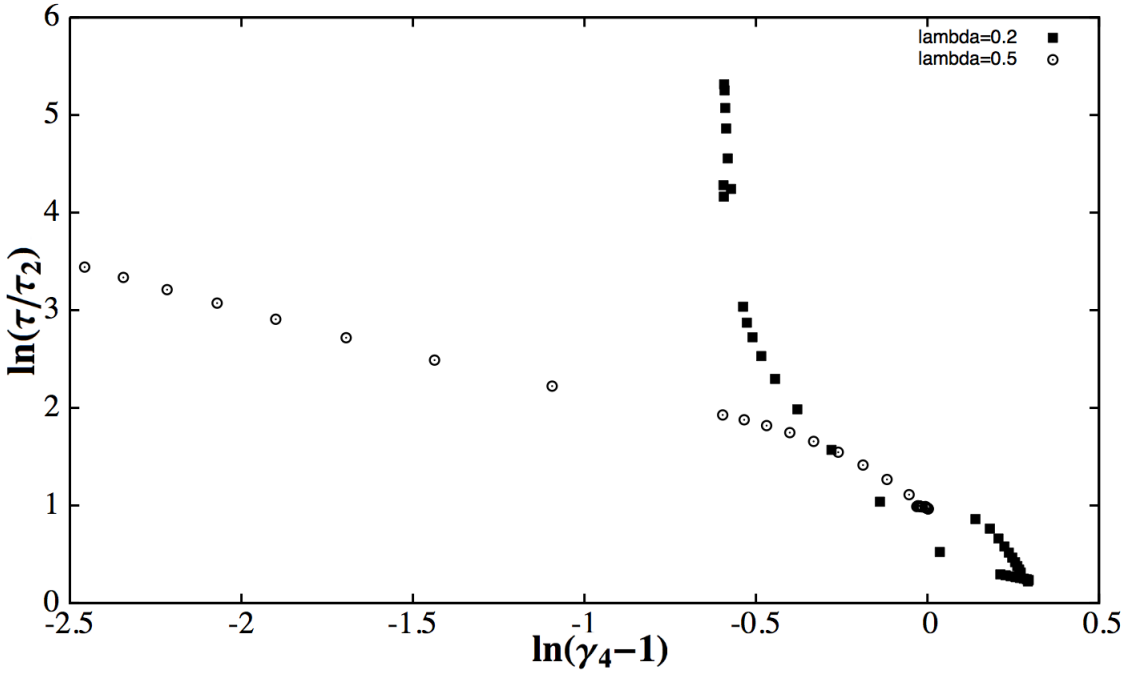

Figure 3.36: VACF of x mode at $\lambda = 0.2$ and $\lambda = 0.5$ in the cubic model

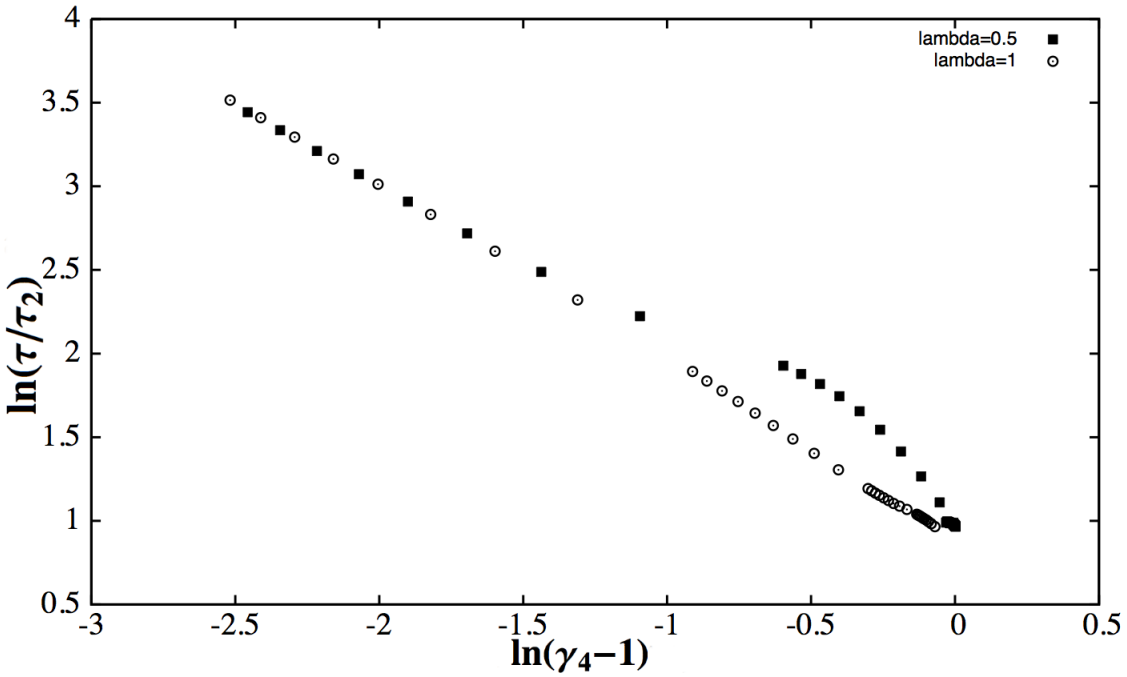

Figure 3.37: VACF of x mode at $\lambda = 0.5$ and $\lambda = 1$. in the cubic model

The following table can summarize the graphs above:

τ/τ_2 vs γ_4	high T	low T
$\lambda = 0.1$ and $\lambda = 0.05$	MAYBE consistent	NOT consistent
$\lambda = 0.1$ and $\lambda = 0.2$	consistent	NOT consistent
$\lambda = 0.2$ and $\lambda = 0.5$	consistent	NOT consistent
$\lambda = 0.5$ and $\lambda = 1$	NOT consistent	consistent

Clearly, there isn't one single trend line to represent the relation between τ/τ_2 and γ_4 which cover the range of the temperature that we have calculated(T$\in (0.01, 100)$), even after dividing the temperature into high and low T area with the transition points, and one trend line each area to represent the behavior of the system is difficult. It is possible that in the even lower and higher temperature beyond the range in which our calculations have been carried out, the behavior system might can be better represented by one trend line.

On the other hand, one explanation of the complexity of the system behavior can be illustrated from the density of the states. Here DOS of $\lambda = 0.2$(potential with 3 global minima) and

DOS of $\lambda = 1$ (potential with one minimum) have been presented.

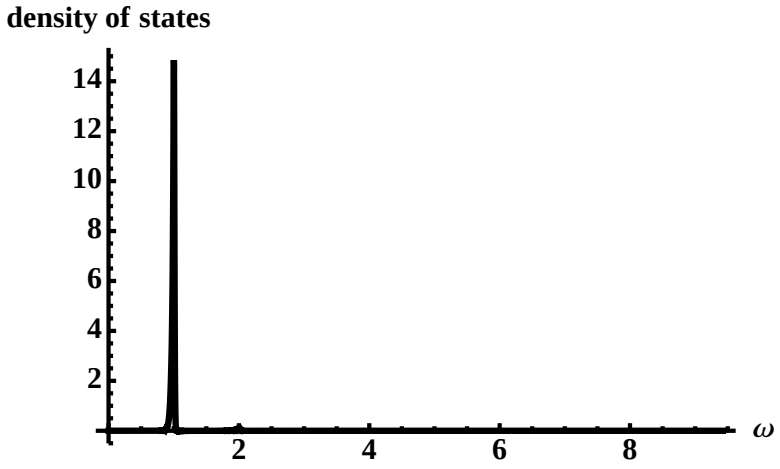

Figure 3.38: DOS in x mode of VACF at $\lambda = 0.2$ and $T = 0.0125$ in the cubic model

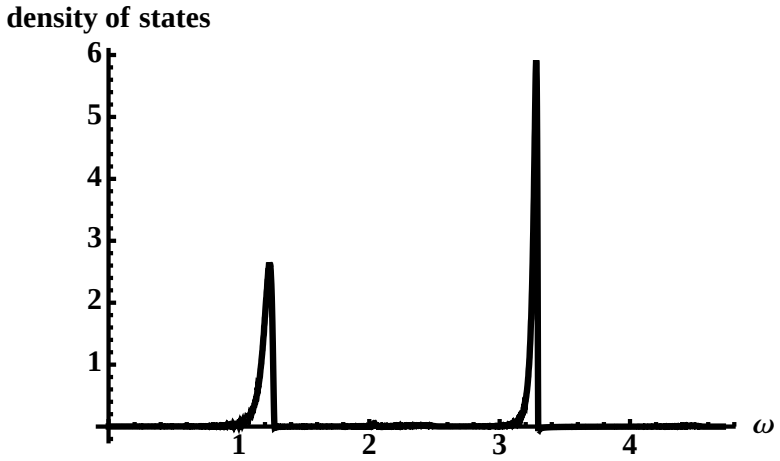

Figure 3.39: DOS in x mode of VACF at $\lambda = 0.2$ and $T = 0.1$ in the cubic model

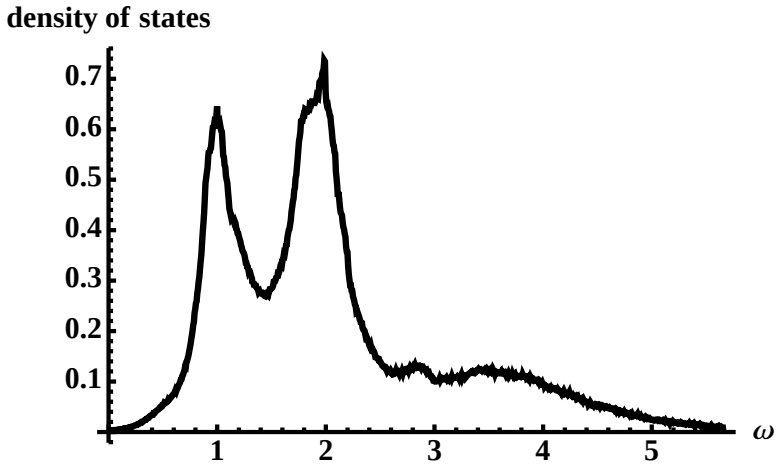

Figure 3.40: DOS in x mode of VACF at $\lambda = 0.2$ and $T = 10$ in the cubic model

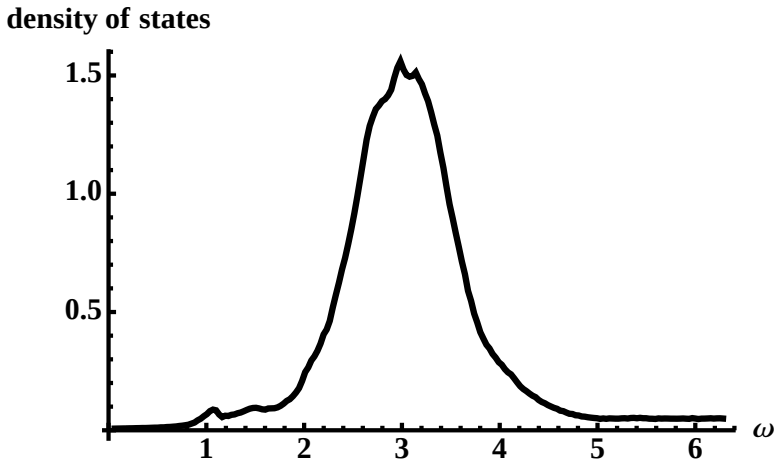

Figure 3.41: DOS in x mode of VACF at $\lambda = 0.2$ and $T = 100$ in the cubic model

At $\lambda = 0.2$ (potential has 3 global minima), DOS (Fig: 3.38, 3.39,3.40,3.41) of the cubic model is much more complicated than that in the x^4 and x^2y^2 model, two parameters (such as height and width) are no longer sufficed to describe DOS, and thus lifetime cannot be approximated with only first two moments (μ_2 and μ_4).

3.9 Analysis of all 3 models

From the previous results, we see that the behavior of the lifetime for the x^4 and x^2y^2 models over a wide range of parameters and temperature is captured in the behavior of the two lowest moments (μ_2 and μ_4) which can be calculated analytically. However, for the cubic model, the behavior is more complex, requiring at least higher moments in the description. We investigate here the reasons for success in one case and not in the other.

Fig. 3.12 shows the insight gained from checking for a data-collapse for $\chi(t)$, by scaling the time t by the lifetime τ for the x^4 model. The results illustrate that while the oscillations of auto-correlation functions vary with temperature, they are contained by one decaying envelope, which is what we are trying to capture.

As one might expect from the data-collapse, the DOS for the x^4 model is also simple, as shown in Fig 3.14 for various temperatures.

The DOS of this model is characterized by a single dominant peak that shifts and broadens with increasing temperature (as one would typically expect of a vibrational mode in an anharmonic solid). In such a case, the lifetime depends mostly on the shape of the DOS around the peak, and two parameters (peak value of the DOS and the width) are sufficient to describe it. At low temperatures, $\gamma_4 \to 1$, while at high temperatures $\gamma_4 \to 2.2$ (for this model). Recalling γ_4 as the (dimensionless) ratio μ_4/μ_2^2, it is aptly designated as a "shape parameter" of the DOS.

The DOS of the x^2y^2 model (Fig. 3.23) is only somewhat more complex than that of the x^4 model.

The simple evolution of the DOS with the temperature and other parameters for these models explains why a simple, generic relationship can exist between τ and the first two moments of the DOS. To explore this point further, let us consider a generic, single-mode DOS that is peaked at an oscillator frequency ω_0 and broadened to a width Ω. Both the oscillator frequency and width will depend on temperature. At low temperatures, $\Omega << \omega_0$, and from Eq. 4.7 we have

$$\tau \approx \Omega^{-1}$$

The leading behavior of the lowest two moments is

$$\mu_2 \approx \omega_0^2(1 + a\Omega^2/\omega_0^2)$$

$$\mu_4 \approx \omega_0^4(1 + b\Omega^2/\omega_0^2)$$

where a and b depend on the details of the DOS. Then

$$\tau/\tau_2 \approx \omega_0/\Omega$$

and

$$\gamma_4 - 1 \approx \Omega^2/\omega_0^2$$

Eliminating Ω and ω_0 among the two relations gives

$$\tau/\tau_2 \approx (\gamma_4 - 1)^{-1/2}$$

just as we found in Eq. 3.13. So long as the DOS has this simple, generic behavior, the same relationship obtained here should hold.

At high temperatures, if the DOS can be assumed to be a mostly featureless and broad distribution with width Ω and height Ω^{-1}, then $\tau \approx \Omega^{-1}$ and $\mu_2 \approx \Omega^2$ so $\tau_2 \approx \Omega^{-1}$. While the shape parameter saturates at some value ($\gamma_4 \approx c$), in which case the variation in τ is tracked by that of τ_2, so that

$$\tau \approx \tau_2$$

which is consistent with the high-T behavior reported by DD.

The DOS of cubic model (Fig. 3.42) is much more complicated than that of x^4 and x^2y^2 model, which explains why the simple 2-parameter scatterplots (Fig. 3.34, 3.35, 3.36, 3.37) do not capture the behavior.

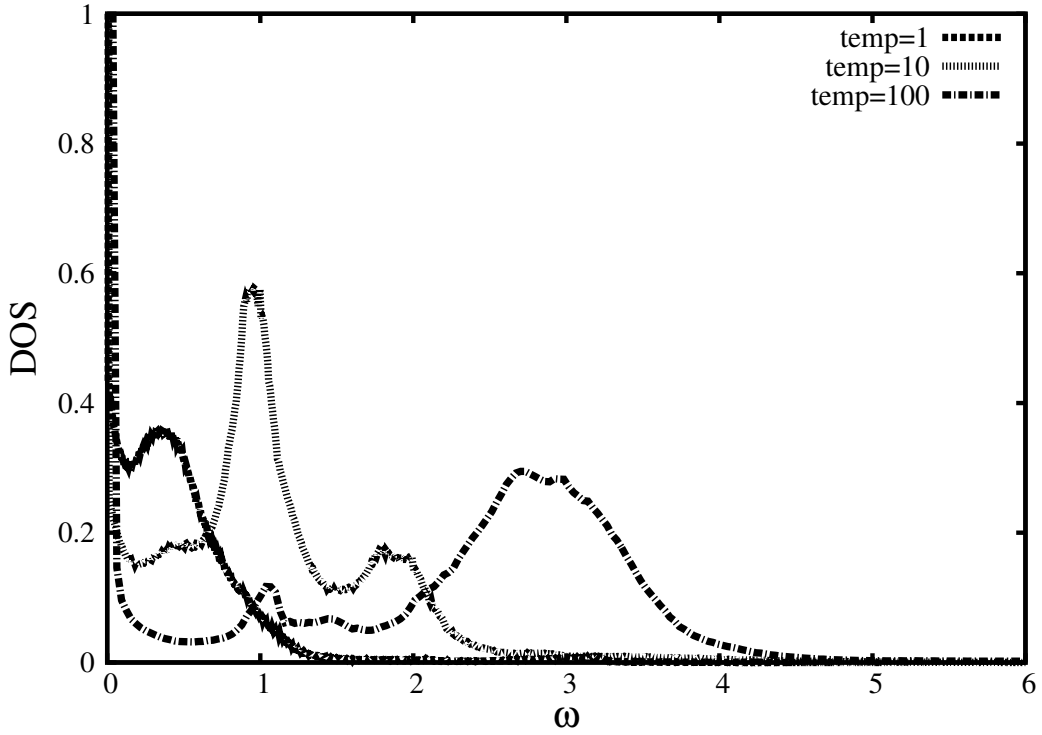

Figure 3.42: Density of states of the x-mode at $\lambda = 0.2$ and various temperatures for the cubic model.

Finally we note that γ_4, in addition to being a simple measure of the shape of the DOS, is also a direct measure of the degree of anharmonicity of the mode as averaged over the ensemble. Specifically, γ_4 is

$$\gamma_4 = \frac{\langle x^2 \rangle \langle f^2 \rangle}{\langle xf \rangle^2} \tag{3.25}$$

A harmonic system is, of course, defined where the force obeys $f + kx = 0$. In the anharmonic ensemble, we could define an effective k by that which minimizes the deviation from linear. That is, we construct the function

$$\alpha = \langle (f + kx)^2 \rangle / \langle f^2 \rangle \tag{3.26}$$

and minimize that with respect to k to determine the effective force constant. The minimum value of α then measures the degree of anharmonicity of the system as effective for the ensemble. For a harmonic system, $\alpha_{\min} = 0$. In general, $k_{\text{eff}} = -\langle xf \rangle / \langle x^2 \rangle = \mu_2$, from which the degree of

anharmonicity is

$$\alpha_{\min} = 1 - \gamma_4^{-1} \tag{3.27}$$

showing how the deviation $\gamma_4 - 1$ is directly related to the temperature-dependent anharmonicity of the system, which highlights again the significance of the observed trend in Eq.3.13.

3.10 Conclusions

We have investigated the proposed method using low-dimensional models and can conclude that in these simple low-dimensional systems, the mode lifetime in equilibrium might be approximated from the two lowest, non-vanishing moments of the Liouvillian. For the generic case of a DOS dominated by a single peak broadened and shifted, as is the case here for the x^4 and x^2y^2 models and for the non-linear lattice rmodel presented here, we see that the fourth moment approximation works well. In the case of the cubic model with two degrees of freedom, the fourth moment approximation is insufficient, which can be understood in terms of the more complex structure of the DOS. The multiple minima of the cubic model creates a more complex dynamics that cannot be captured with just two parameters.

Chapter 4

Fourth Moment Approximation in 1D chain and 3D Lattice[1]

4.1 Introduction

After analyzing the simple systems, we are trying to applying the same method to many body systems in different dimensions. We started with the 1D anharmonic chain (the simplest model in many body cases) to test our hypothesis: that the mode lifetime over full range of temperatures can be well approximated by first two moments as long as the Density of states(DOS) is a single peak.

This chapter has been organized as follows:

- We take a close look at the 1D and 3D models.
- Descriptions of the numerical test of our approximation method and the results have been presented.
- We make an attempt to improve the model by including the sixth moment in our approximation method.
- Estimation of mode lifetimes have been done for different 3D lattice model.
- Conclusion is drawn.

[1]Some of the text and figures have appeared in [35]

4.2 Chosen models

1D model:

$$\begin{aligned} H = \sum_{i=1}^{n} \frac{1}{2}p_i^2 + \frac{1}{2}(u_i - u_{i-1})^2 + \frac{1}{24}(u_i - u_{i-1})^4 \\ u_0 = u_n \text{ (periodic boundary condition)} \\ u_{n+1} = u_1 \end{aligned} \tag{4.1}$$

3D model:

$$\begin{aligned} H = \sum_{i=1}^{L}\sum_{i=j}^{L}\sum_{k=1}^{L}(\frac{1}{2}\vec{p}_{i,j,k}^{\,2} + \frac{1}{2}|\vec{u}_{i,j,k} - \vec{u}_{i-1,j,k}|^2 + \frac{1}{24}|\vec{u}_{i,j,k} - \vec{u}_{i-1,j,k}|^4 \\ + \frac{1}{2}|\vec{u}_{i,j,k} - \vec{u}_{i,j-1,k}|^2 + \frac{1}{24}|\vec{u}_{i,j,k} - \vec{u}_{i,j-1,k}|^4 \\ + \frac{1}{2}|\vec{u}_{i,j,k} - \vec{u}_{i,j,k-1}|^2 + \frac{1}{24}|\vec{u}_{i,j,k} - \vec{u}_{i,j,k-1}|^4) \end{aligned} \tag{4.2}$$

with periodic condition:

$$\begin{aligned} \vec{u}_{0,j,k} = \vec{u}_{L,j,k},\ \vec{u}_{i,0,k} = \vec{u}_{i,L,k} \text{ and } \vec{u}_{i,j,0} = \vec{u}_{i,j,L} \\ \vec{u}_{1,j,k} = \vec{u}_{L+1,j,k},\ \vec{u}_{i,1,k} = \vec{u}_{i,L+1,k} \text{ and } \vec{u}_{i,j,1} = \vec{u}_{i,j,L+1} \end{aligned} \tag{4.3}$$

4.3 Normal mode

We are investigating the lifetime of each normal mode, and all normal modes can be derived with normal mode transformation from the particle positions, and for 1D systems with L even particles:

$$q(n) = \frac{1}{L}\sum_{i=1}^{L} e^{-ik\cdot r}u(r) \tag{4.4}$$

where k is the wavenumber. It is easy to see that $q(k) = q(2\pi - k)^\star$ (mode at $k = 0$ i s the sliding mode whose mode lifetime is infinity and we simply ignore it). Thus, it is sufficient to focus on $q(k)$ at $k \in (0, \pi)$.

For 3D lattice systems:

$$\vec{q}(\vec{k}) = \frac{1}{L^3} \sum_{\vec{r}} e^{-i\vec{r}\cdot\vec{k}} \vec{u}(\vec{r}) \tag{4.5}$$

The wave vector is defined by :

$$\vec{k} = \frac{2\pi}{L}\vec{n} \ , \vec{n} = (n_1, n_2, n_3) \ , n_i \in (1, L)$$

and $\vec{q}(k_1, k_2, k_3) = \vec{q}(L + 2 - k_1, L + 2 - k_2, L + 2 - k_3)^\star$ (mode 1 is the sliding mode, and all other modes are symmetric about the mode $q(\frac{L}{2} + 1)$ with wave number π), and thus it is sufficient to focus on $q(n) \ , n \in (2, \frac{L}{2} + 1)$.

Figure (4.1) gives a pictorial expression of the same mode in systems of different sizes (1D example):

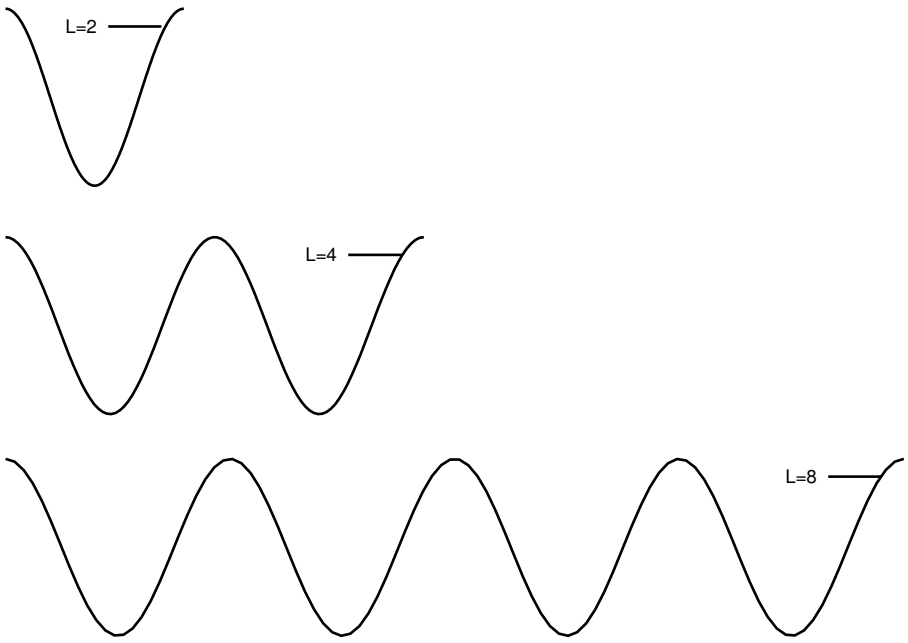

Figure 4.1: Transverse mode with wavenumber $= \pi$ at systems of $L = 2$, $L = 4$ and $L = 8$

4.4 Mode index and degeneracy in 3D Lattice

During the following discussion, index of normal modes mode:($ei,\ n_1,\ n_2,\ n_3$) has been set up in the following way:

- ei is the $x,\ y$ or z component of the normal mode amplitude (which is a vector in 3D system)
- $n_1,\ n_2,\ n_3$ are the index of wave vectors: $\vec{k} = \frac{2\pi}{L}\vec{n}$, $\vec{n} = (n_1, n_2, n_3)$, $n_i \in (1, L)$

Due to the symmetry of the system, there is no preference or difference in the $x,\ y$ and z components of the normal modes. In other words, quantities that we are interested in should be independent of ordering of index, such as:

$$\frac{\langle u(x,i,j,k)(0)u(x,i,j,k)(t)\rangle}{\langle u(x,i,j,k)(0)^2\rangle} = \frac{\langle u(x,i,k,j)(0)u(x,i,k,j)(t)\rangle}{\langle u(x,i,k,j)(0)^2\rangle} = \frac{\langle u(z,j,k,i)(0)u(x,j,k,i)(t)\rangle}{\langle u(x,j,k,i)(0)^2\rangle}$$

Also, in the Hamiltonian (Eq: 4.2): the transverse and longitudinal mode are degenerate, so

$$\frac{\langle u(x,\vec{k})(0)u(x,\vec{k})(t)\rangle}{\langle u(x,\vec{k})(0)^2\rangle} = \frac{\langle u(y,\vec{k})(0)u(y,\vec{k})(t)\rangle}{\langle u(y,\vec{k})(0)^2\rangle} = \frac{\langle u(z,\vec{k})(0)u(z,\vec{k})(t)\rangle}{\langle u(z,\vec{k})(0)^2\rangle}$$

thus, we only focus on one component ($e_i = 1$ or x) to continue the following analysis.

4.5 Numerical test of the 4th moment approximation method

The calculations were done for systems with different size (L=2, 4, 8, 16, 32, 64, etc in 1D and L=2, 4, 8 for 3D) at a wide range of temperatures (temperature=2^{-10} to 2^{10}). mode lifetime is defined [35] as follows:

$$\tau = \int_{-\infty}^{+\infty} dt\ \chi(t)^2 \tag{4.6}$$

Figures (4.2-4.7) shows that mode lifetime τ can be approximated by the first two moments for the 1D anharmonic chains in the wide range of temperatures.

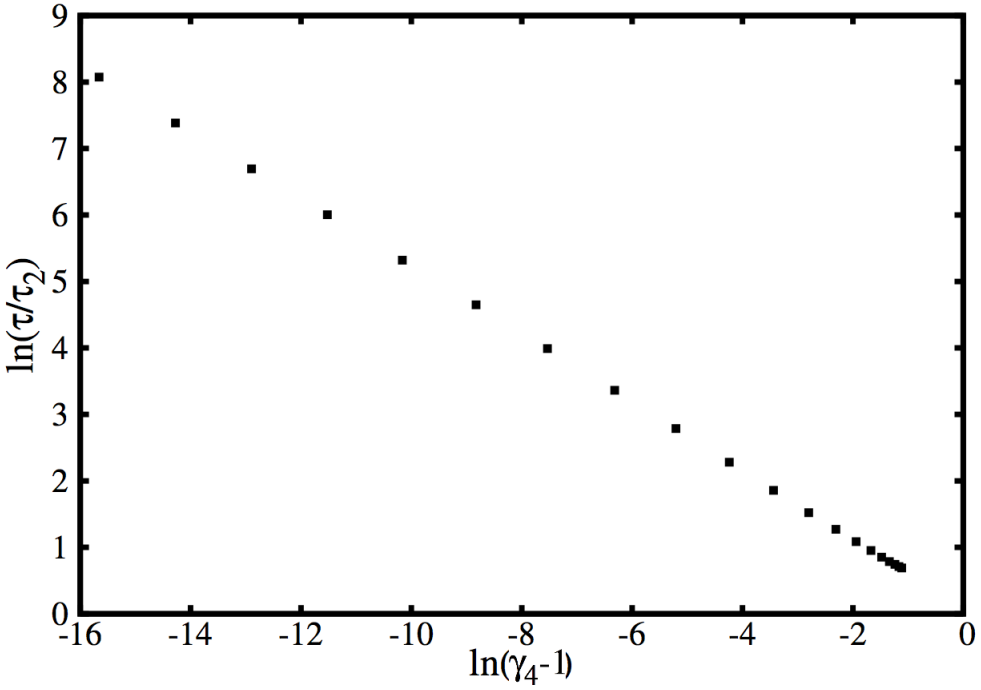

Figure 4.2: $\ln(\tau/\tau_2)$ vs. $\ln(\gamma_4 - 1)$of XACF at $k = \pi$ in the 1D chain of the size of 2

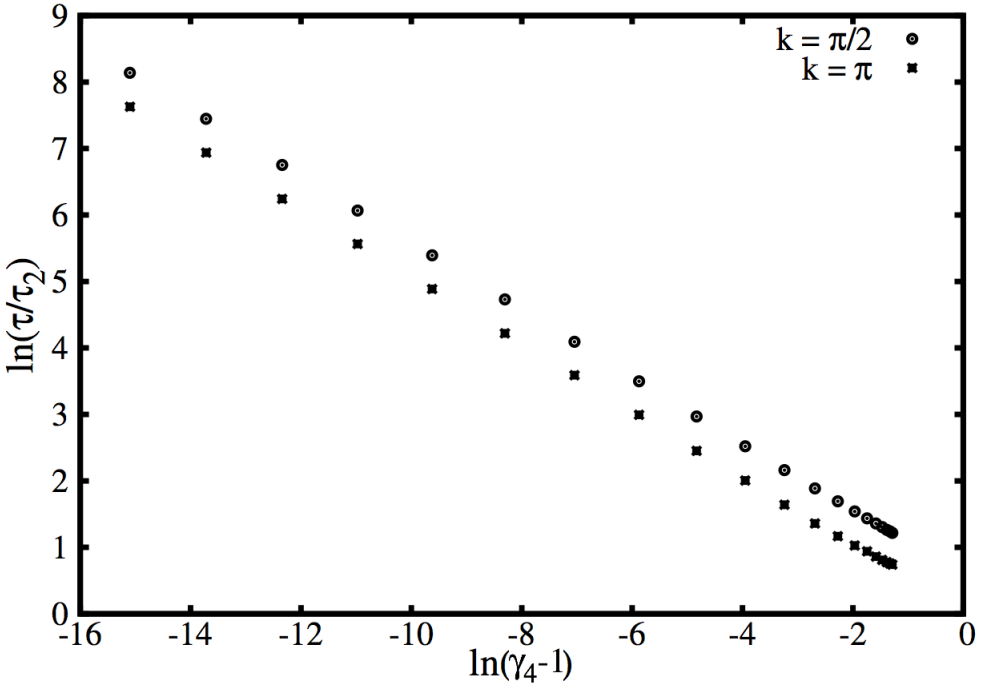

Figure 4.3: $\ln(\tau/\tau_2)$ vs. $\ln(\gamma_4 - 1)$ of XACF in the 1D chain of the size of 4

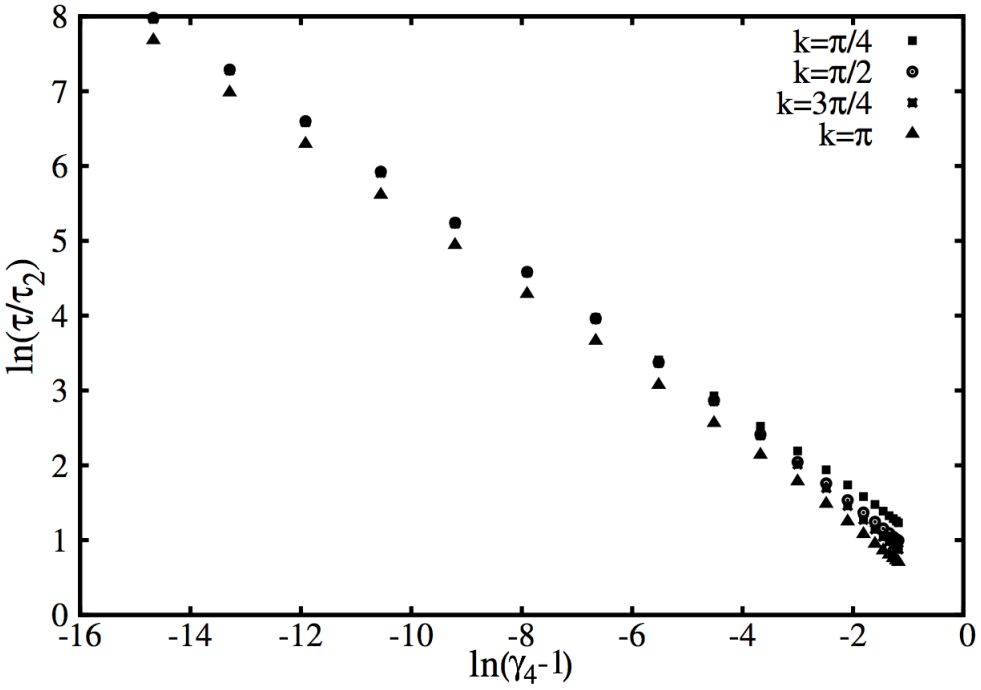

Figure 4.4: $\ln(\tau/\tau_2)$ vs. $\ln(\gamma_4 - 1)$ of XACF in the 1D chain of the size of 8

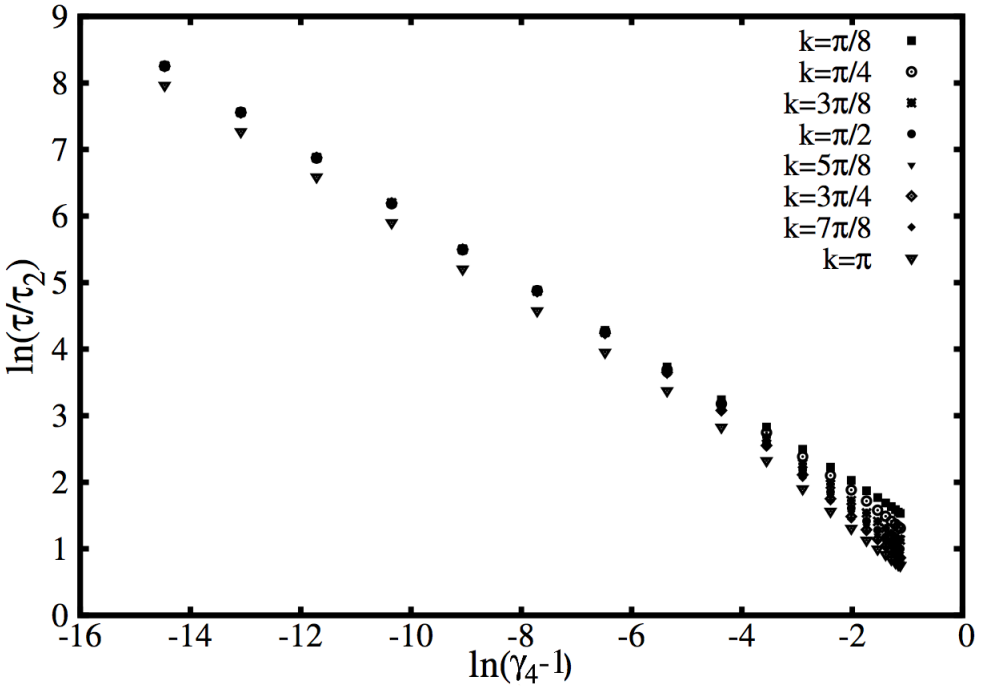

Figure 4.5: $\ln(\tau/\tau_2)$ vs. $\ln(\gamma_4 - 1)$ of XACF in the 1D chain of the size of 16

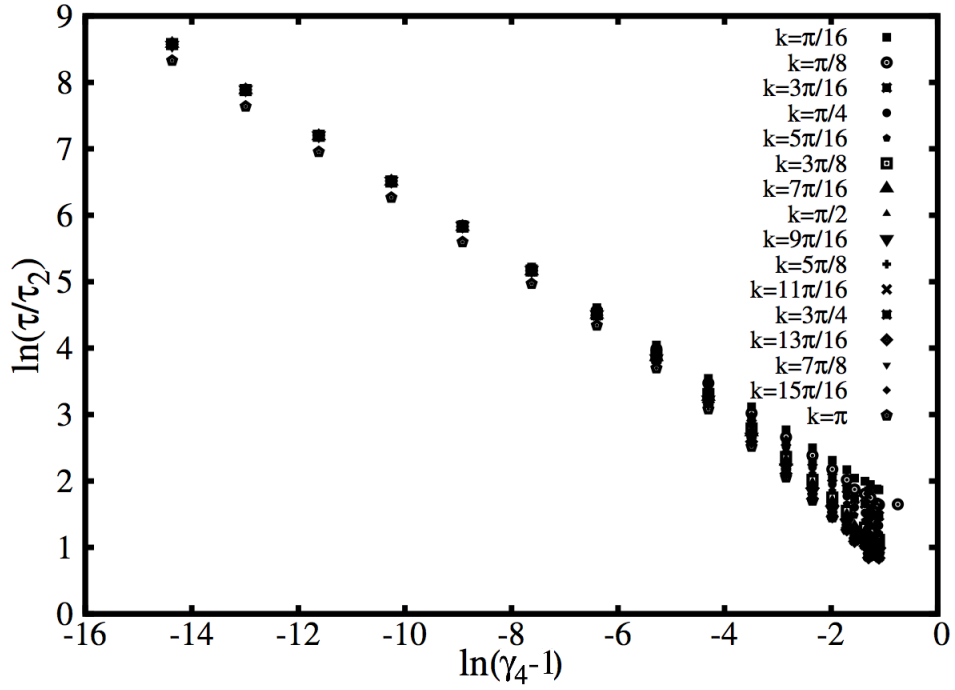

Figure 4.6: $\ln(\tau/\tau_2)$ vs. $\ln(\gamma_4 - 1)$ of XACF in the 1D chain of the size of 32

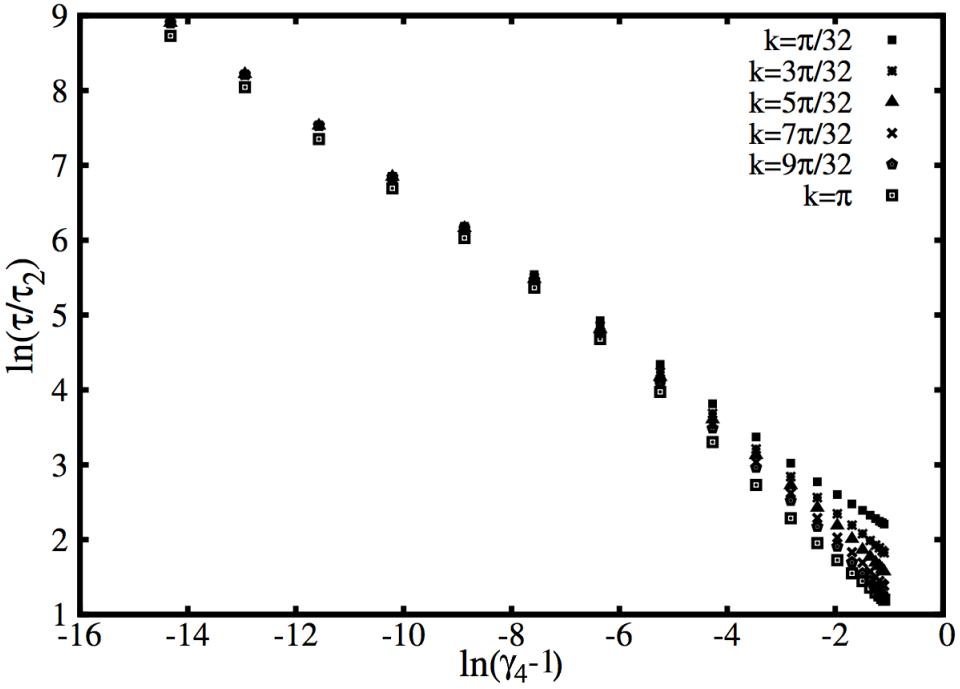

Figure 4.7: $\ln(\tau/\tau_2)$ vs. $\ln(\gamma_4 - 1)$ of XACF (selected modes) in the 1D chain of the size of 64

Figures (4.8, 4.9 and 4.10) shows that mode lifetime τ can be approximated by first two moments for the 3D anharmonic lattice in the wide range of temperatures.

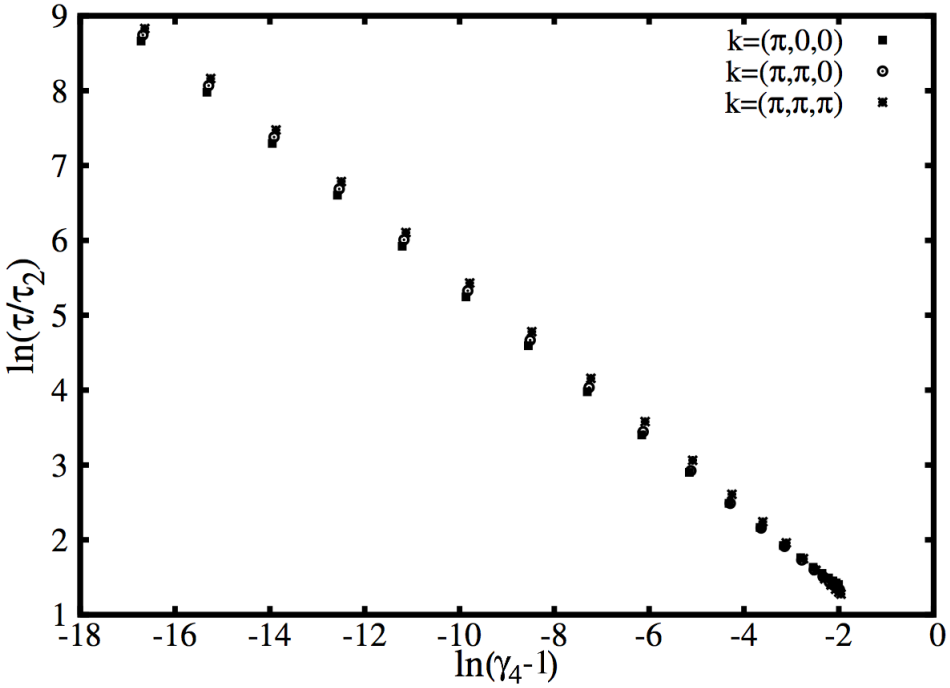

Figure 4.8: $\ln(\tau/\tau_2)$ vs. $\ln(\gamma_4 - 1)$of XACF in the 3D lattice of the size of 2

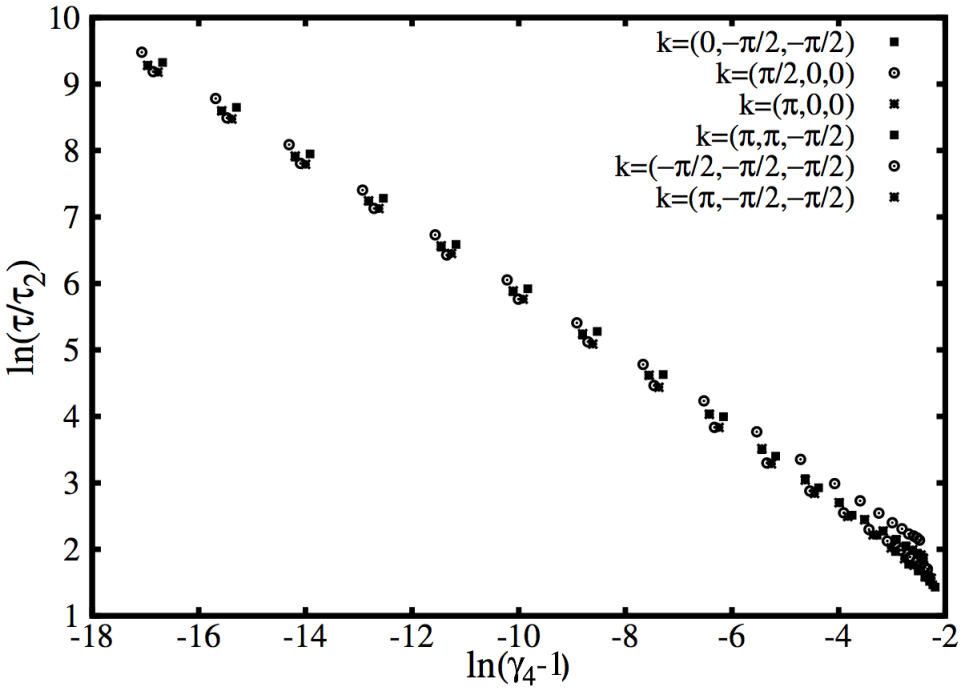

Figure 4.9: $\ln(\tau/\tau_2)$ vs. $\ln(\gamma_4 - 1)$of XACF in the 3D lattice of the size of 4

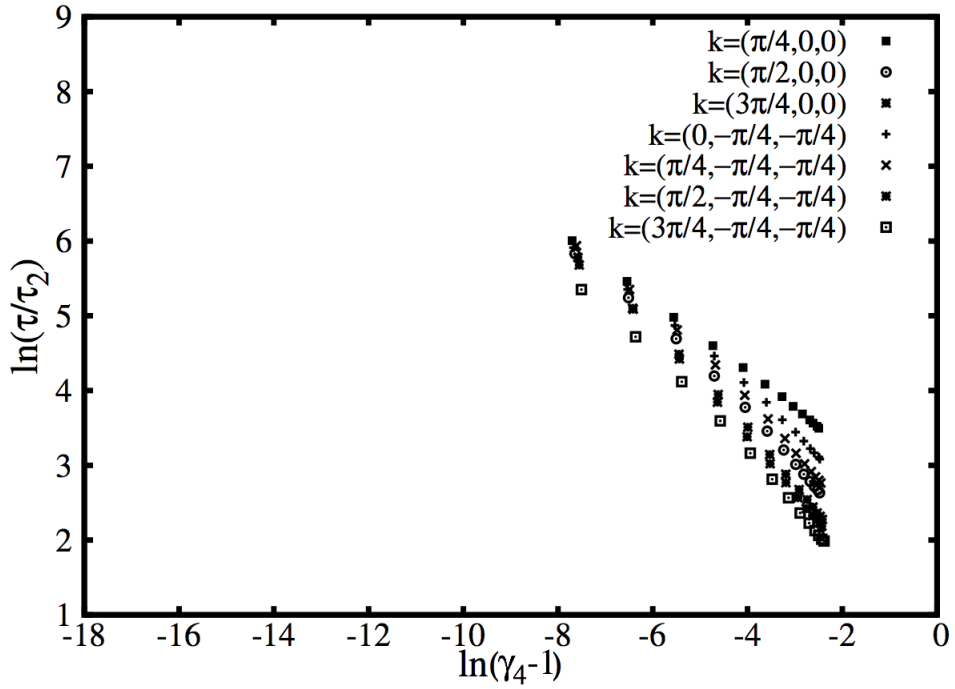

Figure 4.10: $\ln(\tau/\tau_2)$ vs. $\ln(\gamma_4 - 1)$of XACF in the 3D lattice of the size of 8

4.6 The sixth moment

The graphs above showed clearly that there is a simple relation between $\ln(\tau/\tau_2)$ and $\ln(\gamma_4 - 1)$ for any mode in the system, in other words, lifetime τ can be approximated by μ_2 and μ_4. While at the high temperature area, trend line from each mode seems to deviate from each other, which suggests that to make more precise approximation, more moments are needed (such as μ_6). Now we use γ_6 to approximate the mode lifetime in L=32 1D chain.

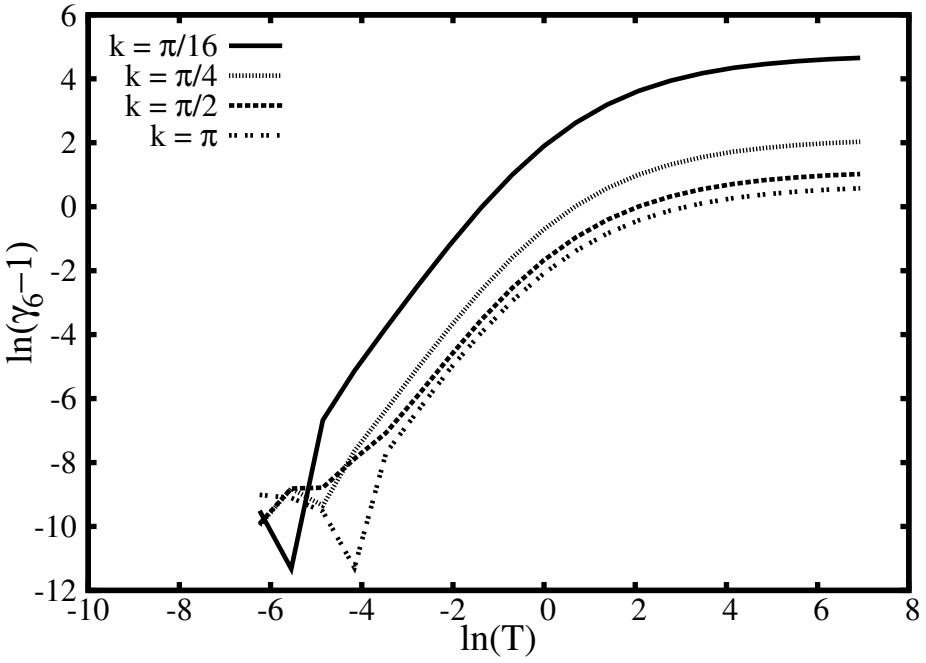

Figure 4.11: $\ln(\gamma_6 - 1)$ in system $L = 32$ vs temperatures

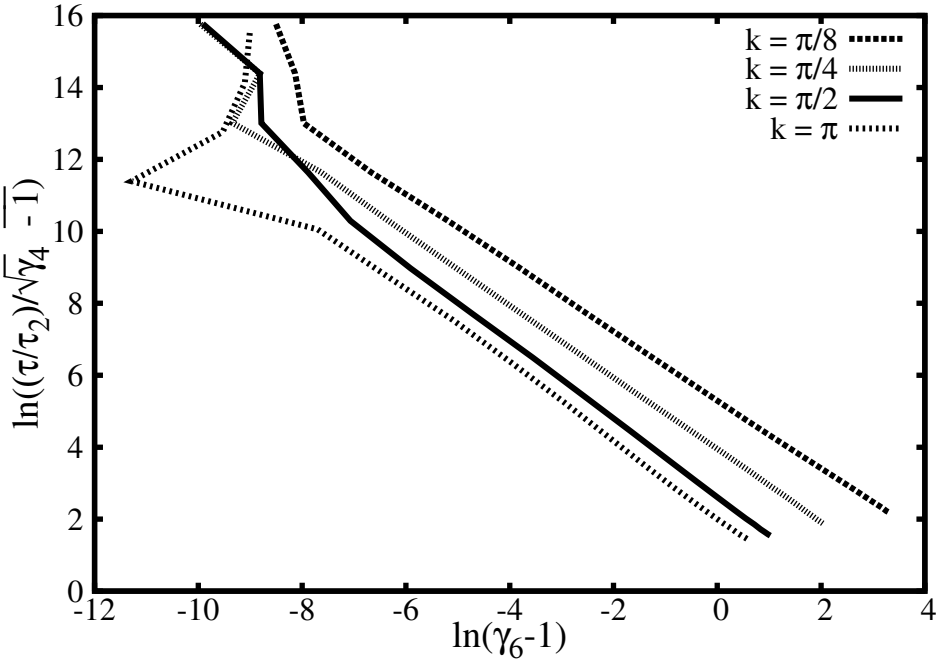

Figure 4.12: $\ln \tau/(\tau 2\sqrt{\gamma 4-1})$ in system $L = 32$ vs $\gamma_6 - 1$

In this section, we attempted to increase the precision of our approximation method by using sixth moment, the plots above show no significant improvement from the 4th moment approximation, which can be explained by two possibilities: it is possible that for our specific 1D model calculation of the sixth moment doesn't bring any new information that has been discovered in the second and fourth moment, or the function of lifetime in terms of μ_2, μ_4 and μ_6 has a more complex form than simple multiplications of terms related each moments.

4.7 Estimated lifetime with moments in 3D lattice systems

From our calculations shown above, it is safe to assume that mode lifetime τ can be estimated by the following form:

$$\tilde{\tau} = \text{Const.} \ * \frac{\tau_2}{\sqrt{\gamma_4 - 1}}$$

As the size of the system increases, calculations of mode lifetime directly are getting more computationally expensive, but with our estimating method by calculating the moments only, one can estimate the mode lifetime for much larger systems. The following graphs show that relation be-

tween the estimated mode lifetime($\tilde{\tau}$ with Const.= 1) and the size of the system (the relation is not monotonic).

Figures (4.13-4.17) show the estimated mode lifetime of different modes at various temperatures vs the size of the system which indicated the complexity of mode lifetimes in terms of the size of the system.

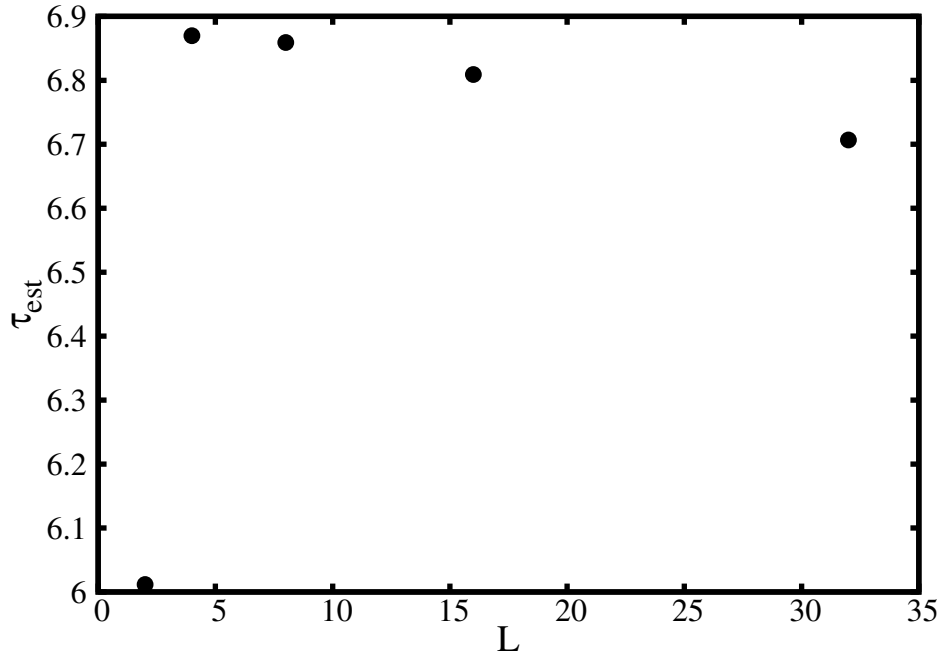

Figure 4.13: Estimated lifetime of mode $(\pi, 0, 0)$ vs. system size at temperature $= 1$

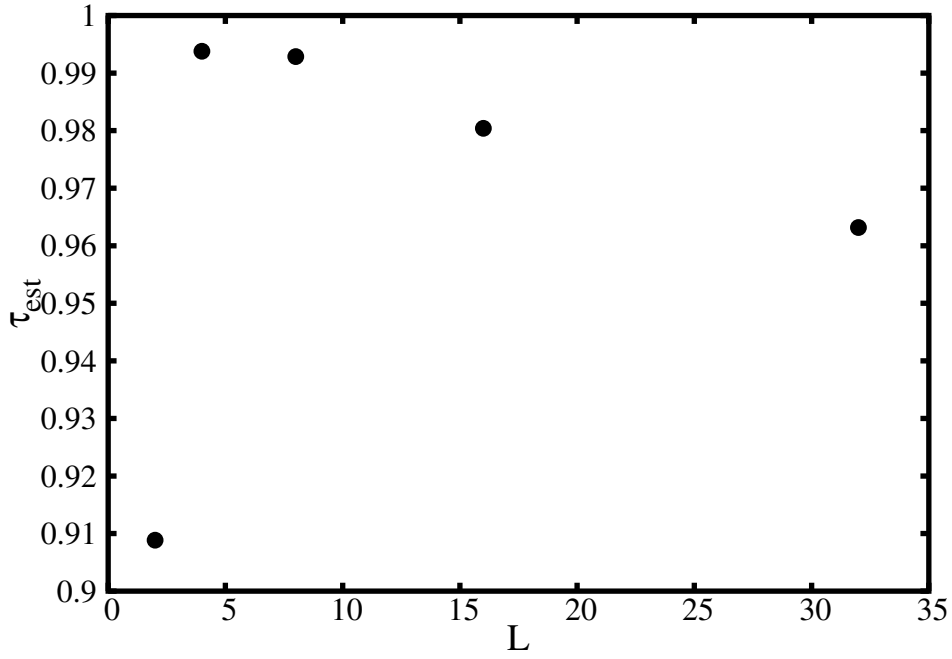

Figure 4.14: Estimated lifetime of mode $(\pi, \pi, 0)$ vs. system size at temperature $= 2^4$

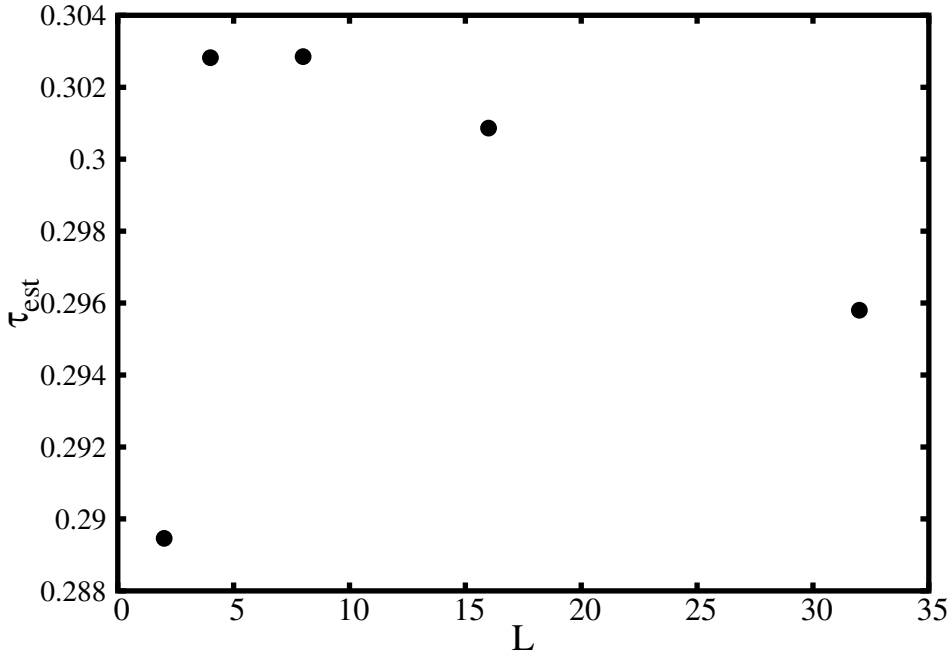

Figure 4.15: Estimated lifetime of mode (π, π, π) vs. system size at temperature $= 2^8$

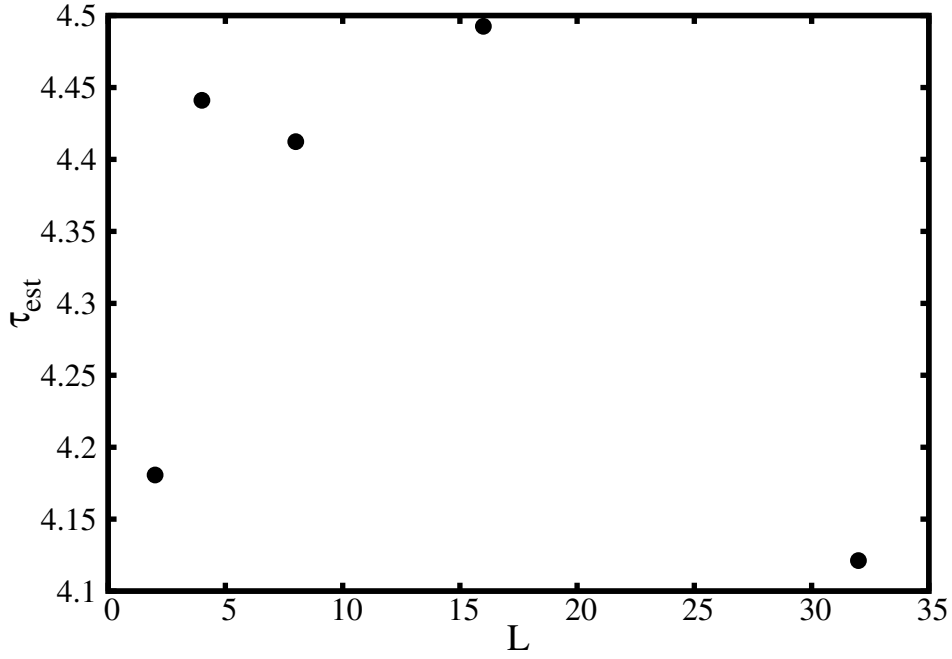

Figure 4.16: Estimated lifetime of mode $(\pi, \pi, 0)$ vs. system size at temperature $= 1$

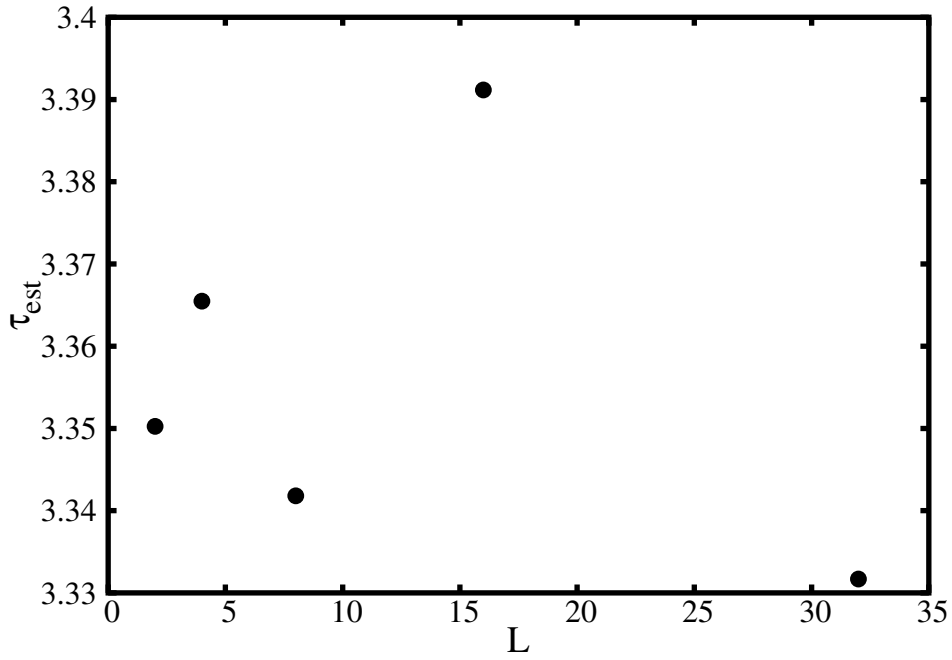

Figure 4.17: Estimated lifetime of mode (π, π, π) vs. system size at temperature $= 1$

4.8 Other characters of the models

In this section, we take a very brief look at some characters of our tested model.

4.8.1 τ and temperature

There is a general monotonic relation between mode lifetimes τ and the temperature T, the higher the temperature is, the shorter the mode lifetime will be.

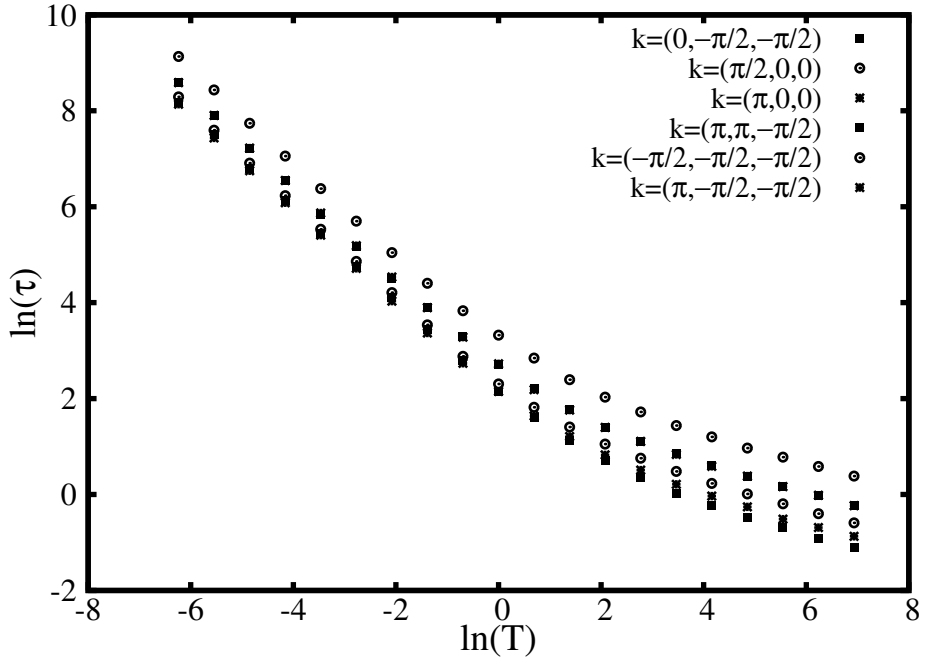

Figure 4.18: Lifetime τ vs. T in XACF in the 3D lattice of the size of 2, 4 and 8

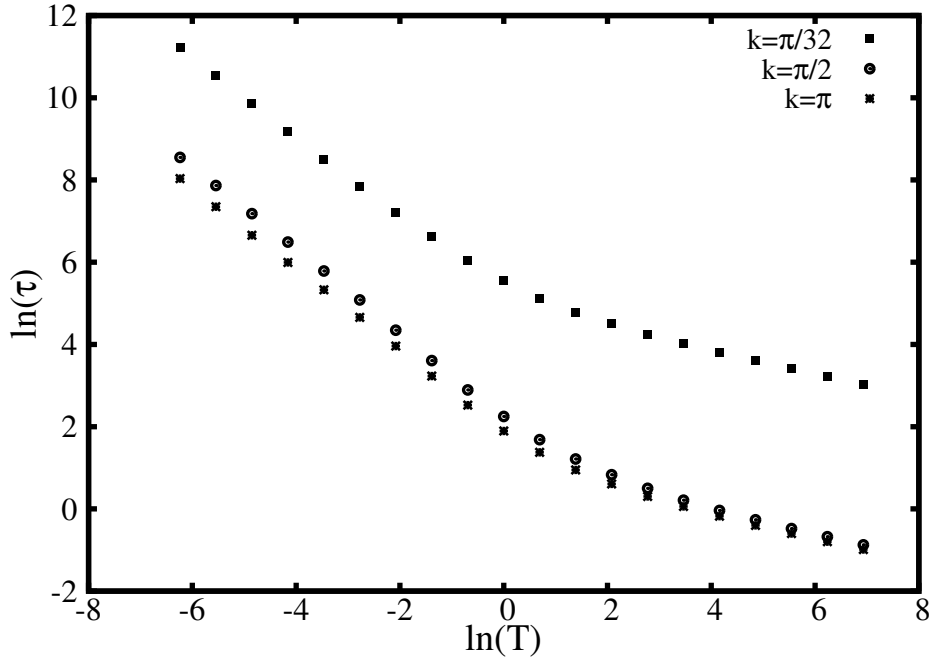

Figure 4.19: Lifetime τ vs. T in XACF in the 1D chain $L = 64$

4.8.2 τ and k

Following are the mode lifetime vs wave number k in many body systems, where more than one mode is available.

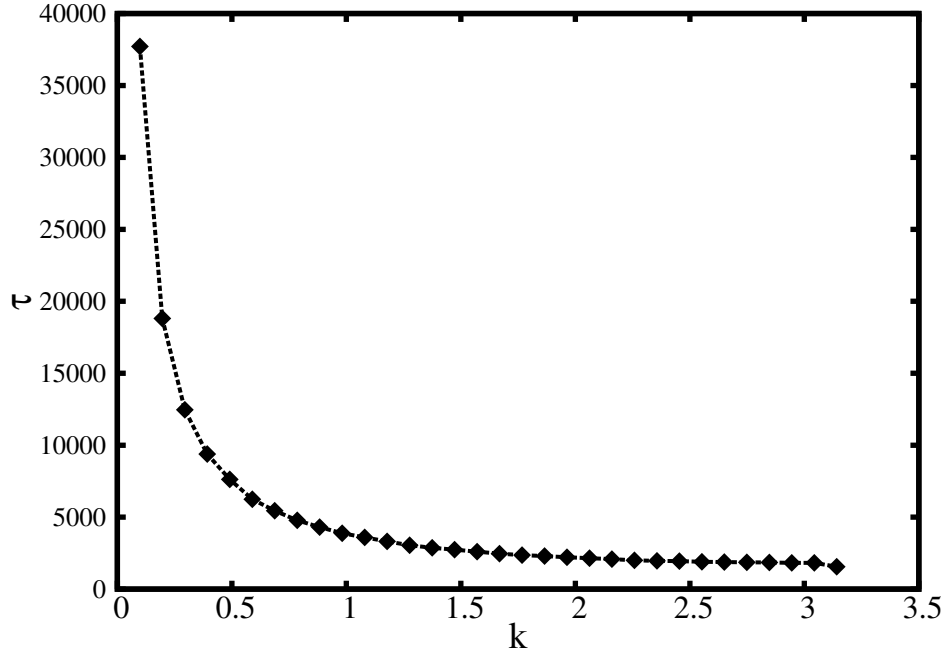

Figure 4.20: Lifetime τ vs k at temperature=2^{-8}, L=64 1D chain

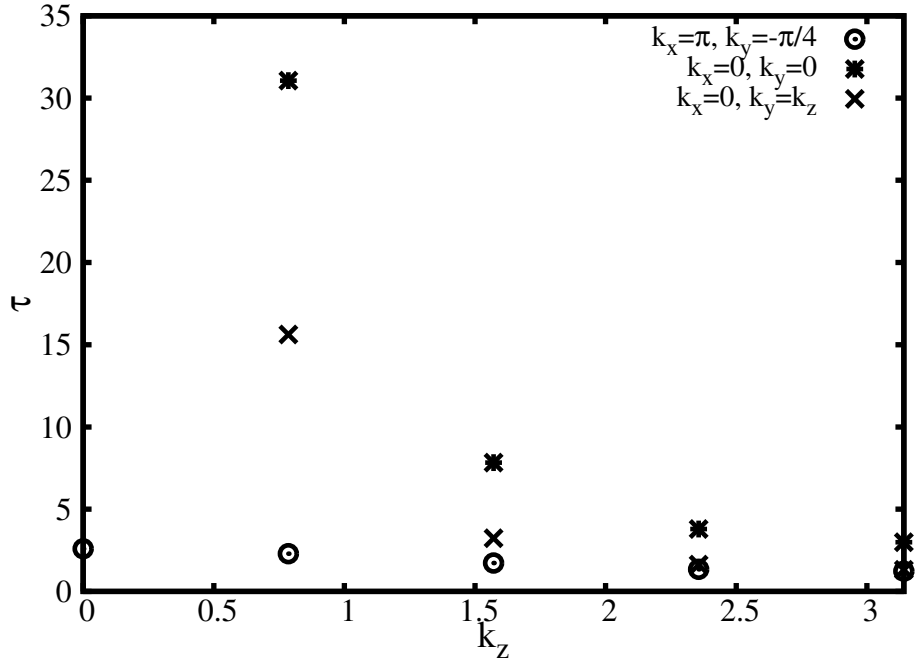

Figure 4.21: Lifetime τ vs. k_x of XACF in the 3D lattice of L=8 at T=2^5

It is clear that at the same temperature, higher-k mode has much shorter lifetime than lower-k ones. Beside, it is interesting to see how fast that the lifetime of each mode falls as the temperature increases.

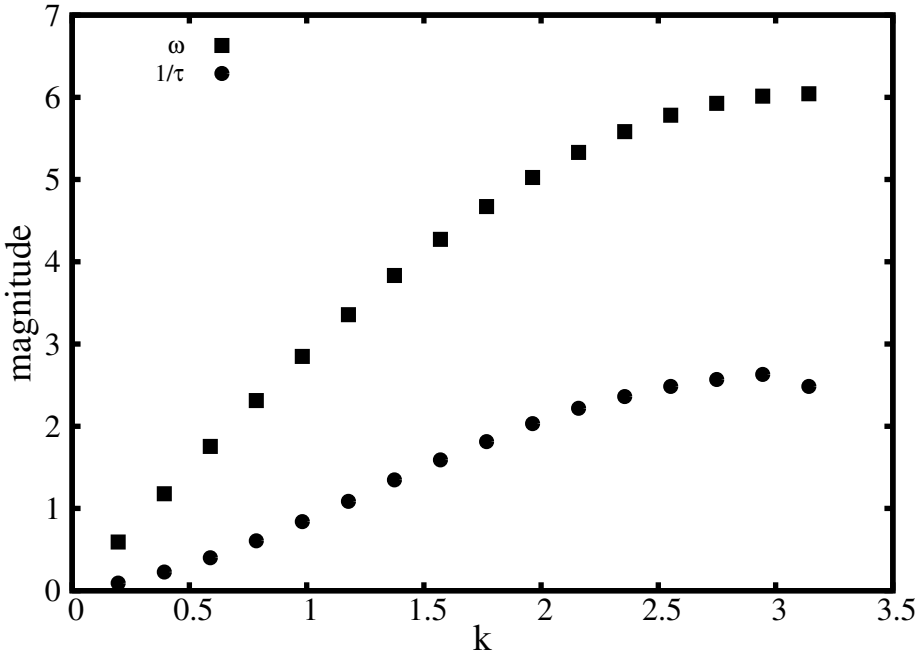

Figure 4.22: ω and $\frac{1}{\tau}$ vs k in the system $L = 32$ 1D chain at $T = 2^8$

Figure (4.22) shows both ω (a measurement of harmonic approximation of the anharmonic system) and $1/\tau$ in terms of wavenumber k. Figure (4.23) shows d_{min}(a measurement of anharmonicity of the system) in terms of temperatures.

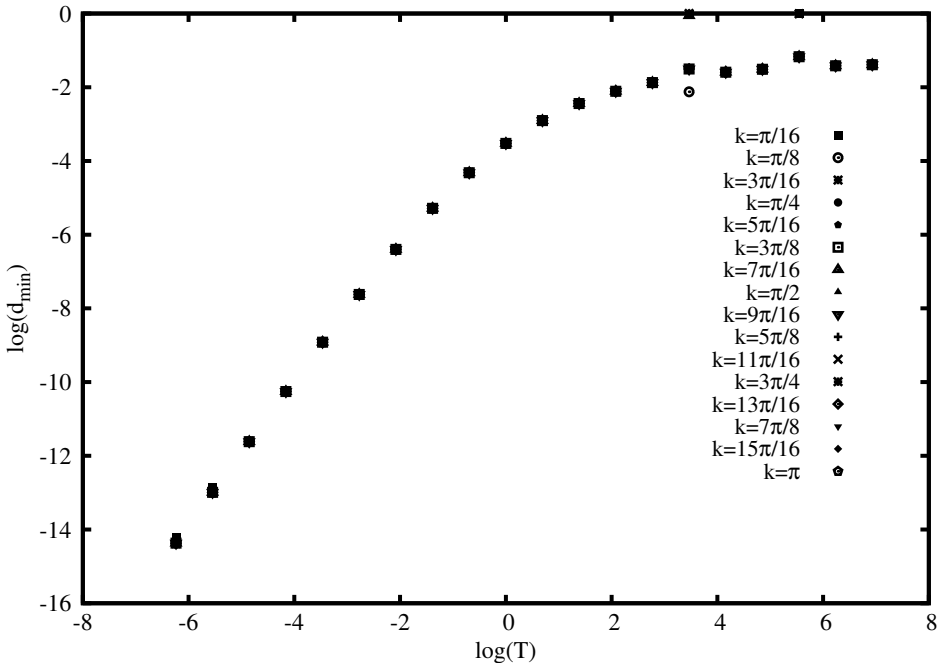

Figure 4.23: d_{min} vs temperature in the system $L = 32$ 1D chain

The following plot (Fig:4.24) shows the harmonicity of the system changes with respect to the temperature.

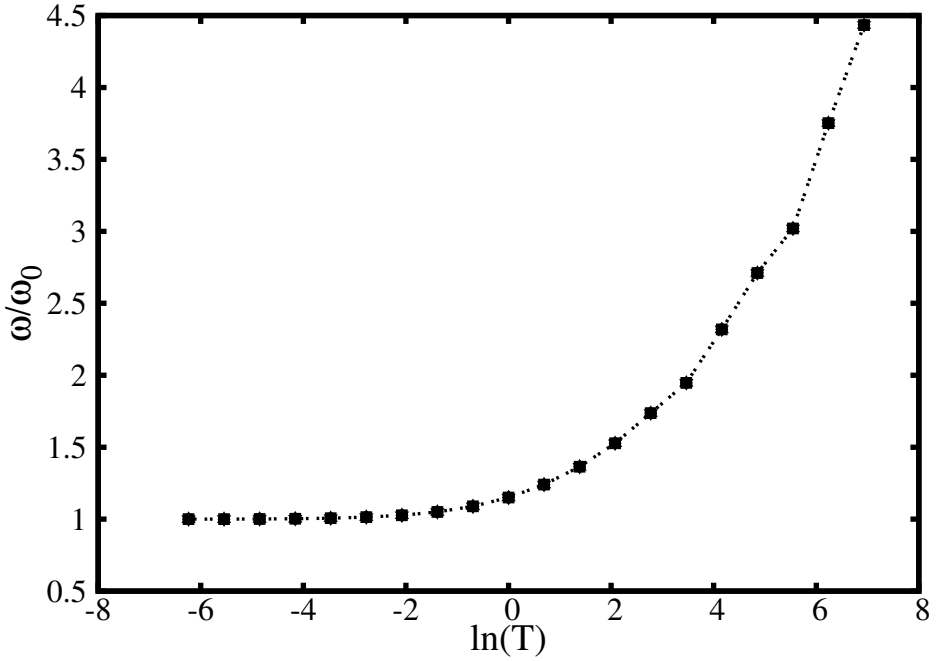

Figure 4.24: ω vs temperature in the system $L = 32$ 1D chain

4.8.3 τ and L

In this part, we explore the relation between mode lifetime τ and the size of the system L (calculations were done at L=2,4,8,16,32 and 64).

Figures (4.25-4.30) show the lifetime τ of different modes vs length of the system L in 1D system at different temperatures:

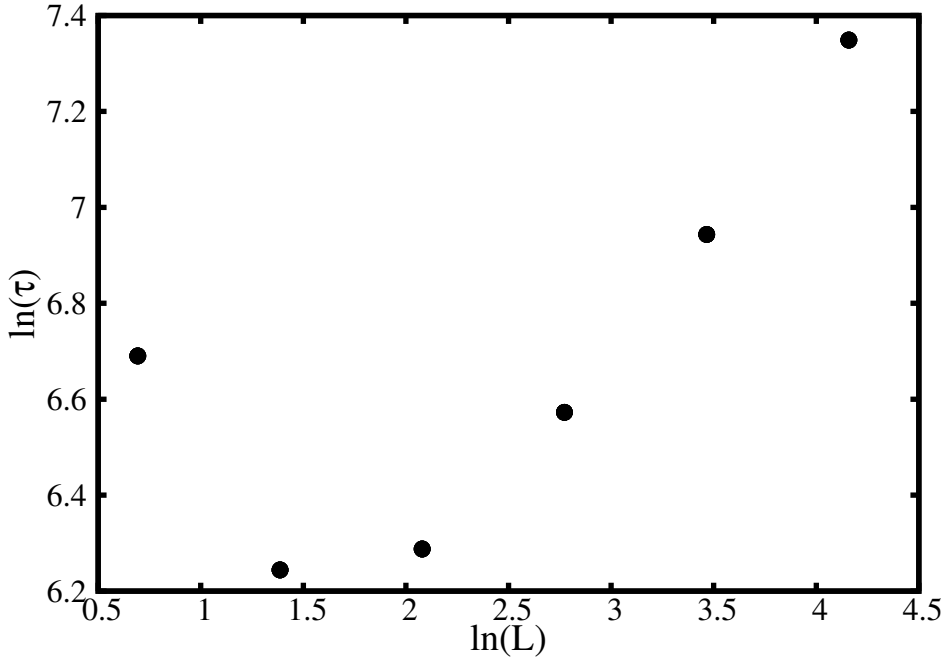

Figure 4.25: τ of mode π vs. L at temp $= 2^{-8}$ in the 1D chain model

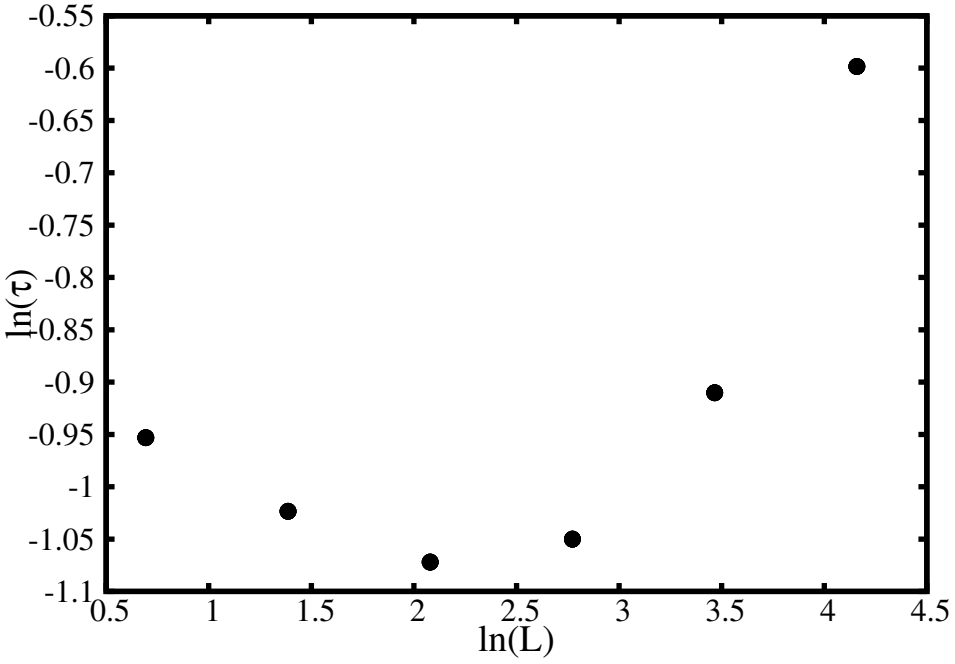

Figure 4.26: τ of mode π vs. L at temp $= 2^{8}$ in the 1D chain model

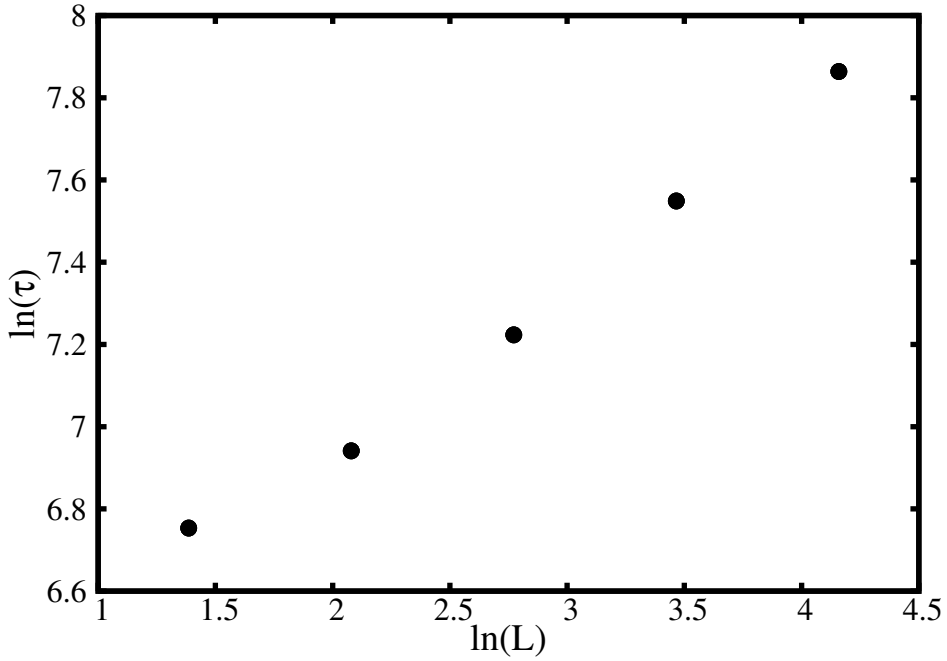

Figure 4.27: τ of mode $\pi/2$ vs. L at temp $= 2^{-8}$ in the 1D chain model

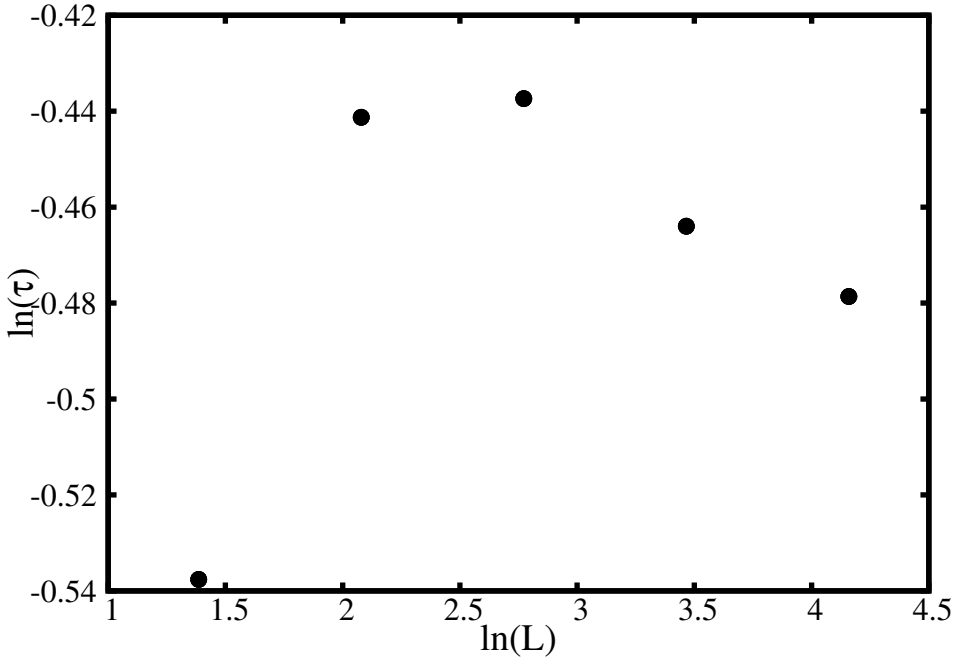

Figure 4.28: τ of mode $\pi/2$ vs. L at temp $= 2^{8}$ in the 1D chain model

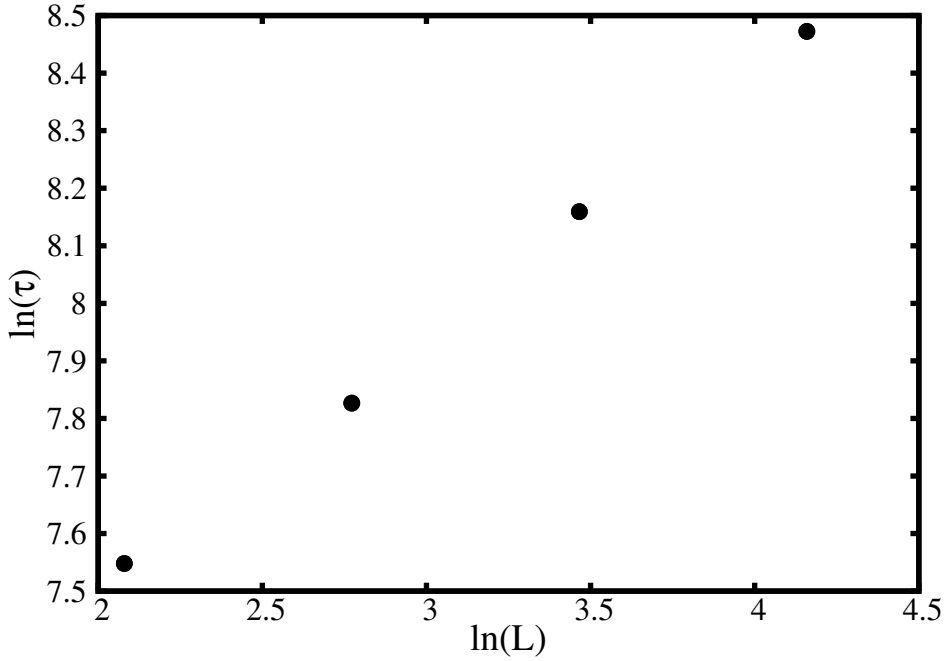

Figure 4.29: τ of mode $\pi/4$ vs. L at temp $= 2^{-8}$ in the 1D chain model

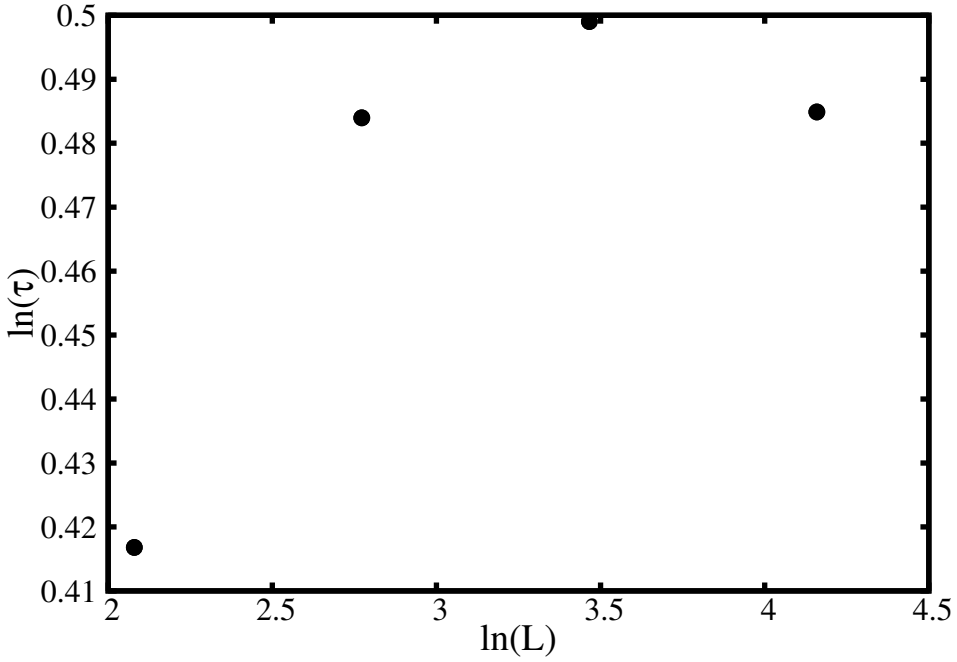

Figure 4.30: τ of mode $\pi/4$ vs. L at temp $= 2^{8}$ in the 1D chain model

Overall, the plots above show that even for very simple models like 1D anharmonic chain and 3D anharmonic lattice, there is no simple relation between lifetime τ and size of the systems L.

4.9 Density of states

Here we use the density of states (DOS) to explain why the low moments approximation works.

Figures (4.31-4.38) show examples of DOS of various modes in both 1D and 3D systems at different temperatures.

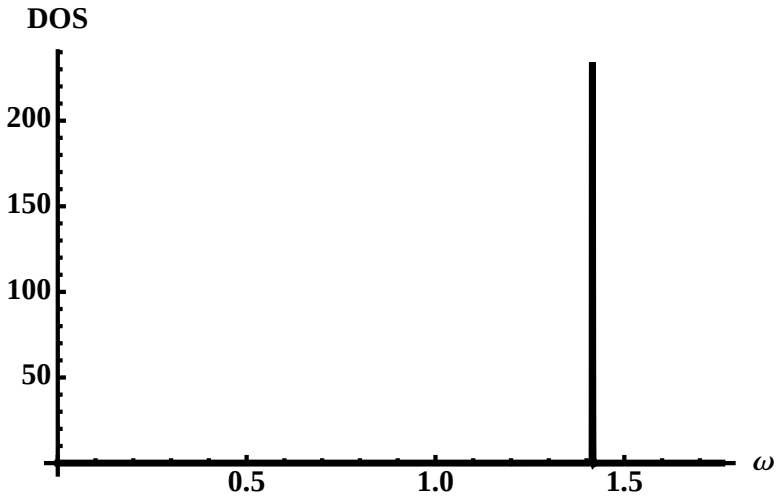

Figure 4.31: *DOS* of XACF of mode 2 in the 1D chain of the size of 8 at temperature=2^{-8}

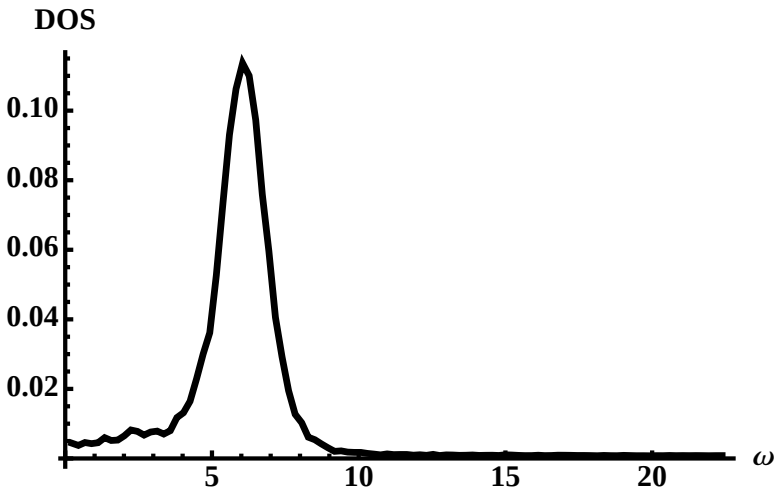

Figure 4.32: *DOS* of XACF of mode 5 in the 1D chain of the size of 8 temperature=2^8

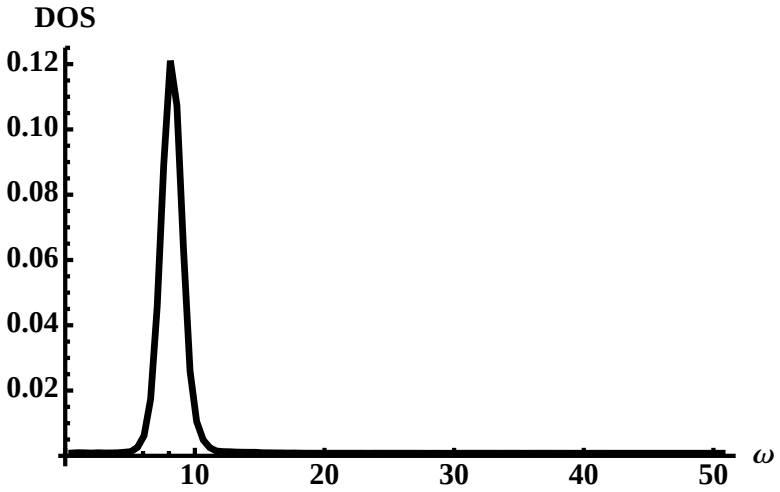

Figure 4.33: *DOS* of XACF in the 3D lattice of L=2 of x component of mode $\vec{k} = (0, 0, \pi)$ at temp=2^{10}

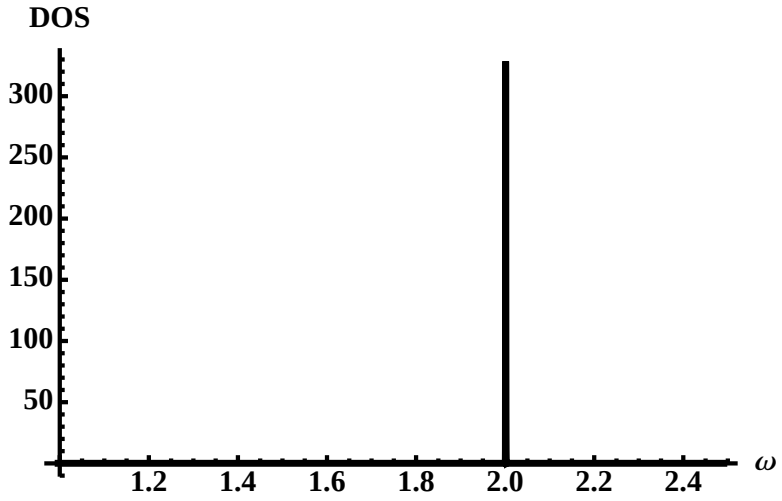

Figure 4.34: *DOS* of XACF in the 3D lattice of L=2 of x component of mode $\vec{k} = (0, 0, \pi)$ at temp=2^{-8}

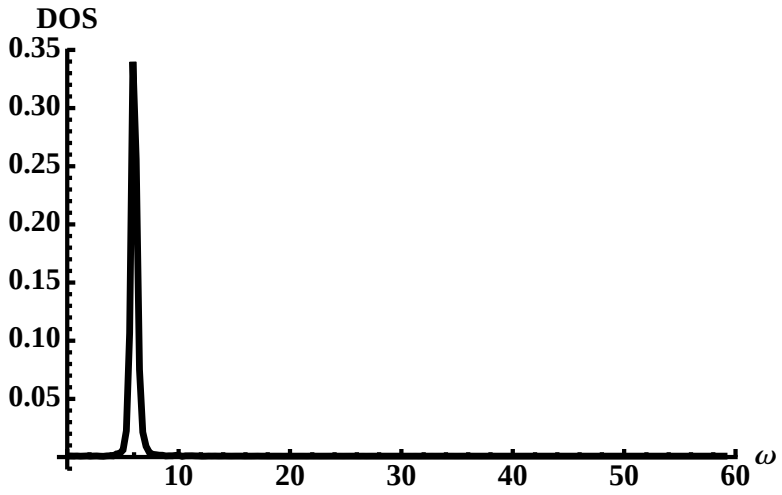

Figure 4.35: *DOS* of XACF in the 3D lattice of L=4 of x component of mode $\vec{k} = (0, 0, \pi/2)$ at temp=2^{10}

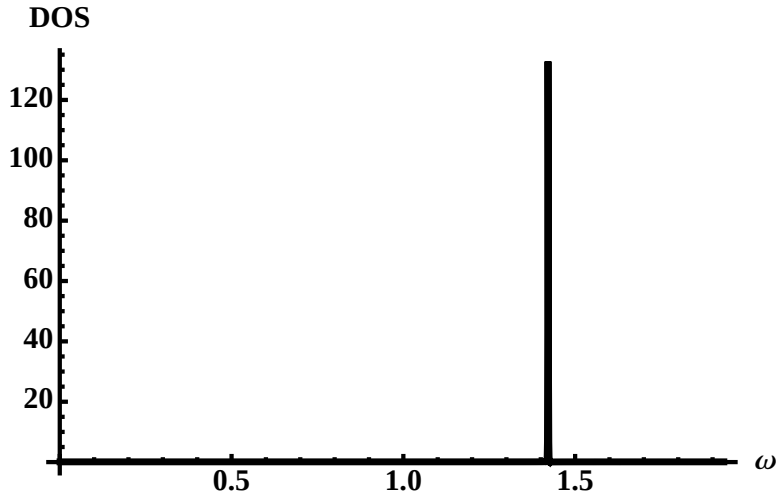

Figure 4.36: *DOS* of XACF in the 3D lattice of L=4 of x component of mode $\vec{k} = (0, 0, \pi/2)$ at temp=2^{-5}

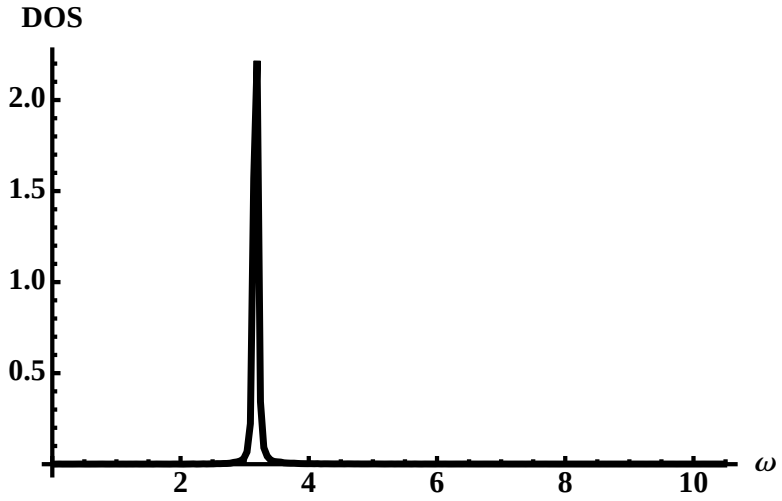

Figure 4.37: *DOS* of XACF in the 3D lattice of L=8 of x component of mode $\vec{k} = (0, 0, \pi/4)$at temp=1024

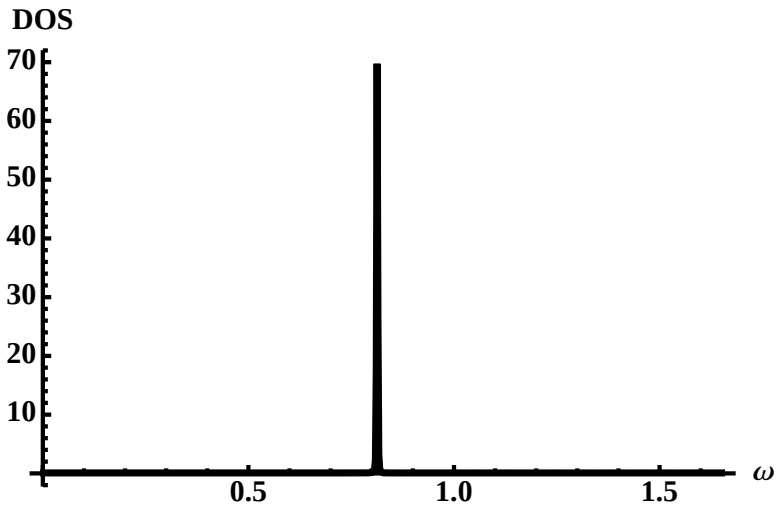

Figure 4.38: *DOS* of XACF in the 3D lattice of L=8 of x component of mode $\vec{k} = (0, 0, \pi/4)$at temp=0.5

The graphs above show that the single peak behavior in the DOS at all temperatures in systems with different sizes, with the DOS in systems we have discussed so far. As the temperature increases, the width of the peak increases and its height decreases.

It is clearer to see the change of DOS with respect to temperature in one plot:

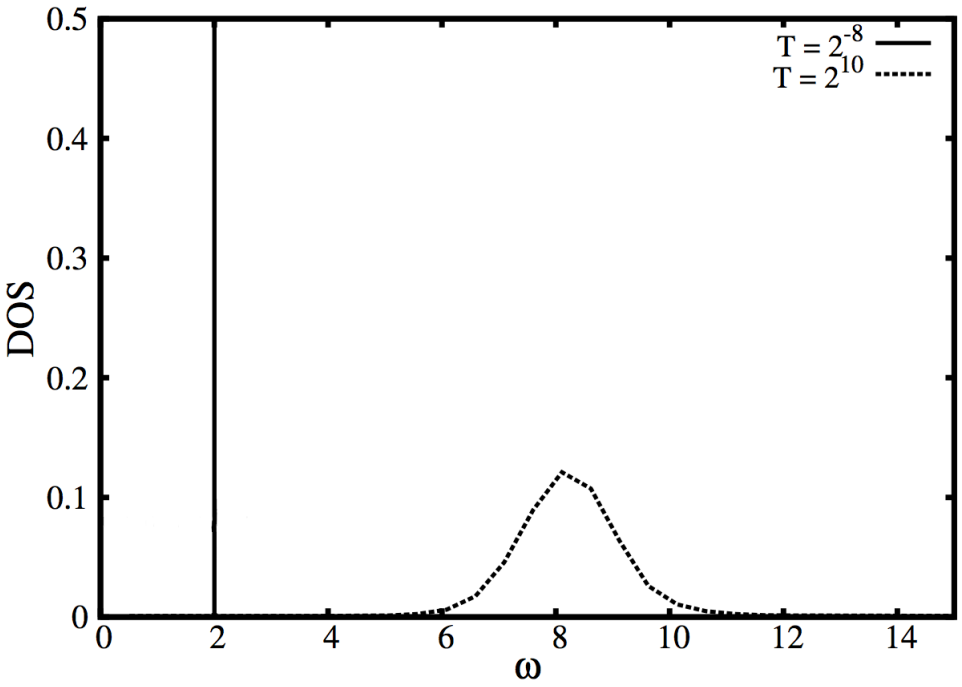

Figure 4.39: *DOS* of XACF in the 3D lattice of L=2 of x component of mode $\vec{k} = (0, 0, \pi)$

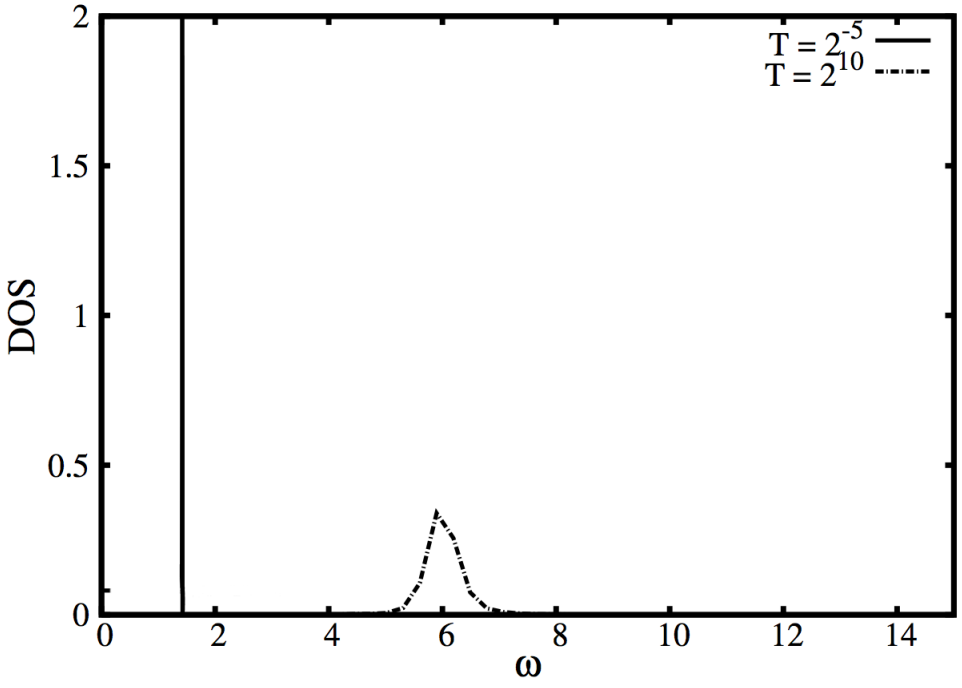

Figure 4.40: *DOS* of XACF in the 3D lattice of L=4 of x component of mode $\vec{k} = (0, 0, \pi/2)$

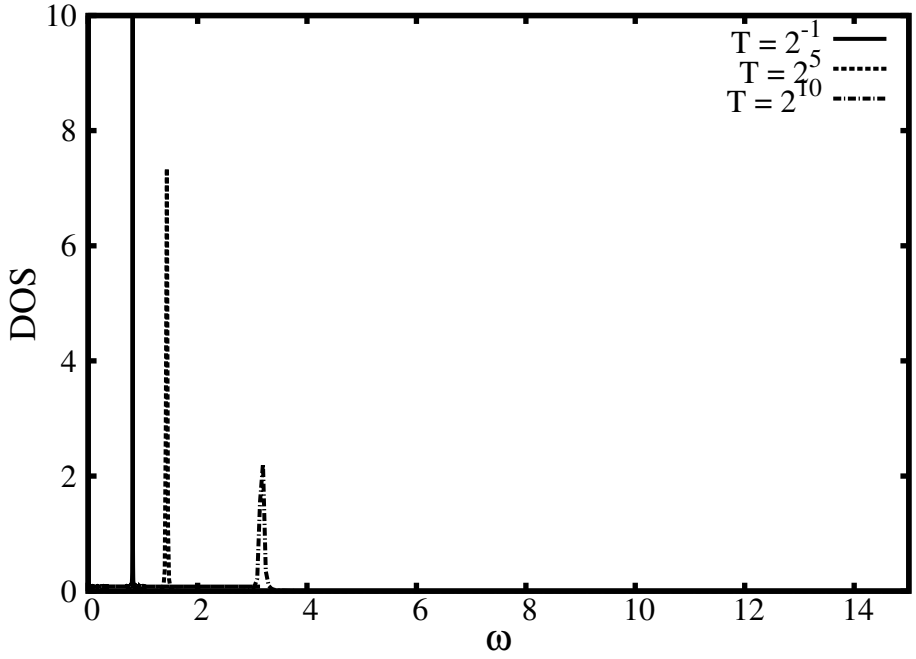

Figure 4.41: *DOS* of XACF in the 3D lattice of L=8 of x component of mode $\vec{k} = (0, 0, \pi/4)$

According to Parseval's Theorem, mode lifetime can be calculated by the integration of the area under the curve of DOS.

$$\tau = \int_{-\infty}^{\infty} dt\ \chi(t)^2 = \int_{-\infty}^{\infty} d\omega\ n(\omega)^2 \tag{4.7}$$

Both DOS above are quite simple, especially the DOS at low temperature which is almost structureless, and the one at the high temperature is only slightly more complicated, yet, both can be characterized by their width and the location of the peak (two parameters). Actually, the DOS of any normal mode in this 1D chain system is characterized by a single peak that shifts with temperatures and also the width of the peak varies as the temperature changes, thus mode lifetime can also be approximated by two parameters, the first two moments.

4.10 Comparison between 1D and 3D model

- τ vs L: In 1D system, the relation between τ and L is not clear, while in 3D model, our estimated mode lifetime shows that as the size of the system increases, mode lifetime will

asymptotically reach a constant.

- τ vs T: in both modes, the relation between $\ln(\frac{\tau}{\tau_2})$ and $\ln(\gamma 4_1 - 1)$ can be approximately represented by a straight line with slope $\frac{1}{2}$:

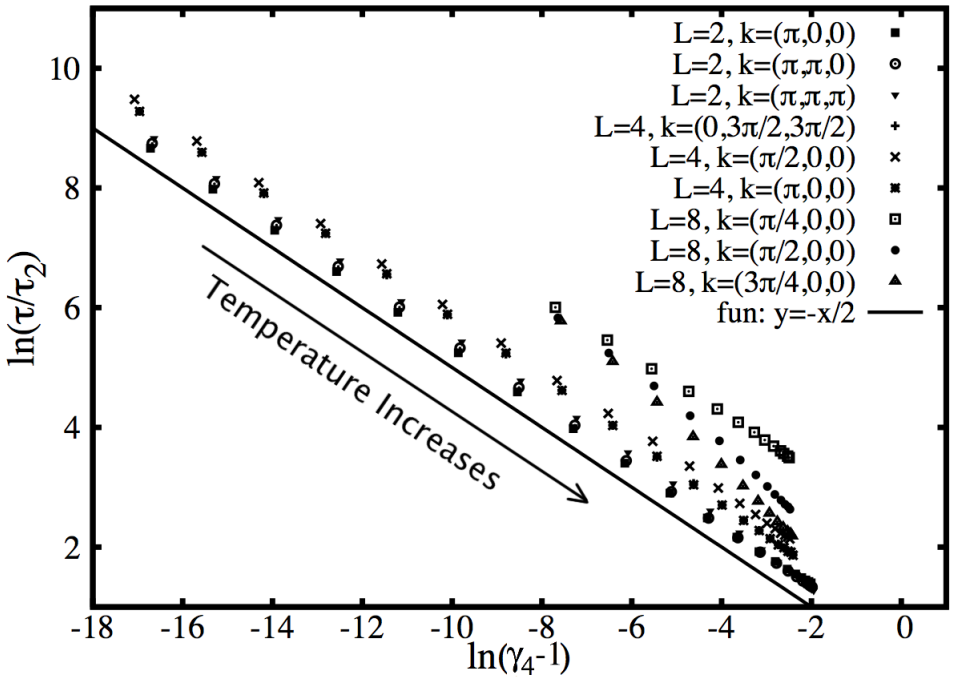

Figure 4.42: $\ln(\tau/\tau_2)$ vs. $\ln(\gamma_4 - 1)$of XACF in the 3D lattice of the size of 2, 4 and 8

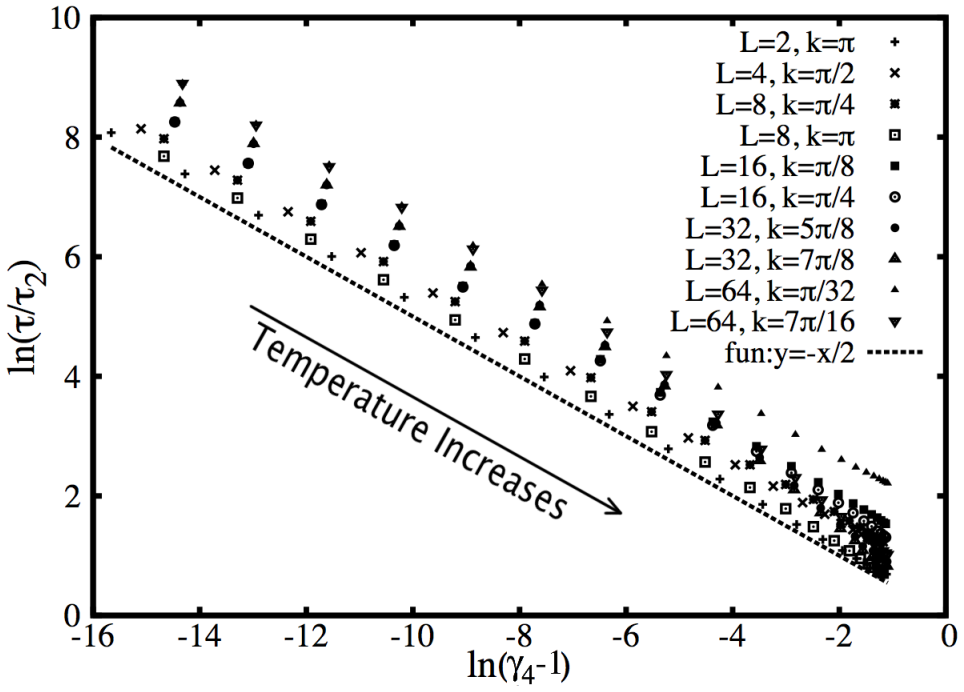

Figure 4.43: $\ln(\tau/\tau_2)$ vs. $\ln(\gamma_4 - 1)$of XACF in the 1D lattice of the size of 2,...,64

- *DOS* vs T: our hypothesis still holds for both 1D and 3D model, with the simple anharmonic potential in these model, the DOS is a single peak, which will get lower and wider as temperature increases

Chapter 5

Fourth Moment Approximation in FCC: Lennard-Jones[1]

5.1 Introduction

In chapters 2-4 [14, 15, 35], we have developed and tested an approximate method to calculate lifetimes of vibrational modes in insulating solids. The method is based on ensemble averages of powers of the Liouvillian, and can be carried out by conventional Monte Carlo in combination with a means of calculating forces, such as interatomic potentials or first-principles electronic structure codes. The approach was tested on a lattice model of non-linear interactions, and it was shown that ensemble averages of the second power of the Liouvillian (that is, so-called "second-moment" approximation) accounted for the mode lifetimes very well at high temperatures but diverged at lower temperatures. The next level of approximation ("fourth-moment") was shown to account very well for the vibrational mode lifetimes in the same model system over the full range of temperatures. It was also determined that the principle reason for the success of the fourth moment was that the density of states (DOS) *for each mode* was simple enough to be described as single broadened peak.

This chapter reports a test of the fourth-moment approximation for a more realistic system: the vibrational modes of an FCC crystal with simple, Lennard-Jones interactions among the atoms. We find in this case that, as before in the simple lattice model, the vibrational mode lifetimes can

[1]Some of the text and figs have appeared in [36]

be captured by the fourth-moment approximation over the full range of temperatures (up to the melting point).

This chapter is organized as follows. First, we describe how we carry out the test of the fourth-moment approximation for FCC Lennard-Jonesium. Then the results of the evaluation are presented, along with some analysis of the densities of states for typical modes. Finally, we draw our conclusions.

5.2 Using FCC Lennard-Jonesium as a test of the 4th-moment approximation

We present here a test of the fourth-moment approximation on a more realistic model, namely the vibrational modes in an FCC lattice of atoms with unit mass interacting via a Lennard-Jones potential[2]:

$$\phi(r) = 4(\frac{1}{r^{12}} - \frac{1}{r^6})$$

The potential energy of a set of atoms is:

$$V = \sum_{\text{pairs}} \phi(r_{\text{pairs}})$$

(Note that the length, energy, and mass scales have been chosen be the natural set of units for the LJ potential.) A periodic cell is chosen, and for that specific cell the force constant matrix

$$\Phi_{i\alpha,j\beta} = \frac{\partial^2 U}{\partial r_{i\alpha} \partial r_{j\beta}}|_0$$

is constructed, i, j denote sites and α, β denote Cartesian coordinates, and the "0" indicates that the second derivative is evaluated at equilibrium. The calculated normal mode transformation X is constructed by finding the eigenvectors of the force constant matrix.

The test consists of two parts, both done according to normal modes: the first part determines the amplitude autocorrelation function (AACF) and the second is strictly an MC calculation of the moments. For the first part, we calculate the AACF by drawing initial conditions from the

[2]Actually, we used the "lj/smooth/linear" potential option in LAMMPS, which subtracts a small term, linear in r, to make the interatomic potential and its first derivative go to zero smoothly at the cutoff distance.

ensemble, which are then evolved using a velocity verlet algorithm with time-step $dt = 0.02$ when temperature < 0.1 and $dt = 0.01$ when temperature ≥ 0.1. The AACF is then averaged over all samples from the ensemble, from a minimum of 4×10^6 samples for the smallest cell to 25×10^6 for the largest. The simulated time of each MD run depends on the temperature (roughly inversely) and is determined such that the AACF for the longest-lived movde has decayed well enough that the calculated lifetime is converged to within 1%. From the AACF we extract the lifetime by Eq. 4.6. The second part of the test consists of calculating the fourth and second moments for each mode by MC sampling.

All calculations were performed using LAMMPS [56] and its python interface, by writing a python wrapper to drive the whole calculation. The wrapper [57] we have written for LAMMPS is completely general, and can easily be modified to use *any* of the interatomic potentials contained in LAMMPS .

In our calculations, we set cutoff distance to 2.57, which is between 5th and 6th nearest neighbor shell at the equilibrium, low-temperature lattice constant ($a = 1.57$).

Unlike constant V calculations, where the lattice constant a is unchanged throughout the temperature range, lattice constant a is dependent of the temperature during constant P calculations. At each temperature T_0, lattice constant a has been calculated by using isothermal-isobaric ensemble("NPT" in LAMMPS) and setting the inner pressure to zero and the temperature to T_0, then with the calculated lattice constant in that temperature, constant V MD calculation has been implemented.

The first part is compared to the second by making a scatterplot of τ/τ_2 to $\gamma_4 - 1$. The test is done on systems of various sizes:

- 4 atoms in a cubic cell
- 8 atoms (doubled along one cube axis)
- 16 atoms (doubled along a second cube axis)
- 32 atoms in a cubic cell

under both constant V and constant P conditions, and at various temperatures (0.05, 0.1, 0.2, 0.4, 0.8 for constant V, 0.05, 0.1, 0.2, 0.4, 0.6 at constant P).[3]

[3]The melting point at constant P for Lennard-Jonesium is reported to be at about 0.8 in these units(citation), which is consistent with our MD simulations.

We checked the mode frequencies as functions of temperature. Under constant V conditions, the mode frequencies shift to higher value as the temperature increases, while under constant P, the frequencies shift down (Fig. 5.1).

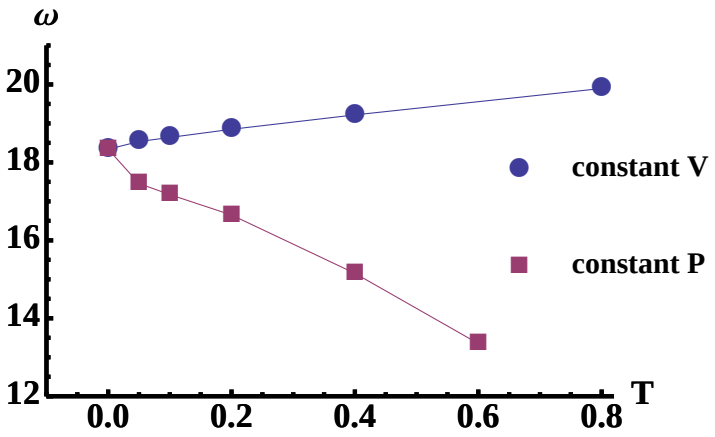

Figure 5.1: The frequency of the peak of the density of states for a typical mode in the 4-atom cell, as a function of temperature showing the up-shift of the mode frequency in constant V and the down-shift of the mode frequency in constant P.

We present here the scatterplots resulting from the two-part test, where we see that the fourth moment does in fact account reasonably well for the mode lifetimes. We then present an analysis of the mode-resolved densities of states.

5.2.1 Scatterplots

The results for FCC4(Fig. 5.2), the smallest cell considered here, are presented first (Fig. 5.2). We find that the mode lifetimes in this small cell can be represented by the same relation as found in the previous work on lattice models [14, 15, 35]), namely:

$$\frac{\tau}{\tau_2} = C\frac{1}{\sqrt{\gamma_4 - 1}} \tag{5.1}$$

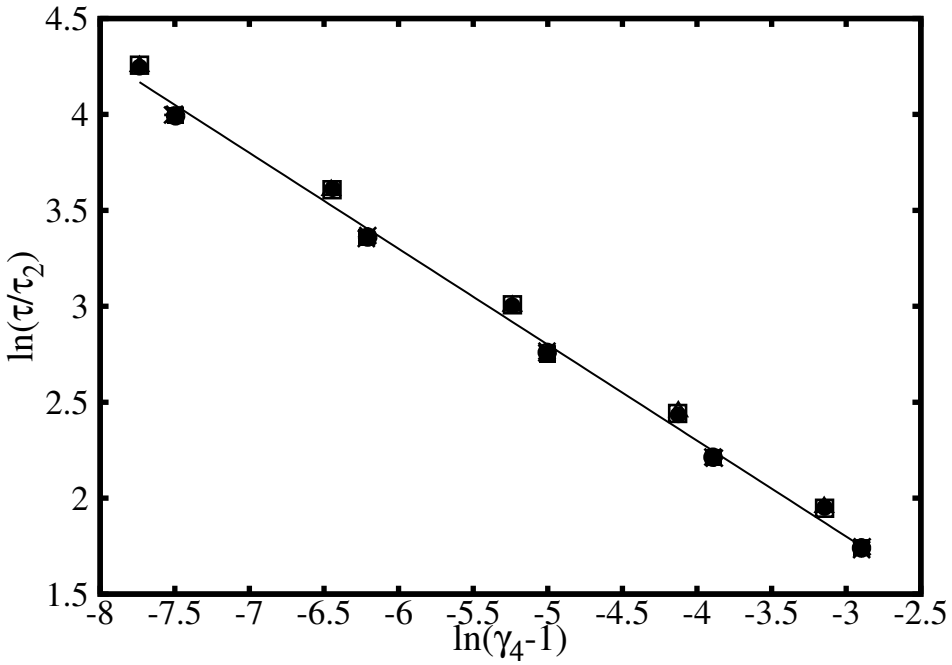

Figure 5.2: Scatter-plot of τ/τ_2 vs. $\gamma_4 - 1$ for all 9 non-sliding modes of the 4-atom cell, at constant V. The degeneracy of the results is in accordance with the symmetry of the cell but is not explicitly imposed in the calculation. The straight line is a fit to the results. The results for constant P condition are very similar.

The results for the other cells (FCC8, FCC16, and FCC32) under constant V conditions are presented all together in Fig. 5.3.

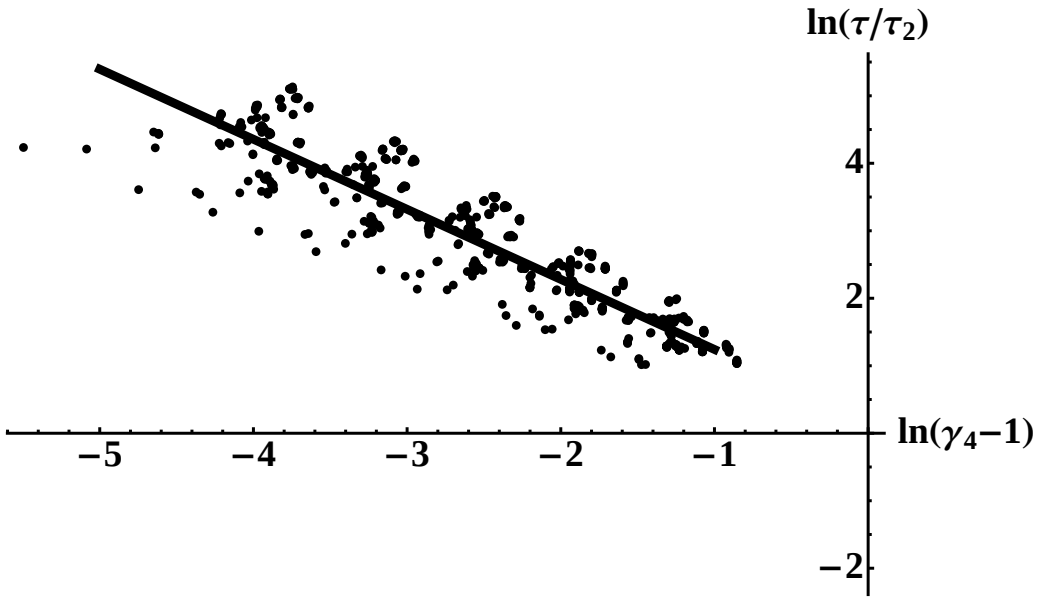

Figure 5.3: Scatter-plot of τ/τ_2 vs. $\gamma_4 - 1$ for all non-sliding modes of the 8-, 16-, and 32-atom cells, at constant V. The straight line is a fit to the results. The results for constant P condition are very similar.

The scatterplots in this figure show that the normal modes in these systems follow a single trendline with a different power, namely Eq. 3.1:

$$\frac{\tau}{\tau_2} = C\frac{1}{\gamma_4 - 1} \tag{5.2}$$

The difference in the two behaviors can be understood in terms of the basic mode couplings present in the system. In the model potentials considered previously, such as Eq. 2.20, the coupling was chosen to be fourth order. This was true also in the simple, low-dimensional models. We find also that if the potential energy is expanded in terms of the normal modes, that the Hamiltonian for the FCC4 cell contains second- and fourth-order terms, but no third order couplings (that is, couplings involving a product of three mode amplitudes, or two modes with one amplitude square, or the third power of a single mode amplitude). Thus, the basic mode coupling dynamics involves only fourth-order couplings in FCC4. However, the larger cells involve more degrees of freedom, which introduce third-order couplings, which are generally expected in solids. Expanding the potential energy for the FCC8 cell in terms of normal mode amplitudes, for example, shows the present of third-order

couplings. So, the primary difference between the larger cells (FCC8, 16, 32) of Lennard-Jonesium on the one hand, and the smallest cell (FCC4) of Lennard-Jonesium along with the previously investigated lattice models, on the other hand, is precisely the difference between systems with and without 3rd order mode couplings.

The scatterplots obtained under condition of constant P are very similar to those obtained under constant V, as we see for Figs. 5.4.

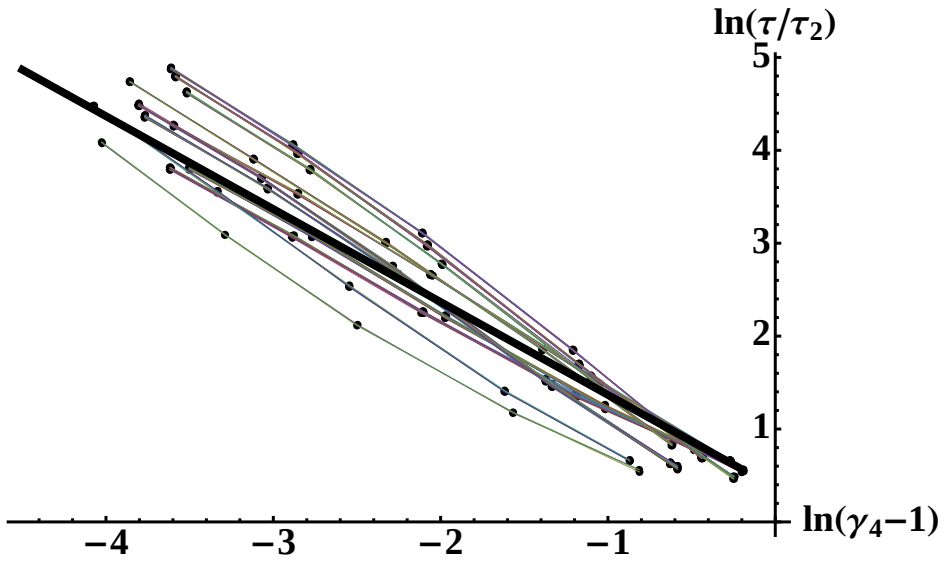

Figure 5.4: Scatter-plot of τ/τ_2 vs. $\gamma_4 - 1$ for all non-sliding modes of 32-atom cells at constant P.

5.2.2 Density of States

Figures 5.5 and 5.6 show the densities of states of some typical modes from the smallest and largest cells we considered, at two different temperatures (the lowest and highest considered). These were obtained under constant P conditions. Typically, the DOS is dominated by single peak that broadens and shifts with increasing temperature.[4]

[4]The highest frequency modes (zone edge) in FCC systems have a small number of multiple frequencies even at low temperatures, but these are atypical modes. All of the other modes display the behavior shown here.

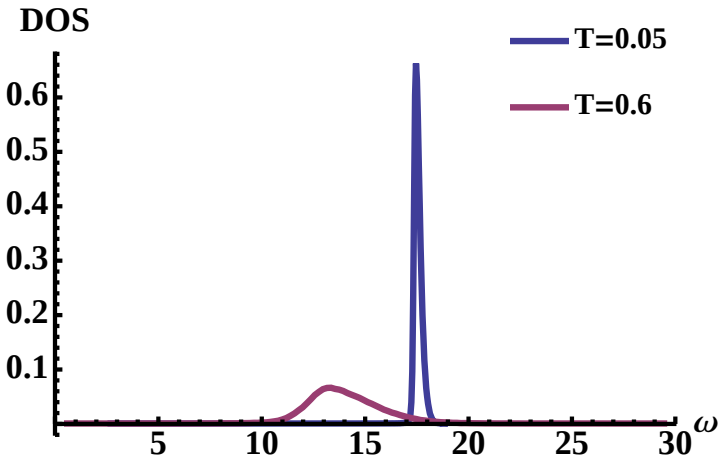

Figure 5.5: The density of states of a typical mode in the 4-atom cell at the lowest and highest temperatures we investigated, for constant P.

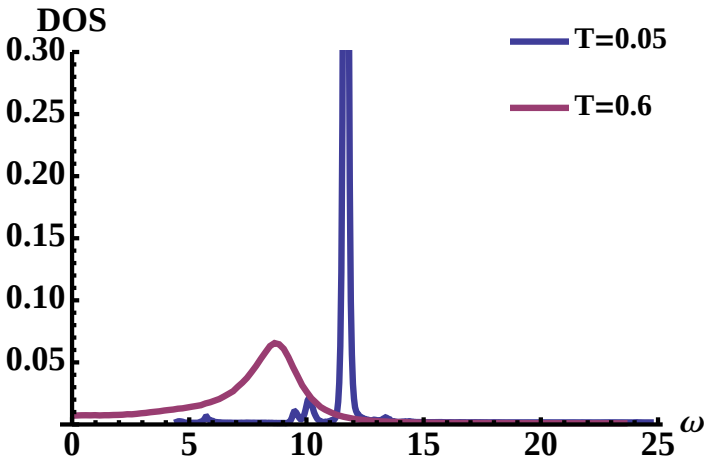

Figure 5.6: The density of states of a typical mode in the 32-atom cell at the lowest and highest temperatures we investigated, for constant P.

5.3 Conclusions

We have investigated the vibrational mode lifetimes in FCC-Lennard Jonesium at various temperatures up to the melting point, constant V and constant P conditions, and for cells ranging from 4 to 64 atoms. Based on previous work, we have tested whether the second and fourth-moments of the Liouvillian are sufficient to capture the behavior of the lifetimes. The second moment reflects basically the temperature-dependent mode frequency, and the fourth moment reflects the temperature-dependent anharmonicity of the mode. We conclude that the fourth-moment approximation captures the basic trends, though some scatter is observed that could be attributed to deviations at higher moment. Because the smallest cell has only 4th-order anharmonic couplings among the modes, the fourth-moment scaling (Eq. 5.1) agrees with that reported in previous work on 4th-order lattice models. The other cells all have 3rd-order anharmonic couplings, and as a result the fourth-moment scaling (Eq. 5.2) is linear. The success of the fourth-moment scaling appears to be due to the simple nature of the mode-resolved densities of states, which are single peaks that are shifted and broadened with increasing temperature.

Chapter 6

Summary and Future work

6.1 Summary

In this dissertation, we have investigated and developed a method of calculation of mode lifetimes, the fourth moment approximation. Based on theoretical conductions, actual numerical applications to multiple models from simple low dimensional anharmonic oscillator to more realistic FCC systems with Lennard-Jones potential and comparison to other numerical scheme (specifically MD in combination with interatomic potential), it is proven that the fourth moment approximation method is overall a reliable, fast and general technique to calculate mode lifetimes in wide range of materials.

Following is a quick recap of this dissertation. In chapter 1, we firstly represented some classic methods of calculation of mode lifetimes by reviewing some important articles. In these articles, each method shows it own strength and weakness, and overall these methods (Fig:1.1) are either hard to apply due to its computational cost or difficult to generalize because of limited availability of empirical potentials comparing with the scale of materials that need to be investigated. Then in chapter 2, we reviewed the second moment approximation method that is proposed by DD. Tested on a 3D model, their numerical calculation shows agreement with classic MD with interatomic potential at high temperatures, but deviates at low temperatures. From chapter 3 to chapter 5, we developed the fourth moment approximation method, and the method was tested on 3 low dimensional model, 1D anharmonic chains, 3D anharmonic lattices, and finally FCC systems with the Lennard-Jones potential. For comparison, the MD method was also applied to all the

models, and calculations showed that results agree with that from MD calculations within the full range of temperatures.

6.2 Future work

The main purpose of this dissertation is to lay the groundwork of a general scheme to calculate mode lifetimes on **any** materials. In the future, this technique will be developed to calculate mode lifetimes using a first-principled electronic structure code.

In this thesis we used MC in combination with empirical potentials, in which empirical potentials provide force constants and MC calculates the ensemble average of chosen dynamic variables. LAMMPS [56] provide a variety of empirical potentials, and it is beneficial to utilize it by having a wrapper to treat LAMMPS as a black box and extract forces from it and then conducting MC calculations.

In the future, it is proposed to use MC in combination with a first-principles electronic structure code. Just like the first scheme, we can extract force constants from first principle calculation software such as VASP [9] and then calculate ensemble average using MC.

With both methods, we can conduct calculations on many materials that haven't been investigated before with relative low computational cost. Furthermore we can even predict mode lifetimes of new materials, which can provide guidance to experiments.

Appendices

Appendix A Table of terms

- ACF: Autocorrelation function
- Clemson Time: $\tau = \int_0^\infty \chi(t)^2 dt$
- DA: Dimensional Analysis
- DD: Dickel & Daw
- GK: Green-Kubo
- MD: Molecular dynamics
- MC: Monte Carlo
- EMD: Ensemble molecular dynamics
- LTC: Lattice thermal conductivity
- OACF: Occupational number autocorrelation function
- VACF: Velocity autocorrelation function
- XACF: displacement autocorrelation function

Bibliography

[1] A. J. C. Ladd, B. Moran and W. G. Hoover, *Phys. Rev. B*, 34, 5058 (1986).

[2] R. W. Zwanzig, *Ann. Rev. Phys. Chem.* 16, 67 (1965).

[3] J. Dong, O.F. Sankey, and C.W. Myles, *Physical Review Letters* 86, 2361 (2001).

[4] P K Schelling, S R Phillpot and P Keblinski *Phys. Rev. B* 65, 144306 (2002).

[5] D. A. Broido, A. Ward and N. Mingo, *Phys. Rev. B* 72, 014308 (2005).

[6] D.A. Broido, M. Malorny, G. Birner, N. Mingo, D.A. Stewart, *Appl.Phys.Lett.* 91, 231911 (2007).

[7] J. M. Ziman, *Electrons and Phonons*, Oxford, New York, 2001.

[8] S. Stackhouse, L. Stixrude and B. B. Karki *Phys. Rev. Lett.* 104, 208501 (2010).

[9] G. Kresse and J. Hafner. *Phys. Rev. B*, 47, 558 (1993).

[10] H. B. Shore, J. H. Rose and E. Zaremba, *Phys. Rev. B* 15, 2858 (1977).

[11] W. Li, N. Mingo, L. Lindsay, D. A. Broido, D. A. Stewart, and N. A. Katcho *Phys. Rev. B* 85, 195436 (2012).

[12] L. Lindsay, D. A. Broido, and T. L. Reinecke, *Phys. Review Lett.* 109, 095901 (2012).

[13] L. Lindsay, D. A. Broido and T. L. Reinecke, *Phys. Review Lett.* 111, 025901 (2013).

[14] D. Dickel and M. S. Daw, *Comp. Mat. Sci.* 47, 698 (2009).

[15] D. Dickel and M. S. Daw, *Comp. Mat. Sci.* 49, 445 (2010).

[16] R. Haydock and D. B. Kim, *Comp. Phys. Comm* 87, 396 (1995)

[17] R. Haydock, C.M.M Nex and B.D.Simons. *Physical Review E* 59, 5 (1999)

[18] R. Haydock and C.M.M Nex. *Physical Review B* 74, 205121 (2006)

[19] L. Van Hove, *Physica* 21, 517 (1955).

[20] L. Van Hove, *Physica* 25, 268 (1959).

[21] I Prigogine. *Nonequilibrium statistical mechanics* (Wiley, 1962)

[22] R. Brout, I. Prigogine, *Physica*, 22, 521 (1956).

[23] I. Prigogine, R. Balescu, *Physica*, 25, 281 (1959) .

[24] I. Prigogine, R. Balescu, *Physica*, 25, 302 (1959).

[25] P. Resibois, *Physica*, 27, 541 (1961).

[26] I. Prigogine, P. Resibois, *Physica*, 27, 629 (1961).

[27] I. Prigogine, *Introduction to Thermodynamics of Irreversible Processes*, Wiley, (1968).

[28] R. Zwanzig, *J. Chem. Phys.* 33, 1338 (1960).

[29] R. Zwanzig, *Phys. Rev.*, 124, 983 (1961).

[30] R. Zwanzig, *Phys. Rev.*, 144, 170 (1966).

[31] H. Mori, Prog. *Theor. Phys.*, 33, 423 (1965).

[32] B. O. Koopman. *Proc. Nat. Acad. Sci.*, 17, 315 (1931).

[33] B. O. Koopman and J. von Neumann. *Proc. Nat. Acad. Sci.*, 18, 255 (1932).

[34] R.S. Wilson, S.K. Kim, *Phys. Rev. B* 7, 4674 (1973).

[35] Y. Gao, D. Dickel, D. Harrison and M. S. Daw, *Comp. Mat. Sci.* 89, 12 (2014).

[36] Y. Gao and M. S. Daw 2014 *Modeling and Simulation in Materials Science and Engineering* in press.

[37] S. Sen, R. S. Sinkovits and S. Chakravarti, *Phys. Rev. Lett.* 77, 4855 (1996).

[38] R. S. Sinkovits, S. Sen, J. C. Phillips and S. Chakravarti, *Phys. Rev. E* 59, 6497 (1999).

[39] T. Tadano, Y Gohda and S Tsuneyuki, *J. Phys. Condens Matter*, 26, 225402 **2014** .

[40] K. Parlinski, Z. Q. Li and Y. Kawazoe *Phys. Rev. Lett.*, 78m 4063 (1997).

[41] S Baroni, S de Gironcoli, A D Corso and P Giannozzi *Rev. Mod. Phys.*, 73, 515 (2001).

[42] X. Gonze *Phys. Rev. B*, 55, 10337 (1997).

[43] C. S. Wang, B. M. Klein, and H. Krakauer, *Phys. Rev. Lett.*, 54, 1852 (1985).

[44] T. C. Leung, C. T. Chan, and B. N. Harmon, *Phys. Rev. B*, 44, 2923 (1991).

[45] J. P. Perdew, J. A. Chevary, S. H. Vosko, K. A. Jackson, M. R. Pederson, D. J. Singh, and C. Fiolhais, *Phys. Rev. B*, 46, 6671 (1992).

[46] J. Tersoff, *Phys. Rev. B*, 39, 5566 (1989).

[47] D W. Brenner*Phys. Rev. B*, 42, 9458 (1990).

[48] D Donadio and G Galli *Phys. Rev. Lett.*, 102, 195901 (2009).

[49] Y He and Galli G *Phys. Rev. Lett.*, 108, 215901 (2012).

[50] M. S. Green, *J. Chem. Phys.* 22, 398 (1954); R. Kubo, M.Yokota and S. Nakajima, *J. Phys. Soc. Jpn.* 12, 1203 (1957).

[51] P. K. Schelling, S. R. Phillpot, *App. Phys. Lett.*, 80, 2484 (2002)

[52] C. W. Myles, J.J. Dong, and O.F. Sankey, *Physica Status Solidi B*, 239, 26 (2003)

[53] C. W. Myles, J. Dong, O.F. Sankey, G.S. Nolas, and C.A. Kendziora, *Physical Review B*, 65, 235208 (2002)

[54] L. Verlet, *Phys. Rev.*, 159, 98 (1967)

[55] G.I. Barenblatt, *Dimensional Analysis* (1987)

[56] S. Plimpton, Fast Parallel Algorithms for Short-Range Molecular Dynamics, *J Comp Phys*, **117**, 1-19 (1995): http://lammps.sandia.gov

[57] Y. Gao, H. Wang and M. S. Daw 2014*Modeling and Simulation in Materials Science and Engineering* in press: http://sourceforge.net/projects/jazzforlammps/

[58] A J. C. Ladd,B Moran and W G. Hoover *Physical Review B*, 34, 5058 (1986)